ISSN 2686-7575 (Online)

ТОНКИЕ ХИМИЧЕСКИЕ ТЕХНОЛОГИИ

Fine Chemical Technologies

- Theoretical Bases of Chemical Technology
- Chemistry and Technology of Organic Substances
- Chemistry and Technology of Medicinal Compounds and Biologically Active Substances
- Synthesis and Processing of Polymers and Polymeric Composites
- Chemistry and Technology of Inorganic Materials
- Analytical Methods in Chemistry and Chemical Technology
- Mathematical Methods and Information Systems in Chemical Technology

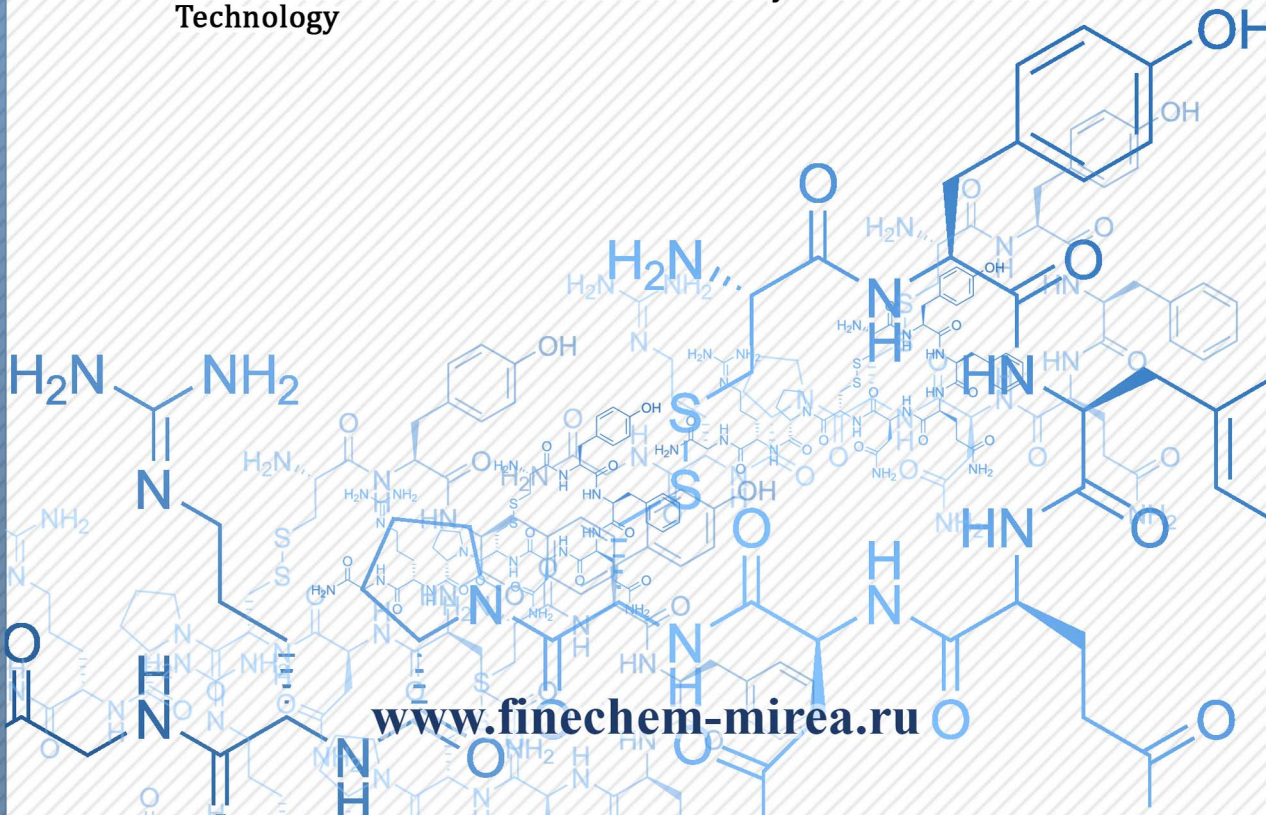

15(3)
2020

www.finechem-mirea.ru

ISSN 2686-7575 (Online)

ТОНКИЕ ХИМИЧЕСКИЕ ТЕХНОЛОГИИ

Fine Chemical Technologies

- Theoretical Bases of Chemical Technology
- Chemistry and Technology of Organic Substances
- Chemistry and Technology of Medicinal Compounds and Biologically Active Substances
- Synthesis and Processing of Polymers and Polymeric Composites
- Chemistry and Technology of Inorganic Materials
- Analytical Methods in Chemistry and Chemical Technology
- Mathematical Methods and Information Systems in Chemical Technology

Tonkie Khimicheskie Tekhnologii =
Fine Chemical Technologies
Vol. 15, No. 3, 2020

Тонкие химические технологии =
Fine Chemical Technologies
Том 15, № 3, 2020

https://doi.org/10.32362/2410-6593-2020-15-3
www.finechem-mirea.ru

https://doi.org/10.32362/2410-6593 ***www.finechem-mirea.ru***

Tonkie Khimicheskie Tekhnologii = Fine Chemical Technologies 2020, vol. 15, no. 3

The peer-reviewed scientific and technical journal Fine Chemical Technologies highlights the modern achievements of fundamental and applied research in the field of fine chemical technologies, including theoretical bases of chemical technology, chemistry and technology of medicinal compounds and biologically active substances, organic substances and inorganic materials, synthesis and processing of polymers and polymeric composites, analytical and mathematical methods and information systems in chemistry and chemical technology.

Founder and Publisher

Federal State Budget
Educational Institution
of Higher Education
"MIREA – Russian Technological University"
78, Vernadskogo pr., Moscow 119454, Russian Federation.

Six issues a year are published.
The journal was founded in 2006. The name was Vestnik MITHT until 2015 (ISSN 1819-1487).

The journal is included into the List of peer-reviewed science press of the State Commission for Academic Degrees and Titles of the Russian Federation.
The journal is indexed:
DOAJ, Chemical Abstracts, Science Index, RSCI, Ulrich's International Periodicals Directory

86, Vernadskogo pr., Moscow 119571, Russian Federation.
Phone: +7(495) 246-05-55 (#2-88)
E-mail: *vestnik@mitht.ru*

Registration Certificate ПИ № ФС 77–74580, issued on December 14, 2018 by the Federal Service for Supervision of Communications, Information Technology, and Mass Media of Russia

The subscription index of *Pressa Rossii*: **36924**

Тонкие химические технологии = Fine Chemical Technologies 2020, том 15, № 3

Научно-технический рецензируемый журнал «Тонкие химические технологии» освещает современные достижения фундаментальных и прикладных исследований в области тонких химических технологий, включая теоретические основы химической технологии, химию и технологию лекарственных препаратов и биологически активных соединений, органических веществ и неорганических материалов, синтез и переработку полимеров и композитов на их основе, аналитические и математические методы и информационные системы в химии и химической технологии.

Учредитель и издатель

федеральное государственное бюджетное
образовательное учреждение
высшего образования
«МИРЭА – Российский технологический университет»
119454, РФ, Москва, пр-кт Вернадского, д. 78.

Периодичность: 6 раз в год.
Журнал основан в 2006 году. До 2015 года издавался под названием «Вестник МИТХТ» (ISSN 1819-1487).

Журнал входит в Перечень ведущих рецензируемых научных журналов ВАК РФ.
Индексируется:
DOAJ, Chemical Abstracts, РИНЦ (Science Index), RSCI, Ulrich's International Periodicals Directory

119571, Москва, пр. Вернадского, 86, оф. Л-119.
Тел.: +7(495) 246-05-55 (#2-88)
E-mail: *vestnik@mitht.ru*

Свидетельство о регистрации СМИ: ПИ № ФС 77-74580 от 14.12.2018 г. выдано Федеральной службой по надзору в сфере связи, информационных технологий и массовых коммуникаций (Роскомнадзор)

Индекс по Объединенному каталогу «Пресса России»: **36924**

ТОНКИЕ ХИМИЧЕСКИЕ ТЕХНОЛОГИИ | Fine Chemical Technologies

15(3)
2020

CONTENTS

СОДЕРЖАНИЕ

ISSN 2686-7575 (Online)

https://doi.org/10.32362/2410-6593-2020-15-3-7-20

UDC 66.011:66.048.3

Areas of energy advantage for flowsheets of separation modes for mixtures containing components with similar volatilities

Margarita E. Peshekhontseva, Mark A. Maevskiy, Ivan S. Gaganov, Anastasiya V. Frolkova[@]

MIREA – Russian Technological University (M.V. Lomonosov Institute of Fine Chemical Technologies), Moscow, 119571 Russia

[@]Corresponding author, e-mail: frolkova_nastya@mail.ru

Objectives*. The conditions for the effective application of the sharp distillation technique (without a component distributed between the distillate and bottom flows) for the separation of quaternary zeotropic mixtures containing components with similar volatilities were determined. The area of energy advantage for the flowsheet based on the preliminary fractionation of the mixture, compared with the flowsheet, the first distillation column of which works based on the indirect separation mode, was identified for an ethyl acetate–benzene–toluene–butyl acetate system. Energy savings of up to 20% were achieved. The direct and indirect distillation modes can become competitive when the point of the original composition is located near single K-surfaces or in a region with a different ratio of distribution coefficients. Sharp distillation is not suitable for the separation of a mixture containing a pair of components exhibiting relative unity volatility with medium boiling points.*

Methods. *The mathematical modeling in the Aspen Plus V.10.0 software package was chosen as the research method. The simulation was based on the Wilson local composition equation. The relative errors in the description of the phase equilibrium did not exceed 3%.*

Results. *The structure of the vapor–liquid equilibrium diagram and diagram of surfaces of the unit component distribution coefficients were studied for the ethyl acetate–benzene–toluene–butyl acetate and acetone–toluene–butyl acetate–o-xylene systems. Flowsheets based on the sharp, indirect (both systems), or direct (second system) distillation modes were proposed. The distillation process was simulated, and the parameters of the column work were determined (the quality of the substances meets the State Standard requirements of the Russian Federation for minimal energy consumption).*

Conclusions. *Recommendations regarding the use of sharp distillation for the separation of quaternary mixtures containing components with similar volatilities were devised.*

Keywords: *distillation, sharp distillation, liquid–vapor equilibrium, components relative volatility, components distribution coefficients.*

For citation: Peshekhontseva M.E., Maevskiy M.A., Gaganov I.S., Frolkova A.V. Areas of energy advantage for flowsheets of separation modes for mixtures containing components with similar volatilities. *Tonk. Khim. Tekhnol. = Fine Chem. Technol.* 2020;15(3):7-20. https://doi.org/10.32362/2410-6593-2020-15-3-7-20

Области энергетического преимущества схем разделения смесей, содержащих компоненты с близкими летучестями

М.Е. Пешехонцева, М.А. Маевский, И.С. Гаганов, А.В. Фролкова[@]

МИРЭА – Российский технологический университет (Институт тонких химических технологий им. М.В. Ломоносова), Москва, 119571 Россия
[@]Автор для переписки, e-mail: frolkova_nastya@mail.ru

Цели. *Для ректификации четырехкомпонентных зеотропных смесей, содержащих компоненты с близкими летучестями, определены условия эффективности применения промежуточного заданного разделения (при отсутствии компонента, распределенного между дистиллятным и кубовым потоками). На примере системы этилацетат–бензол–толуол–бутилацетат выделена область энергетического преимущества схемы, основанной на использовании предварительного фракционирования смеси, по сравнению со схемой, первая ректификационная колонна которой работает по второму заданному разделению. Экономия энергозатрат составляет до 20%. Реализация первого и второго заданного разделения может стать конкурентной при расположении точки исходного состава вблизи единичных K-поверхностей или в области с другим соотношением коэффициентов распределения. Промежуточное разделение не может быть рекомендовано для разделения смеси с близкой к единице относительной летучестью пары компонентов со средними температурами кипения.*

Методы. *В качестве метода исследования выбрано математическое моделирование в программном комплексе Aspen Plus V.10.0. Моделирование основывалось на уравнении локального состава Wilson. Относительные ошибки описания фазового равновесия не превышают 3%.*

Результаты. *Исследована структура диаграммы парожидкостного равновесия и диаграммы поверхностей единичных коэффициентов распределения компонентов для систем этилацетат–бензол–толуол–бутилацетат и ацетон–толуол–бутилацетат–о-ксилол. Предложены схемы, основанные на использовании промежуточного, второго (обе системы) или первого (вторая система) заданного разделения. Проведен расчет процесса ректификации и подобраны параметры работы колонн, обеспечивающие получение веществ, качество которых отвечает требованиям ГОСТ при минимальных энергозатратах.*

Выводы. *На основе проведенных исследований сформулированы рекомендации по использованию промежуточного разделения при ректификации четырехкомпонентных смесей, содержащих компоненты с близкими летучестями.*

Ключевые слова: *ректификация, промежуточное разделение, равновесие жидкость–пар, относительная летучесть компонентов, коэффициенты распределения компонентов.*

Для цитирования: Пешехонцева М.Е., Маевский М.А., Гаганов И.С., Фролкова А.В. Области энергетического преимущества схем разделения смесей, содержащих компоненты с близкими летучестями. *Тонкие химические технологии.* 2020;15(3):7-20. https://doi.org/10.32362/2410-6593-2020-15-3-7-20

INTRODUCTION

Choosing an energy-efficient version of the separation flowsheet is one of the key challenges in basic organic and petrochemical synthesis. This is primarily because the separation unit of the reaction mixture accounts for 60–80% of the total energy consumption [1–3]. Developing a separation flowsheet for multicomponent mixtures is a polyvariant task, since the same mixture can be separated using different modes (direct, indirect, or sharp distillation) or using special methods [1, 2, 4–8]. The formulation of practical recommendations for the use of a particular technique or method will significantly reduce the time expended at the pre-project development stage of the separation technology.

In [9], we evaluated the possibility of using sharp distillation (provided that there is no component distributed between the cube and the distillate) for the separation of quaternary non-ideal mixtures containing azeotropes and/or components with similar volatilities. Based on the analysis of the diagrams

of surfaces of the unit component distribution coefficients, the areas of compositions are identified for which the use of the sharp distillation mode is not only possible but also potentially more energy-efficient than the direct or indirect distillation modes.

In this paper, a comparative analysis of the separation flowsheets of multicomponent zeotropic mixtures (containing components with similar volatilities) based on various types of separation modes is carried out. The conditions, under which sharp distillation is more energy-efficient than other separation modes, as well as the restrictions to its application, are determined.

The objects of research are quaternary systems: ethyl acetate (EA)–benzene (B)–toluene (T)–butyl acetate (BA) (a mixture of solvents produced by biodegradable polymers [10]) and acetone (A)–toluene (T)–butyl acetate (BA)–*o*-xylene (*o*-X) (a mixture of solvents produced by epoxy primers [11]). Both systems are zeotropic and contain pairs of components with similar volatiles: ethyl acetate–benzene and toluene–butyl acetate.

MATERIALS AND METHODS

Phase equilibrium modeling was performed in the AspenPlus V.10.0 software package using the Wilson equation:

$$\ln y_i = 1 - \ln\left(\sum_j A_{ij} x_j\right) - \sum_j \frac{A_{ji} x_j}{\sum_k A_{jk} x_k}$$

where $A_{ij} = a_{ij} + \frac{b_{ij}}{T} + c_{ij} \ln T + d_{ij} T + \frac{e_{ij}}{T^2}$, a_{ij}, a_{ji}, b_{ij} and b_{ji} are the parameters of the Wilson equation.

This equation has been proven to be instrumental in the study of the phase equilibrium of homogeneous systems, including the changes in the external conditions. This model is chosen to enable the simulation of the phase equilibrium and the distillation process at low pressures.

The parameters of the binary interaction and errors in the description of the phase equilibrium are given in Table 1.

RESULTS AND DISCUSSION

Based on the analysis of the phase equilibrium curves of the binary systems, ethyl acetate–benzene and toluene–butyl acetate [12–13], it was shown that the separation of ethyl acetate from benzene using conventional distillation is impossible under any condition. This fact restricts the use of direct distillation for the separation of the EA–B–T–BA mixture. The separation of toluene from BA without special methods is possible in a distillation column at a low pressure (the relative volatility of the components is increased by more than 1.5 times). Thus, for the separation of the EA–B–T–BA mixture at the first stage, it is possible to use a sharp distillation (at reduced pressure) specified separation technique; for the A–T–BA–*o*-X mixture, any technique can be utilized.

The efficiency of using a particular separation technique for mixtures of different compositions characterized by different ratios of component distribution coefficients was evaluated. To select the original compositions, diagrams of the unit surfaces of the component distribution coefficients were constructed (Fig. 1).

The area of compositions in which the distribution coefficients of two components are

Table 1. Wilson equation parameters for the binary constituents of the benzene (B)–toluene (T)–ethyl acetate (EA)–butyl acetate (BA) and acetone (A)–toluene (T)–butyl acetate (BA)–*o*-xylene (*o*-X) systems

Binary system	a_{ij}	a_{ji}	b_{ij}	b_{ji}	ΔT, %	ΔY, %
B–T	−1.5857	2.3275	634.7787	−913.6505	0.17	1.06
B–EA	8.2122	−11.6434	−2841.5425	4010.0664	0.07	0.31
B–BA	0	0	−19.0272	54.5272	0.20	1.12
T–A*	5.10951	−4.14947	−2010.08	1570.5	0.20	0.94
T–BA*	−2.0001	1.53945	951.97	−848.68	0.27	4.56
EA–BA	0	0	−5.6575	−15.65	0.37	1.67

Table 1. Continued

Binary system	a_{ij}	a_{ji}	b_{ij}	b_{ji}	ΔT, %	ΔY, %
A–T	0.8857	−0.8619	−461.065	247.597	0.57	1.47
A–BA	0	0	−0.1353	−87.2465	0.44	0.55
A–*o*-X	0	0	−163.265	−96.3392	0.00	0.10
T–*o*-X*	0	0	−151.016	126.916	–	–
BA–*o*-X**	0	0	245.808	−409.273	–	–

Note: *parameters are estimated from experimental data [12–14];
**parameters were evaluated using the UNIFAC model.

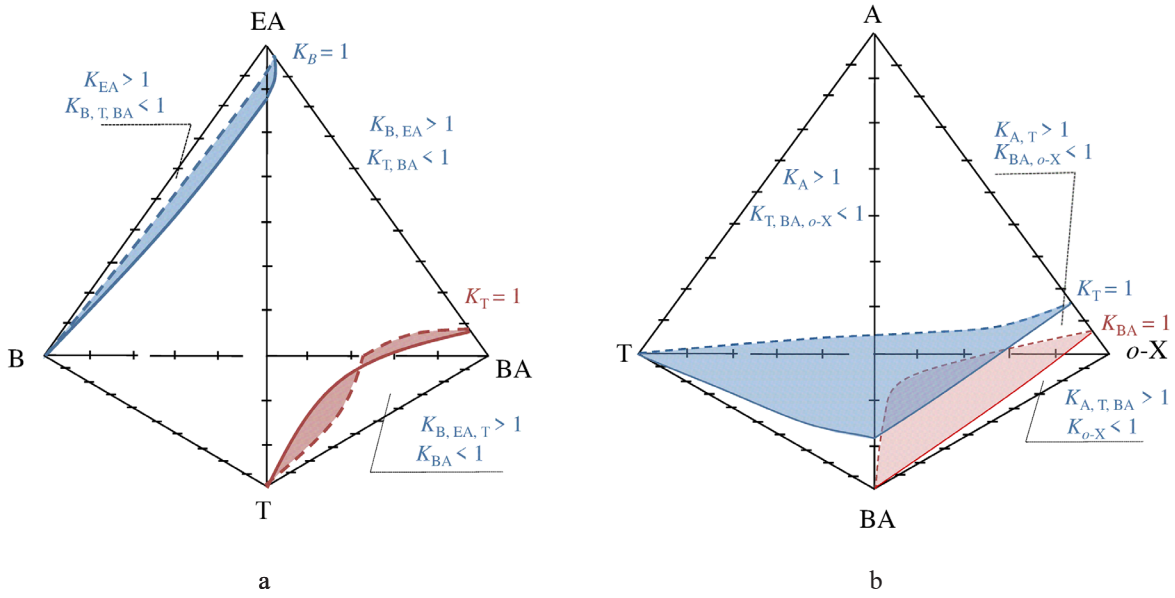

a b

Fig. 1. Diagrams of the unit *K*-surfaces of the systems: ethyl acetate (EA)–benzene (B)–toluene (T)–butyl acetate (BA) (a) and acetone (A)–toluene (T)–butyl acetate (BA)–*o*-xylene (*o*-X) (b) at 760 mm Hg.

characterized by a value greater than one, and the rest by less than one, is favorable for the implementation of sharp distillation. For the system shown in Fig. 1a, this area occupies a significant part of the composition simplex. For the system in Fig. 1b, this region is quite narrow, which is due to the proximity of the volatile components with intermediate boiling points (toluene and butyl acetate).

For the EA–B–T–BA system, the points of original compositions belonging to different secants are selected (secant 1 corresponds to the equimolar ratio of benzene, toluene, and butyl acetate; for secants 2, 3, and 4, the compositions are enriched with butyl acetate, benzene, and toluene, respectively). For each section, five compositions are considered, corresponding to sections 1–5 with constant concentrations of ethyl acetate: 0.05 (1), 0.25 (2), 0.45 (3), 0.65 (4), and 0.82 (5). The original composition of the mixture is represented by two digits, the first of which indicates the number of the secant, and the second—the section number. Composition **2.1** ($x_{EA} = 0.05$, $x_B = 0.05$, $x_T = 0.3$, $x_{BA} = 0.6$ mol. fractions) belongs to the area where only butyl acetate is a highly volatile component; the other components are highly volatile. Other compositions are characterized by the following ratio of distribution coefficients: $K_{EA} > 1, K_B > 1, K_T < 1, K_{BA} < 1$.

For the A–T–BA–*o*-K system, two original compositions, belonging to regions with different ratios of distribution coefficients, will be considered: equimolar ($K_A > 1, K_T > 1, K_{BA} > 1, K_{o\text{-X}} < 1$) and $x_A = 0.04$, $x_T = 0.32$, $x_{BA} = 0.32$, $x_{o\text{-X}} = 0.32$ mol. fractions ($K_A > 1$, $K_T > 1$, $K_{BA} < 1$, $K_{o\text{-X}} < 1$).

For each system, the separation flowsheets for different structures are proposed, the distillation process is simulated, and the parameters of the columns are selected to ensure the production of substances whose quality meets the requirements of GOST (benzene No. 5955-75; ethyl acetate, butyl acetate No. 8981-78; toluene No. 14710-78; acetone No. 2768-84; *o*-xylene No. 9410-78) with minimal energy consumption (the column reboiler duty is considered).

Ethyl acetate–benzene–toluene–butyl acetate system

Two flowsheets are proposed for the separation of the mixtures (Fig. 2).

The parameters of the columns (NTS: the number of theoretical stages; *P*: the pressure (mm Hg); F_{init}/F_{SA}: the ratio of the amounts of the initial mixture and the separating agent (SA); FS: the feed stage; *R*: the reflux ratio), as well as the energy consumption (*Q*) for both flowsheets and 20 original compositions, are shown in Tables 2–5.

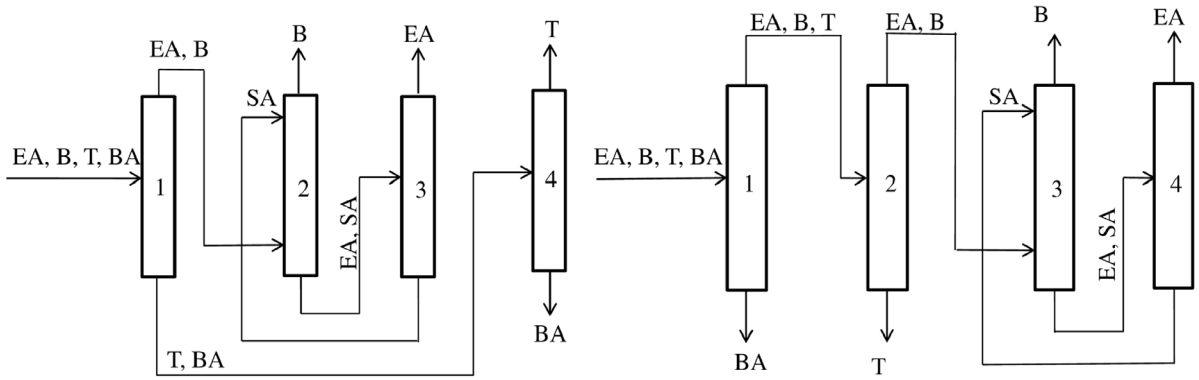

a b

Fig. 2. Ethyl acetate (EA)–benzene (B)–toluene (T)–butyl acetate (BA) mixture separation flowsheets based on the sharp (a) and indirect (b) distillation modes (separating agent (SA): phenol).

Table 2. Parameters of the columns work of the separation flowsheets shown in Fig. 2 (for the original compositions from **1.1** to **1.5**)

Column	NTS (F_{init}/F_{SA})	*P*	FS mix/SA	*R*	*Q*, kW	NTS (F_{init}/F_{SA})	*P*	FS mix/SA	*R*	*Q*, kW
	Sharp distillation					Indirect distillation				
The original composition of the mixture is **1.1** (x_{EA} = 0.04, x_B = 0.32, x_T = 0.32, x_{BA} = 0.32 mol. fract.)										
1	34	760	14	2.7	1189.2	36	100	10	1.1	1551.0
2	24 (1/1)	760	13/6	1	766.6	34	760	18	1.7	850.1
3	36	760	6	4.8	222.0	24 (1/1)	760	13/6	1	766.6
4	32	110	10	3.5	1492.7	36	760	6	4.8	222.0
					$\sum Q$ = 3670.5					**$\sum Q$ = 3389.7**
The original composition of the mixture is **1.2** (x_{EA} = 0.25, x_B = 0.25, x_T = 0.25, x_{BA} = 0.25 mol. fract.)										
1	24	760	14	2	1346.9	24	100	9	1	1669.5
2	30 (1/1.7)	760	9/4	3	608.6	24	760	12	1.4	1064.2
3	22	760	9	3	987.4	30 (1/1.7)	760	9/4	3	608.6
4	24	110	12	3.8	1230.6	22	760	9	3	987.4
					$\sum Q$ = 4173.5					**$\sum Q$ = 4329.7**

Table 2. Continued

Column	NTS (F_{init}/F_{SA})	*P*	FS mix/SA	*R*	*Q*, kW	NTS (F_{init}/F_{SA})	*P*	FS mix/SA	*R*	*Q*, kW
	Sharp distillation					Indirect distillation				
The original composition of the mixture is **1.3** (x_{EA} = 0.46, x_B = 0.18, x_T = 0.18, x_{BA} = 0.18 mol. fract.)										
1	32	760	19	1.4	1413.6	28	100	8	0.4	1419.1
2	36 (1/3)	760	10/4	1.3	1417.2	32	760	21	1.2	1278.3
3	28	760	5	1.3	1172.5	36 (1/3)	760	10/4	1.3	1417.2
4	36	110	12	3.1	766.6	28	760	5	1.3	1172.5
					$\sum Q$ = 4769.9					**$\sum Q$ = 5287.1**
The original composition of the mixture is **1.4** (x_{EA} = 0.64, x_B = 0.12, x_T = 0.12, x_{BA} = 0.12 mol. fract.)										
1	36	760	23	1.3	1598.5	28	100	8	0.3	1417.1
2	36 (1/4)	760	10/4	1.3	1943.1	32	760	22	1.3	1582.6
3	32	760	5	1.6	1791.0	36 (1/4)	760	10/4	1.3	1943.1
4	32	110	11	3.5	559.7	32	760	5	1.6	1791.0
					$\sum Q$ = 5892.3					**$\sum Q$ = 6733.8**
The original composition of the mixture is **1.5** (x_{EA} = 0.82, x_B = 0.06, x_T = 0.06, x_{BA} = 0.06 mol. fract.)										
1	36	760	24	1.2	1751.0	24	100	8	0.2	1339.1
2	32 (1/5.5)	760	11/4	0.9	2885.0	32	760	21	1.3	1821.2
3	32	760	5	2.1	2708.6	32 (1/5.5)	760	11/4	0.9	2885.0
4	32	110	11	3.6	285.9	32	760	5	2.1	2708.6
					$\sum Q$ = 7630.5					**$\sum Q$ = 8753.9**

Note: the separating agent is phenol.

Table 3. Parameters of the columns work of the separation flowsheets shown in Fig. 2 (for the original compositions from **2.1** to **2.5**)

Column	NTS (F_{init}/F_{SA})	*P*	FS mix/SA	*R*	*Q*, kW	NTS (F_{init}/F_{SA})	*P*	FS mix/SA	*R*	*Q*, kW
	Sharp distillation					Indirect distillation				
The original composition of the mixture is **2.1** (x_{EA} = 0.05, x_B = 0.05, x_T = 0.3, x_{BA} = 0.6 mol. fract.)										
1	58	760	16	8	832.6	37	100	11	4.3	2296.7
2	33 (1/2)	760	11/6	0.5	175.7	36	760	15	4.6	509.8
3	28	760	6	1.3	125.9	33 (1/2)	760	11/6	0.5	175.7
4	37	110	12	6.1	2195.6	28	760	6	1.3	125.9
					$\sum Q$ = 3329.8					**$\sum Q$ = 3108.1**

Table 3. Continued

Column	NTS (F_{init}/F_{SA})	*P*	FS mix/SA	*R*	*Q*, kW	NTS (F_{init}/F_{SA})	*P*	FS mix/SA	*R*	*Q*, kW
	Sharp distillation					Indirect distillation				
The original composition of the mixture is **2.2** (x_{EA} = 0.25, x_B = 0.039, x_T = 0.237, x_{BA} = 0.474 mol. fract.)										
1	37	760	17	2.5	960.1	36	100	10	2.1	1900.8
2	32 (1/5)	760	11/5	0.5	882.2	33	760	20	1.9	767.9
3	33	760	5	2.1	818.2	32 (1/5)	760	11/5	0.5	882.2
4	40	110	12	5.7	1638.4	33	760	5	2.1	818.2
					∑*Q* = 4298.9					**∑*Q* = 4369.1**
The original composition of the mixture is **2.3** (x_{EA} = 0.45, x_B = 0.029, x_T = 0.173, x_{BA} = 0.348 mol. fract.)										
1	36	760	21	1.6	1176.5	33	100	9	1.2	1689.8
2	33 (1/5.5)	760	13/5	0.4	1550.1	28	760	18	1.6	1131.9
3	28	760	5	2.2	1525.1	33 (1/5.5)	760	13/5	0.4	1550.1
4	37	110	12	6.2	1283.6	28	760	5	2.2	1525.1
					∑*Q* = 5535.3					**∑*Q* = 5896.9**
The original composition of the mixture is **2.4** (x_{EA} = 0.65, x_B = 0.0184, x_T = 0.1108, x_{BA} = 0.2208 mol. fract.)										
1	37	760	25	1.4	1485.0	28	100	8	0.7	1519.8
2	32 (1/6.5)	760	12/5	0.5	2599.0	29		19	1.8	1686.3
3	33	760	5	2.6	2443.6	32 (1/6.5)	760	12/5	0.5	2599.0
4	37	110	12	6.1	810.9	33	760	5	2.6	2443.6
					∑*Q* = 7338.5					**∑*Q* = 8248.7**
The original composition of the mixture is **2.5** (x_{EA} = 0.85, x_B = 0.008, x_T = 0.048, x_{BA} = 0.094 mol. fract.)										
1	36	760	25	1.3	1786.6	29	100	9	0.2	1172.9
2	33 (1/8)	760	15/8	0.4	4075.4	32	760	21	1.8	2152.2
3	36	760	5	3.2	3689.0	33 (1/8)	760	15/8	0.4	4075.4
4	33	110	12	7	395.0	36	760	5	3.2	3689.0
					∑*Q* = 9946.0					**∑*Q* = 11089.5**

Note: the separating agent is phenol.

The stage numbering begins at the top of the column. To separate the pair of components: ethyl acetate–benzene, phenol, recommended in the literature [15], is used, which increases the volatility of benzene relative to that of ethyl acetate.

Figure 3 shows graphs of the dependence of the total energy consumption of the separation flowsheets on the concentration of EA in the original mixture (for secants 1 and 2). For the compositions located in the other two sections, similar graphs were not obtained because the energy consumption of the flowsheet based on the sharp distillation is lower than that of the flowsheets, the first column of which operates in the indirect distillation mode.

The graphs, shown in Fig. 3, were used to determine the coordinates of the intersection points

Table 4. Parameters of the columns work of the separation flowsheets shown in Fig. 2 (for the original compositions from **3.1** to **3.5**)

Column	NTS (F_{init}/F_{SA})	*P*	FS mix/SA	*R*	*Q*, kW	NTS (F_{init}/F_{SA})	*P*	FS mix/SA	*R*	*Q*, kW
	Sharp distillation					Indirect distillation				
The original composition of the mixture is **3.1** (x_{EA} = 0.05, x_B = 0.6, x_T = 0.05, x_{BA} = 0.3 mol. fract.)										
1	30	760	15	1.8	1616.23	30	100	7	1.4	1745.58
2	30 (1/1)	760	14/7	1.2	1123.41	36	760	23	1	1318.31
3	32	760	5	6.2	359.27	30 (1/1)	760	14/7	1.2	1123.41
4	47	110	14	18.3	859.27	32	760	5	6.2	359.31
					$\sum Q$ = 3958.18					**$\sum Q$ = 4546.61**
The original composition of the mixture is **3.2** (x_{EA} = 0.25, x_B = 0.474, x_T = 0.039, x_{BA} = 0.237 mol. fract.)										
1	30	760	15	1.4	1571.93	29	100	9	0.8	1629.03
2	22 (1/2.6)	760	10/6	2.4	1332.27	36	760	23	1	1606.97
3	24	760	5	4	1240.14	22 (1/2.6)	760	10/6	2.4	1332.27
4	47	110	14	18.5	671.34	24	760	5	4	1240.16
					$\sum Q$ = 4815.68					**$\sum Q$ = 5808.43**
The original composition of the mixture is **3.3** (x_{EA} = 0.45, x_B = 0.348, x_T = 0.029, x_{BA} = 0.173 mol. fract.)										
1	30	760	16	1.4	1745.25	28	100	9	0.6	1674.92
2	38 (1/2.4)	760	9/4	3.5	1218.12	33	760	21	1	1850.27
3	20	760	5	1.6	1275.53	38 (1/2.4)	760	9/4	3.5	1218.19
4	47	110	14	18.5	500.86	20	760	5	1.6	1275.58
					$\sum Q$ = 4739.76					**$\sum Q$ = 6018.96**
The original composition of the mixture is **3.4** (x_{EA} = 0.65, x_B = 0.2208, x_T = 0.0184, x_{BA} = 0.1108 mol. fract.)										
1	30	760	16	1.4	1901.95	28	100	10	0.5	1720.68
2	38 (1/4.4)	760	10/5	8.5	1616.26	34	760	21	1	2043.17
3	24	760	5	2.4	2326.96	38 (1/4.4)	760	10/5	8.5	1620.69
4	47	110	14	18.3	313.27	24	760	5	2.4	2327.07
					$\sum Q$ = 6158.44					**$\sum Q$ = 7711.61**
The original composition of the mixture is **3.5** (x_{EA} = 0.85, x_B = 0.094, x_T = 0.008, x_{BA} = 0.048 mol. fract.)										
1	30	760	17	1.5	2128.95	27	100	10	0.5	1756.05
2	38 (1/5)	760	10/4	29	2159.29	36	760	23	1.1	2239.51
3	23	760	5	2.2	2893.40	38 (1/5)	760	10/4	29	2164.64
4	47	110	14	16.4	137.03	23	760	5	2.2	2893.40
					$\sum Q$ = 7318.67					**$\sum Q$ = 9053.60**

Note: the separating agent is phenol.

Table 5. Parameters of the columns work of the separation flowsheets shown in Fig. 2 (for the original compositions from **4.1** to **4.5)**

Column	NTS (F_{init}/F_{SA})	*P*	FS mix/SA	*R*	*Q*, kW	NTS (F_{init}/F_{SA})	*P*	FS mix/SA	*R*	*Q*, kW
	Sharp distillation					Indirect distillation				
The original composition of the mixture is **4.1** (x_{EA} = 0.05, x_B = 0.3, x_T = 0.6, x_{BA} = 0.05 mol. fract.)										
1	36	760	17	4	1543.79	25	100	9	0.4	1406.04
2	29 (1/0.8)	760	13/5	1	503.63	32	760	15	2.1	1244.33
3	22	760	5	3.3	209.09	29 (1/0.8)	760	13/5	1.3	580.73
4	25	110	10	1.1	1094.80	22	760	5	3.3	212.09
					∑*Q* = 3351.31					**∑*Q* = 3443.19**
The original composition of the mixture is **4.2** (x_{EA} = 0.25, x_B = 0.237, x_T = 0.474, x_{BA} = 0.039 mol. fract.)										
1	32	760	16	3	1769.60	23	100	8	0.3	1405.04
2	33 (1/2.4)	760	9/4	3.1	767.02	29	760	14	1.7	1540.01
3	23	760	5	1.7	729.90	33 (1/2.4)	760	9/4	3.2	788.41
4	25	110	10	1.1	864.99	23	760	5	1.7	730.26
					∑*Q* = 4131.51					**∑*Q* = 4463.72**
The original composition of the mixture is **4.3** (x_{EA} = 0.45, x_B = 0.173, x_T = 0.348, x_{BA} = 0.029 mol. fract.)										
1	30	760	16	3	2270.55	22	100	7	0.2	1368.67
2	38 (1/3.2)	760	10/5	7.9	1182.36	24	760	13	1.2	1641.69
3	22	760	5	1.6	1276.29	35 (1/3.2)	760	10/5	7.5	1109.44
4	25	110	10	1.1	634.97	22	760	5	1.7	1287.29
					∑*Q* = 5364.17					**∑*Q* = 5407.09**
The original composition of the mixture is **4.4** (x_{EA} = 0.65, x_B = 0.1108, x_T = 0.2208, x_{BA} = 0.0184 mol. fract.)										
1	30	760	18	2.8	2621.59	20	100	6	0.2	1408.87
2	38 (1/6)	760	9/4	17	1533.78	23	760	13	1.3	2008.85
3	22	760	5	3.2	2825.41	38 (1/6)	760	9/4	17	1528.09
4	25	110	10	1.1	402.88	22	760	5	3.2	2817.44
					∑*Q* = 7383.66					**∑*Q* = 7763.25**
The original composition of the mixture is **4.5** (x_{EA} = 0.85, x_B = 0.048, x_T = 0.094, x_{BA} = 0.008 mol. fract.)										
1	30	760	18	2.6	2907.61	18	100	5	0.2	1376.49
2	40 (1/9.5)	760	11/5	50	1883.38	24	760	13	1.4	2339.91
3	24	760	5	4.9	5077.87	40 (1/9.5)	760	11/5	50	1887.00
4	25	110	10	1.1	171.47	24	760	5	4.9	5075.90
					∑*Q* = 10040.33					**∑*Q* = 10679.30**

Note: the separating agent is phenol.

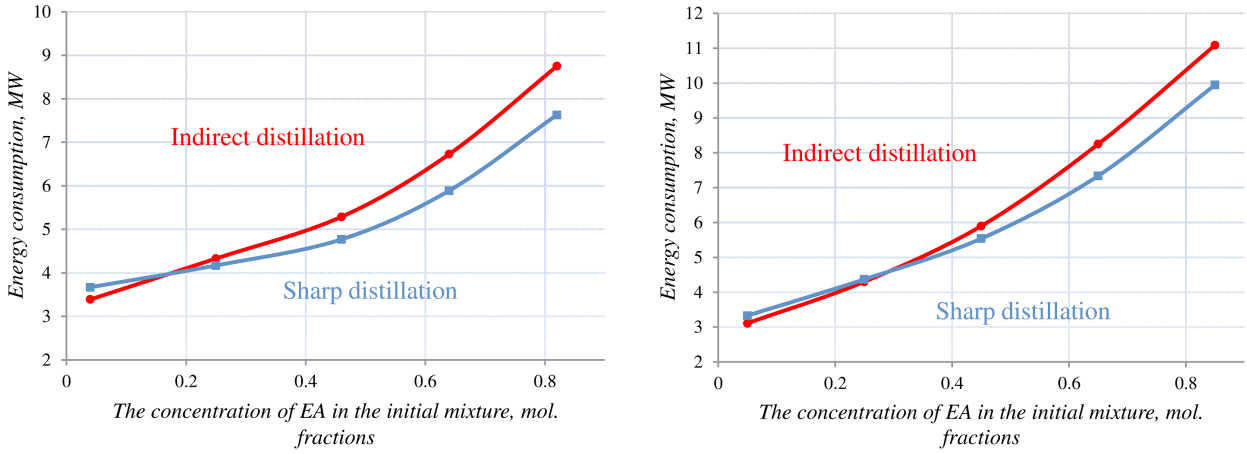

Fig. 3. Dependence of the energy consumption of the ethyl acetate–benzene–toluene–butyl acetate mixture separation flowsheets on the content of ethyl acetate (EA) in the initial mixture:
(a) secant 1 (compositions **1.1**–**1.5**); (b) secant 2 (compositions **2.1**–**2.5**).

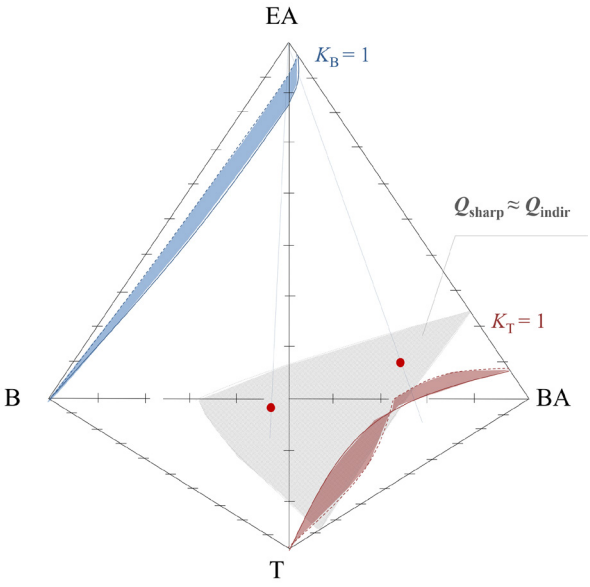

Fig. 4. Areas of energy advantage of the separation flowsheet based on the sharp distillation (above $Q_{sharp} \approx Q_{indir}$ surface) and indirect distillation (below $Q_{sharp} \approx Q_{indir}$ surface).

of the energy consumption dependences of the schemes on the content of ethyl acetate in the original mixture: for secant 1, x_{EA} = 0.17 mol. fractions; for secant 2, x_{EA} = 0.29 mol. fractions. Figure 4 shows a qualitative border (the surface is highlighted by hatching), where the energy consumptions of the considered separation schemes are almost identical.

The area of energy advantage of the flowsheet shown in Fig. 2a is located above the surface $Q_{sharp} \approx Q_{indir}$ diagram, and in Fig. 2b, it is located below $Q_{sharp} \approx Q_{indir}$ surface.

Acetone–toluene–butyl acetate–o-xylene system

For the separation of this mixture, five flowsheets of different structures are considered: the first column implements the direct (Figs. 5a, 5b), indirect (Figs. 5c, 5d), or sharp (Fig. 5e) distillation mode. The flowsheets in Figs. 5a and 5b and in Figs. 5c and 5d differ in the use of the direct and indirect distillation modes for the separation of the ternary mixture of toluene–butyl acetate–*o*-xylene (acetone–toluene–butyl acetate).

Preliminary calculations have shown that when separating toluene from a mixture of butyl acetate–*o*-xylene, it is impossible to achieve the required quality of toluene, even at a pressure of 50 mm Hg. This is because the volatility of toluene, in comparison with that of butyl acetate, in a ternary mixture is lower than that in a binary one.

The results of the simulation of the distillation process (parameters of the columns and energy consumption) for the other flowsheets are shown in Table 6.

The results obtained show that for the A–T–BA–*o*-X system, the use of sharp distillation for the separation of the original mixture is uneconomical (energy consumption is 20–30% higher compared to those for other separation modes).

CONCLUSIONS

If the original composition of a quaternary non-ideal zeotropic mixture, *i*–*j*–*k*–*l* ($T_i^0 < T_j^0 < T_k^0 < T_l^0$), belongs to a region for which the ratio, $K_i > 1$, $K_j > 1$, $K_k < 1$, $K_l < 1$, is observed, then we can recommend pre-fractionation

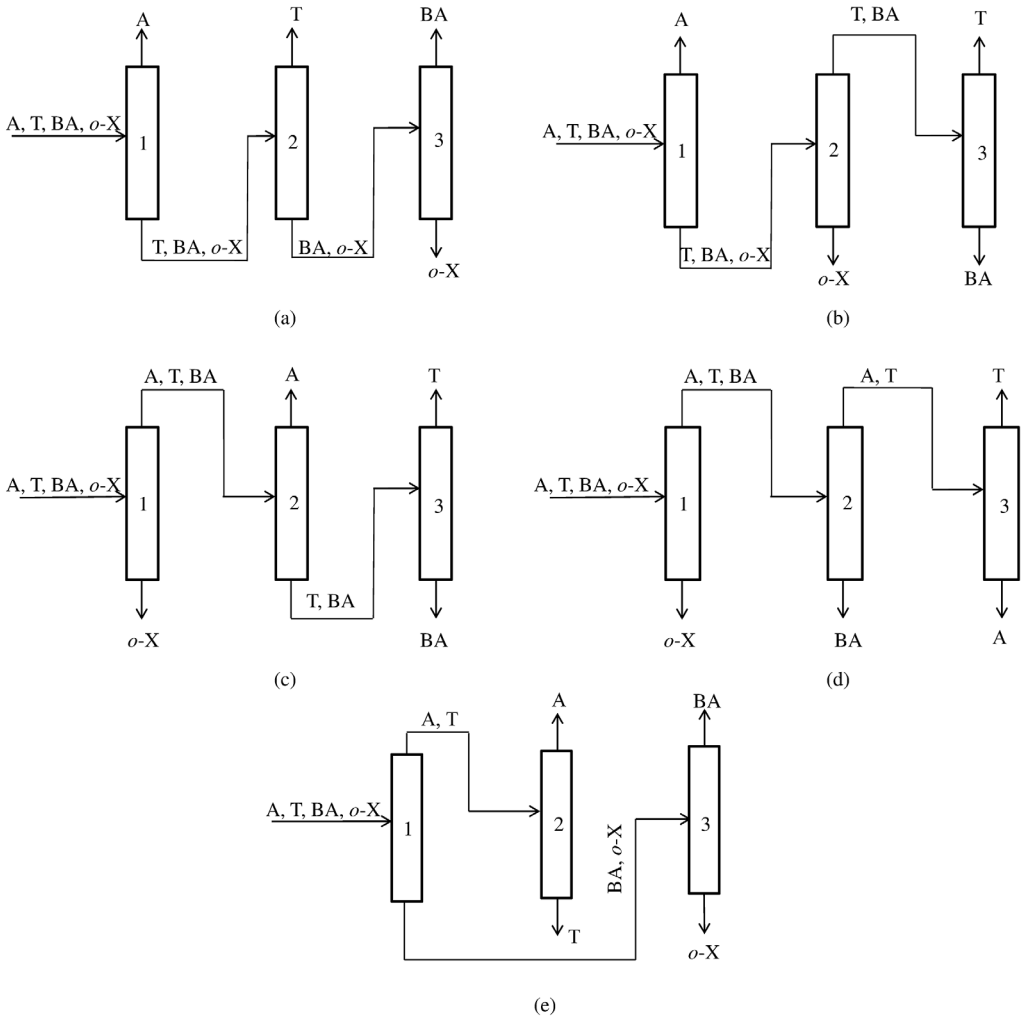

Fig. 5. Flowsheets of the separation of the mixture: acetone (A)–toluene (T)–butyl acetate (BA)–*o*-xylene (*o*-X), based on the direct (a)–(b), indirect (c)–(d) and sharp (e) distillation modes.

Table 6. Parameters of the columns work of the separation flowsheets shown in Fig. 5

Column	NTS	*P*	FS	*R*	*Q*, kW	NTS	*P*	FS	*R*	*Q*, kW
The original composition of x_A = 0.25, x_T = 0.25, x_{BA} = 0.25, $x_{o\text{-}X}$ = 0.25 mol. fract.										
Direct distillation (Fig. 5b)						Sharp distillation (Fig. 5e)				
1	20	760	11	0.6	491.3	48	760	16	4.6	2832.3
2	33	760	16	2.3	1687.3	24	760	18	0.7	388.6
3	36	110	12	4.4	1397.2	40	760	24	4.8	1476.6
					$\sum Q$ = 3575.8					**$\sum Q$ = 4697.5**
Indirect distillation (Fig. 5c)						Indirect distillation (Fig. 5d)				
1	36	760	17	1.2	1868.0	36	760	17	1.2	1868.0
2	25	760	11	0.6	424.5	33	110	10	1.2	1208.5
3	40	110	13	4.5	1422.9	28	760	22	0.6	368.0
					$\sum Q$ = 3715.4					**$\sum Q$ = 3444.5**

Table 6. Continued

Column	NTS	*P*	FS	*R*	*Q*, kW	NTS	*P*	FS	*R*	*Q*, kW
The original composition of x_A = 0.04, x_T = 0.32, x_{BA} = 0.32, $x_{o\text{-}X}$ = 0.32 mol. fract.										
Direct distillation (Fig. 5b)						Sharp distillation (Fig. 5e)				
1	20	760	9	3.6	213.7	80	760	24	8	3260.0
2	33	760	16	2.2	2090.1	24	760	13	1.6	110.5
3	36	110	12	3.1	1363.6	40	760	25	4.8	1889.5
					$\sum Q$ = 3667.4					**$\sum Q$ = 5260.0**
Indirect distillation (Fig. 5c)						Indirect distillation (Fig. 5d)				
1	38	760	18	1.8	2056.5	38	760	18	1.8	2056.5
2	25	760	11	3.2	177.3	33	110	11	2.7	1469.6
3	36	110	12	3.1	1363.7	24	760	13	1.6	110.6
					$\sum Q$ = 3597.5					**$\sum Q$ = 3636.7**

for the first stage of separation. The region with the specified ratio of distribution coefficients will occupy a large part of the volume of the composition simplex if the system is characterized by the presence of components with similar volatilities for pairs *i*–*j* and/or *k*–*l*. When a mixture of compositions belonging to this area are separated, the use of sharp distillation will be more energy-efficient (up to 20% energy savings) than the use of direct and indirect distillation modes. The latter modes can become competitive when the point of the original composition is located near the unit *K*-surfaces or in a region with a different ratio of distribution coefficients. These patterns are illustrated using the ethyl acetate–benzene–toluene–butyl acetate system as an example.

If the relative volatility of a pair of components with average boiling points (*j*–*k*) is close to one, the region of compositions with the ratio of distribution coefficients, $K_i > 1$, $K_j > 1$, $K_k < 1$, $K_l < 1$, will be small; consequently, sharp distillation would be unsuitable for separating the mixture, which is confirmed using the example of the acetone–toluene–butyl acetate–*o*-xylene system.

Acknowledgments

The study was supported by the Russian Foundation for Basic Research, project No. 19-19-00620.

The authors declare no conflicts of interest.

REFERENCES

1. Zharov V.T., Serafimov L.A. *Fiziko-khimicheskie osnovy distillyatsii i rektifikatsii* (Physico-chemical principles of distillation and rectification. Leningrad: Khimiya; 1975. 240 p. (in Russ.).

2. Timofeev V.S., Serafimov L.A., Timoshenko A.V. *Printsipy tekhnologii osnovnogo organicheskogo i neftekhimicheskogo sinteza* (The principles of the technology of basic organic and petrochemical synthesis). Moscow: Vysshaya shkola; 2010. 408 p. (in Russ.). ISBN 978-5-06-006067-6

3. Frolkova A.K. *Razdelenie azeotropnykh smesei. Fiziko-khimicheskie osnovy i tekhnologicheskie priemy: monografiya* (Separation of azeotropic mixtures. Physico-chemical fundamentals and technological methods). Moscow: VLADOS; 2010. 192 p. (in Russ.).

4. Petlyuk F.B. Distillation Theory and Its Application to Optimal Design of Separation Units. Cambridge, UK: Cambridge University Press; 2004. https://doi.org/10.1017/CBO9780511547102

СПИСОК ЛИТЕРАТУРЫ

1. Жаров В.Т., Серафимов Л.А. Физико-химические основы дистилляции и ректификации. Л.: Химия; 1975. 240 с.

2. Тимофеев В.С., Серафимов Л.А., Тимошенко А.В. Принципы технологии основного органического и нефтехимического синтеза. М.: Высшая школа; 2010. 408 с. ISBN 978-5-06-006067-6

3. Фролкова А.К. Разделение азеотропных смесей. Физико-химические основы и технологические приемы: монография. М.: ВЛАДОС; 2010. 192 с.

4. Petlyuk F.B. Distillation Theory and Its Application to Optimal Design of Separation Units. Cambridge, UK: Cambridge University Press; 2004. https://doi.org/10.1017/CBO9780511547102

5. Green D.W., Southard M.Z. (Eds.). Approximate Multicomponent Distillation Methods. In: Perry's Chemical Engineers' Handbook. New York, USA: McGraw-Hill Education; 2019. Section 13. P. 25-28.

5. Green D.W., Southard M.Z. (Eds.). Approximate Multicomponent Distillation Methods. In: Perry's Chemical Engineers' Handbook. New York, USA: McGraw-Hill Education; 2019. Section 13. P. 25-28.

6. Mavletkulova P.O., Serafimov L.A., Danilov R.Yu. Comparative Analysis of Sharp Separation Regimes in the Distillation of Ternary Zeotropic Mixtures. *Theor. Found. Chem. Eng.* 2014;48(5):622-628. https://doi.org/10.1134/S0040579514050200

7. Serafimov L.A., Chelyuskina T.V., Mavletkulova P.O. Special Distillation Regime Involving an Infinite Reflux Ratio and an Infinite Number of Separation Stages. *Theor. Found. Chem. Eng.* 2014;48(1):48-54. https://doi.org/10.1134/S0040579514010138

8. Khalili-Garakani A., Ivakpour J., Kasiri N. Three-component Distillation Columns Sequencing: Including Configurations with Divided-wall Columns. *Iranian J. Oil Gas Sci. Technol.* 2016;5(2):66-83. https://dx.doi.org/10.22050/ijogst.2016.15799

9. Frolkova A.V., Peshekhontseva M.E., Gaganov I.S. Sharp separation for quatrenary mixtures. *Tonk. Khim. Tekhnol. = Fine Chem. Technol.* 2018;13(3):41-48 (in Russ.). https://doi.org/10.32362/24106593-2018-13-3-41-48

10. Kleymenova M.N., Komarova L.F., Lazutkina Y.S. Technology for Treatment of Solvents' Liquid Waste from Silicone Enamels Production. *Ekologiya i promyshlennost' Rossii = Ecology and Industry of Russia.* 2014;3:11-15 (in Russ.).

11. Il'ina E.S., Tarasova M.N., Lazutkina Yu.S. The study of the physicochemical properties of solvent components in the production of epoxy primers. In: Proc. 3rd Russian scientific and technical conference of students, postgraduates and young scientists "Science and Youth." Section "Chemical technologies." Subsection "Chemical engineering and engineering ecology." Barnaul: Polzunov Altai State Technical University; 2006. P. 27-28 (in Russ.).

12. Mato F., Bonilla D., Benito G. Liquid-vapor equilibrium of the *n*-heptane-isobutyl acetate, toluene-isobutyl acetate, and toluene-*n*-butyl acetate systems at 760 mmHg. *An. Quim.* 1991;87:660-663.

13. Carr A.D., Kropholler H.W. Vapor Liquid Equilibria at Atmospheric Pressure. Binary Systems of Ethyl Acetate-Benzene, Ethyl Acetate-Toluene, and Ethyl Acetate-*p*-Xylene. *J. Chem. Eng. Data.* 1962;7(1):26-28. https://doi.org/10.1021/je60012a007

14. Gupta B.S., Lee M.-J. Isobaric vapor-liquid equilibrium for binary systems of toluene + *o*-xylene, benzene + *o*-xylene, nonane + benzene and nonane + heptane at 101.3 kPa. *Fluid Phase Equilib.* 2013;352:86-92. https://doi.org/10.1016/j.fluid.2013.05.016

15. Kogan V.B. *Azeotropnaya i ekstraktivnaya rektifikatsiya* (Azeotropic and extractive distillation). Leningrad: Khimiya; 1971. 432 p. (in Russ.).

6. Mavletkulova P.O., Serafimov L.A., Danilov R.Yu. Comparative Analysis of Sharp Separation Regimes in the Distillation of Ternary Zeotropic Mixtures. *Theor. Found. Chem. Eng.* 2014;48(5):622-628. https://doi.org/10.1134/S0040579514050200

7. Serafimov L.A., Chelyuskina T.V., Mavletkulova P.O. Special Distillation Regime Involving an Infinite Reflux Ratio and an Infinite Number of Separation Stages. *Theor. Found. Chem. Eng.* 2014;48(1):48-54. https://doi.org/10.1134/S0040579514010138

8. Khalili-Garakani A., Ivakpour J., Kasiri N. Three-component Distillation Columns Sequencing: Including Configurations with Divided-wall Columns. *Iranian J. Oil Gas Sci. Technol.* 2016;5(2):66-83. https://dx.doi.org/10.22050/ijogst.2016.15799

9. Фролкова А.В., Пешехонцева М.Е., Гаганов И.С. Промежуточное заданное разделение при ректификации четырехкомпонентных смесей. *Тонкие химические технологии.* 2018;13(3):41-48. https://doi.org/10.32362/24106593-2018-13-3-41-48

10. Клейменова М.Н., Комарова Л.Ф., Лазуткина Ю.С. Технология переработки жидких отходов растворителей в производстве кремний органических эмалей. *Экология и промышленность России.* 2014;3:11-15.

11. Ильина Е.С., Тарасова М.Н., Лазуткина Ю.С. Изучение физико-химических свойств компонентов растворителей в производстве эпоксидных грунтовок. 3-я Всероссийская научно-техническая конференция студентов, аспирантов и молодых ученых «Наука и молодежь». Секция «Химические технологии». Подсекция «Химическая техника и инженерная экология». Алтайский государственный технический университет им. И.И. Ползунова. Барнаул: изд-во АлтГТУ; 2006. С. 27-28.

12. Mato F., Bonilla D., Benito G. Liquid-vapor equilibrium of the *n*-heptane-isobutyl acetate, toluene-isobutyl acetate, and toluene-*n*-butyl acetate systems at 760 mmHg. *An. Quim.* 1991;87:660-663.

13. Carr A.D., Kropholler H.W. Vapor Liquid Equilibria at Atmospheric Pressure. Binary Systems of Ethyl Acetate-Benzene, Ethyl Acetate-Toluene, and Ethyl Acetate-*p*-Xylene. *J. Chem. Eng. Data.* 1962;7(1):26-28. https://doi.org/10.1021/je60012a007

14. Gupta B.S., Lee M.-J. Isobaric vapor–liquid equilibrium for binary systems of toluene + *o*-xylene, benzene + *o*-xylene, nonane + benzene and nonane + heptane at 101.3 kPa. *Fluid Phase Equilib.* 2013;352:86-92. https://doi.org/10.1016/j.fluid.2013.05.016

15. Коган В.Б. Азеотропная и экстрактивная ректификация. 2 изд. Л.: Химия; 1971. 432 с.

About the authors:

Margarita Ye. Peshekhontseva, Student, Department of Chemistry and Technology of Basic Organic Synthesis, M.V. Lomonosov Institute of Fine Chemical Technologies, MIREA − Russian Technological University (86, Vernadskogo pr., Moscow, 119571, Russia). E-mail: peshekhontseva-m@mail.ru, https://orcid.org/0000-0002-9446-2462

Mark A. Maevskiy, Postgraduate Student, Department of Chemistry and Technology of Basic Organic Synthesis, M.V. Lomonosov Institute of Fine Chemical Technologies, MIREA − Russian Technological University (86, Vernadskogo pr., Moscow, 119571, Russia). E-mail: markhirurg@list.ru, https://orcid.org/0000-0002-7752-4115

Ivan S. Gaganov, Student, Department of Chemistry and Technology of Basic Organic Synthesis, M.V. Lomonosov Institute of Fine Chemical Technologies, MIREA − Russian Technological University (86, Vernadskogo pr., Moscow, 119571, Russia). E-mail: ivan.gaganov@yandex.ru. https://orcid.org/0000-0003-4837-2332

Anastasiya V. Frolkova, Cand. of Sci. (Engineering), Associate Professor, Department of Chemistry and Technology of Basic Organic Synthesis, M.V. Lomonosov Institute of Fine Chemical Technologies, MIREA − Russian Technological University (86, Vernadskogo pr., Moscow, 119571, Russia). E-mail: frolkova_nastya@mail.ru. https://orcid.org/0000-0001-5675-5777, ResearcherID N-4517-2014

Об авторах:

Пешехонцева Маргарита Евгеньевна, студентка кафедры химии и технологии основного органического синтеза Института тонких химических технологий им. М.В. Ломоносова ФГБОУ ВО «МИРЭА − Российский технологический университет» (119571, Россия, Москва, пр-т Вернадского, д. 86). E-mail: peshekhontseva-m@mail.ru. https://orcid.org/0000-0002-9446-2462

Маевский Марк Александрович, аспирант кафедры химии и технологии основного органического синтеза Института тонких химических технологий им. М.В. Ломоносова ФГБОУ ВО, «МИРЭА - Российский технологический университет» (119571, Россия, Москва пр-т. Вернадского, 86, Москва,). E-mail: markhirurg@list.ru. https://orcid.org/0000-0002-7752-4115

Гаганов Иван Сергеевич, студент кафедры химии и технологии основного органического синтеза Института тонких химических технологий им. М.В. Ломоносова ФГБОУ ВО «МИРЭА − Российский технологический университет» (119571, Россия, Москва, пр-т Вернадского, д. 86). E-mail: ivan.gaganov@yandex.ru. https://orcid.org/0000-0003-4837-2332

Фролкова Анастасия Валериевна, кандидат технических наук, доцент кафедры химии и технологии основного органического синтеза Института тонких химических технологий им. М.В. Ломоносова ФГБОУ ВО «МИРЭА − Российский технологический университет» (119571, Россия, Москва, пр-т Вернадского, д. 86). E-mail: frolkova_nastya@mail.ru. https://orcid.org/0000-0001-5675-5777, ResearcherID N-4517-2014

Submitted: January 10, 2020; Reviewed: January 27, 2020; Accepted: May 11, 2020.

Translated from Russian into English by N. Isaeva
Edited for English language and spelling by Enago, an editing brand of Crimson Interactive Inc.

ISSN 2686-7575 (Online)

https://doi.org/10.32362/2410-6593-2020-15-3-21-30

UDC 66.048.625

Comparison of extractive distillation flowsheets for methanol–tetrahydrofuran–water mixtures

Valentina M. Raeva[1,@], Alexey M. Dubrovsky[2]

[1]MIREA – Russian Technological University (M.V. Lomonosov Institute of Fine Chemical Technologies), Moscow, 119571 Russia
[2]MosFarma, Moscow, 125239 Russia
[@]Corresponding author, e-mail: raevalentina1@gmail.com

Objectives. *Synthesis and comparative analysis of the extractive distillation flowsheets for aqueous mixtures of solvents utilized in pharmaceutical industries using the example of a methanol–tetrahydrofuran–water system with various compositions. The ternary system contains two minimally boiling azeotropes that exist in a vapor–liquid phase equilibrium. To evaluate the selective effect of glycerol, the phase equilibria of the methanol–tetrahydrofuran–water and methanol–tetrahydrofuran–water–glycerol systems at 101.32 kPa were studied.*

Methods. *The calculations were carried out in the Aspen Plus V.9.0 software package. The vapor–liquid equilibria were simulated using the non-random two-liquid (NRTL) equation with the binary interaction parameters of the software package database. To account for the non-ideal behavior of the vapor phase, the Redlich–Kwong equation of state was used. The calculations of the extractive distillation schemes were carried out at 101.32 kPa.*

Results. *The conceptual flowsheets of extractive distillation are proposed. The flowsheets consist of three (schemes I–III) or four (scheme IV) distillation columns operating at atmospheric pressure. In schemes I and II, the extractive distillation of the mixtures is carried out with tetrahydrofuran isolation occurring in the distillate stream. Further separation in the schemes differs in the order of glycerol isolation: in the third column for scheme I (traditional extractive distillation complex) or in the second column for scheme II (two-column extractive distillation complex + methanol/water separation column). Scheme III caters to the complete dehydration of the basic ternary mixtures, followed by the extractive distillation of the azeotropic methanol–tetrahydrofuran system, also with glycerol. Scheme IV includes a preconcentration column (for the partial removal of water) and a traditional extractive distillation complex.*

Conclusions. *According to the criterion of least energy consumption for separation (the total load of the reboilers of distillation columns), scheme I (a traditional complex of extractive distillation) is recommended. Additionally, the energy expended for the separation of the basic equimolar mixture using glycerol as the extractive agent was compared with that expended using another selective agent: 1,2-ethanediol. Glycerol is an effective extractive agent because it reduces energy consumption, in comparison with 1,2-ethanediol, by more than 5%.*

Keywords: *extractive distillation, scheme, relative volatility, effective agent, methanol, tetrahydrofuran, water, glycerol.*

For citation: Raeva V.M., Dubrovsky A.M. Comparison of extractive distillation flowsheets for methanol–tetrahydrofuran–water mixtures. *Tonk. Khim. Tekhnol. = Fine Chem. Technol.* 2020;15(3):21-30. https://doi.org/10.32362/2410-6593-2020-15-3-21-30

Сравнение схем экстрактивной ректификации смесей метанол–тетрагидрофуран–вода

В.М. Раева[1,@], А.М. Дубровский[2]

[1]МИРЭА – Российский технологический университет (Институт тонких химических технологий имени М.В. Ломоносова), Москва, 119571 Россия
[2]ЗАО «МосФарма», Москва, 125239 Россия
[@]Автор для переписки, e-mail: raevalentina1@gmail.com

Цели. *Синтез и сравнительный анализ схем экстрактивной ректификации водных смесей растворителей фармацевтических производств на примере системы метанол–тетрагидрофуран–вода различного состава. Трехкомпонентная система содержит два минимально кипящих азеотропа, которые присутствуют в диапазоне существования парожидкостного равновесия. Для оценки селективного действия глицерина исследованы фазовые равновесия систем метанол–тетрагидрофуран–вода и метанол–тетрагидрофуран–вода–глицерин при 101.32 кПа.*
Методы. *Вычислительный эксперимент выполнен на платформе Aspen Plus V.9.0. Проведены расчеты фазовых равновесий по уравнению NRTL (Non-Random Two-Liquid) с параметрами бинарного взаимодействия базы данных программного комплекса. Для учета неидеального поведения паровой фазы использовали уравнение состояния Редлиха–Квонга. Расчеты схем экстрактивной ректификации проведены при 101.32 кПа.*
Результаты. *Предложены принципиальные технологические схемы разделения (I–IV), состоящие из трех (I–III) или четырех (IV) ректификационных колонн, работающих при атмосферном давлении. В схемах I, II проводилась экстрактивная ректификация базовых смесей с различным содержанием воды для выделения в дистиллатном потоке тетрагидрофурана. Дальнейшее разделение в схемах различалось очередностью выделения глицерина: в третьей колонне схемы I (традиционный трехколонный комплекс экстрактивной ректификации) или во второй колонне схемы II (двухколонный комплекс экстрактивной ректификации + колонна разделения метанола и воды). В схеме III предусмотрено полное обезвоживание базовых трехкомпонентных смесей с последующей экстрактивной ректификацией азеотропной системы метанол–тетрагидрофуран также с глицерином. Схема IV состоит из колонны концентрирования (частичного удаления воды) и традиционного комплекса экстрактивной ректификации.*
Выводы. *По критерию наименьших энергозатрат на разделение (суммарная нагрузка кипятильников ректификационных колонн) рекомендована схема I (традиционный комплекс экстрактивной ректификации). Дополнительно проведено сравнение энергозатрат схемы I при разделении смеси эквимолярного состава с другим селективным веществом – этиленгликолем, предложенным ранее в качестве агента. Глицерин является эффективным экстрактивным агентом, поскольку обеспечивает снижение энергозатрат более чем на 5%.*

Ключевые слова: *экстрактивная ректификация, схема, относительная летучесть, эффективный агент, метанол, тетрагидрофуран, вода, глицерин.*

Для цитирования: Раева В.М., Дубровский А.М. Сравнение схем экстрактивной ректификации смесей метанол–тетрагидрофуран–вода. *Тонкие химические технологии.* 2020;15(3):21-30. https://doi.org/10.32362/2410-6593-2020-15-3-21-30

INTRODUCTION

To separate ternary azeotropic mixtures containing water, special distillation methods including extractive distillation (ED) are used in industries [1–7]. The structures of schemes for the ED of different types of ternary systems are provided in [1, 8]. The task of synthesizing possible schemes for the ED process can be considered via two approaches: for a certain set of agents that differ in selective effect or for a specific agent, which uniquely determines the result of the ED when added to the basic mixture [9, 10].

It is known that the preliminary concentration of binary aqueous mixtures makes it possible to reduce the energy consumption of ED schemes [11–16]. In this regard, it is necessary to additionally evaluate the feasibility of the preliminary partial dehydration (concentration) of basic ternary mixtures.

In this study, ED schemes of methanol–tetrahydrofuran–water mixtures were considered. Their separation is of interest to the chemical industry [4, 17]. Glycerol was chosen as the separating agent since it is recommended for the ED of tetrahydrofuran–water mixtures [18–20], as well as for methanol–tetrahydrofuran–water mixtures [4, 21].

MATERIALS AND METHODS

The basic system contains two azeotropes (Fig. 1, Table 1). The properties of the substances required for the empirical selection of extractive agents are given in Table 2. Glycerol has the highest boiling point and vaporization enthalpy and does not form azeotropes with the substances to be separated.

The simulation of phase equilibria was carried out on the Aspen Plus V. 9.0 platform using the non-random two-liquid (NRTL) equation with the parameters of the software package database. The non-ideal behavior of the vapor phase was considered using the Redlich–Kwong equation of state.

The component relative volatility diagrams of the basic methanol (1)–tetrahydrofuran (2)–water (3) system are shown in Fig. 2. The relative volatilities for the azeotropic pairs were calculated according to the vapor–liquid equilibrium data.

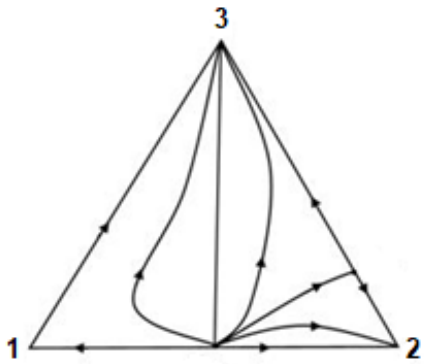

Fig. 1. Diagram of distillation lines in the methanol (1)−tetrahydrofuran (2)−water (3) system.

Table 1. Required properties of substances to be used as extractive agents

Substance	Normal boiling point, K	Vaporization molar enthalpy, kJ/mol
Methanol	337.85	37.6 ± 0.5
Tetrahydrofuran	339.15	32.0
Water	373.15	43.99
Glycerol	563.15	91.7 ± 0.9

Table 2. Calculated azeotropic data at 101.32 kPa

Azeotropic system	Composition, mol. fract.			Temperature, K
	x_1	x_2	x_3	
Methanol–tetrahydrofuran	0.4910	0.5090	–	332.90
Tetrahydrofuran–water	–	0.8304	0.1696	336.59

RESULTS AND DISCUSSION

The volatility of tetrahydrofuran relative to that of methanol (α_{21}) increases with increasing water content in the basic mixtures, i.e., water exerts an extractive effect (Fig. 2a). The volatility of tetrahydrofuran relative to that of water (α_{23}) also increases in the ternary mixtures (Fig. 2b).

For comparison, the compositions of the basic mixtures (x^0_F) with different water contents located on secant $x_1 : x_2 = 1 : 1$ were chosen (Fig. 3). The relative volatilities in the presence of different amounts of the agent (4) are given in Table 3. The selective effects of water and glycerol are unidirectional. The concentration of tetrahydrofuran in the distillate is

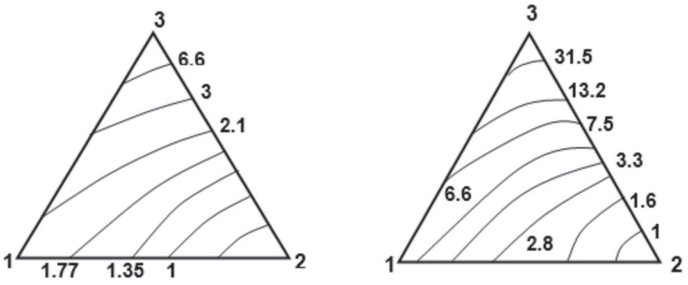

a b

Fig. 2. Diagrams of the relative volatilities of the components of the methanol (1)−tetrahydrofuran (2)−water (3) system at 101.32 kPa (a: α_{21}; b: α_{23}).

determined upon the ED of the basic mixtures. When separating basic mixtures with high water contents, a low concentration of the agent is required.

Notably, the glycerol amount had a different effect on the tetrahydrofuran volatility. For the basic compositions of $x^0_{F\text{-}I}$ and $x^0_{F\text{-}II}$, the values of α_{21} and α_{23} increased, and for the $x^0_{F\text{-}III}$ composition enriched with water, they decreased. In the latter case, it is important to accurately determine the smallest amount of the high-boiling point component, glycerol, which exerts sufficient extractive effect, since excessive consumption of the agent will result in a decrease in

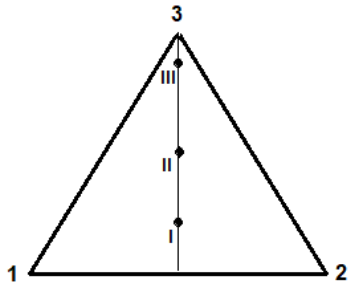

Fig. 3. Compositions (mol. fract.) of the basic methanol (1)−tetrahydrofuran (2)−water (3) mixture: I – $x^0_{F\text{-}I}$ (0.392; 0.408; 0.200); II – $x^0_{F\text{-}II}$ (0.333; 0.333; 0.334); III – $x^0_{F\text{-}III}$ (0.049; 0.051; 0.900).

glycerol selectivity and an increase in the load of the ED column reboiler.

The principal flowsheets of ED with glycerol are shown in Fig. 4. It is predicted that the azeotrope-forming component, tetrahydrofuran, will be obtained in the distillate of the ED column. Therefore, schemes I and II can be considered. Scheme I is traditional, with glycerol regeneration occurring in the last column. In scheme II, the heavy agent is separated in the second column.

Scheme III caters to the complete dehydration of the basic mixtures, after which the ED of the methanol–tetrahydrofuran mixture is carried out with glycerol. Thus, the ternary mixtures located to the left of secant $x_1 : x_2 = 1 : 1$ can be separated (Fig. 3).

Table 3. Relative volatilities of the components of the methanol (1)−tetrahydrofuran (2)−water (3)−glycerol (A) system at 101.32 kPa

$F_A : F^*$	x_A	$x^0_{F\text{-}I}$		$x^0_{F\text{-}II}$		$x^0_{F\text{-}III}$	
		α_{21}	α_{23}	α_{21}	α_{23}	α_{21}	α_{23}
0 : 1	0	1.33	2.90	1.64	4.05	6.64	35.8
0.1 : 1	0.09	1.51	4.56	1.77	5.63	5.00	27.5
0.25 : 1	0.2	1.70	7.04	1.91	7.86	3.89	21.7
0.5 : 1	0.333	1.90	10.6	2.06	10.9	3.10	17.75
0.75 : 1	0.429	2.02	13.2	2.13	13.2	2.72	16.0
1 : 1	0.5	2.09	15.1	2.17	14.8	2.49	15.1
1.5 : 1	0.6	2.15	17.5	2.19	16.85	2.22	14.2

*F_A : F is the ratio of glycerol to the basic mixture (kmol).

In scheme IV, the preliminary concentration (partial dehydration) of the basic mixtures occurs, i.e., the separation option is intermediate for schemes I and III.

The operating parameters of the distillation columns were optimized by minimizing the reboiler duty in the distillation columns (Q) for the distillate composition of 0.995 mol. fraction. The variable parameter was the reflux number (R). At the first stage, we determined the lowest efficiencies for the ED columns (N is the number of theoretical stages) and the amount of glycerol (F_A), at which the required quality of product flows is achieved. The input levels of the feed flow (F) and agent (A) for the extractive columns were varied in the calculation experiment, i.e., the effect of the magnitude and position of the extractive part on the separation results was evaluated.

The calculation conditions comply with the data of [19]. Glycerol was introduced at a temperature (T) of 333.15 K to reduce the viscosity, and the feed flows of the columns were introduced at temperatures close to the boiling points of the separated mixtures.

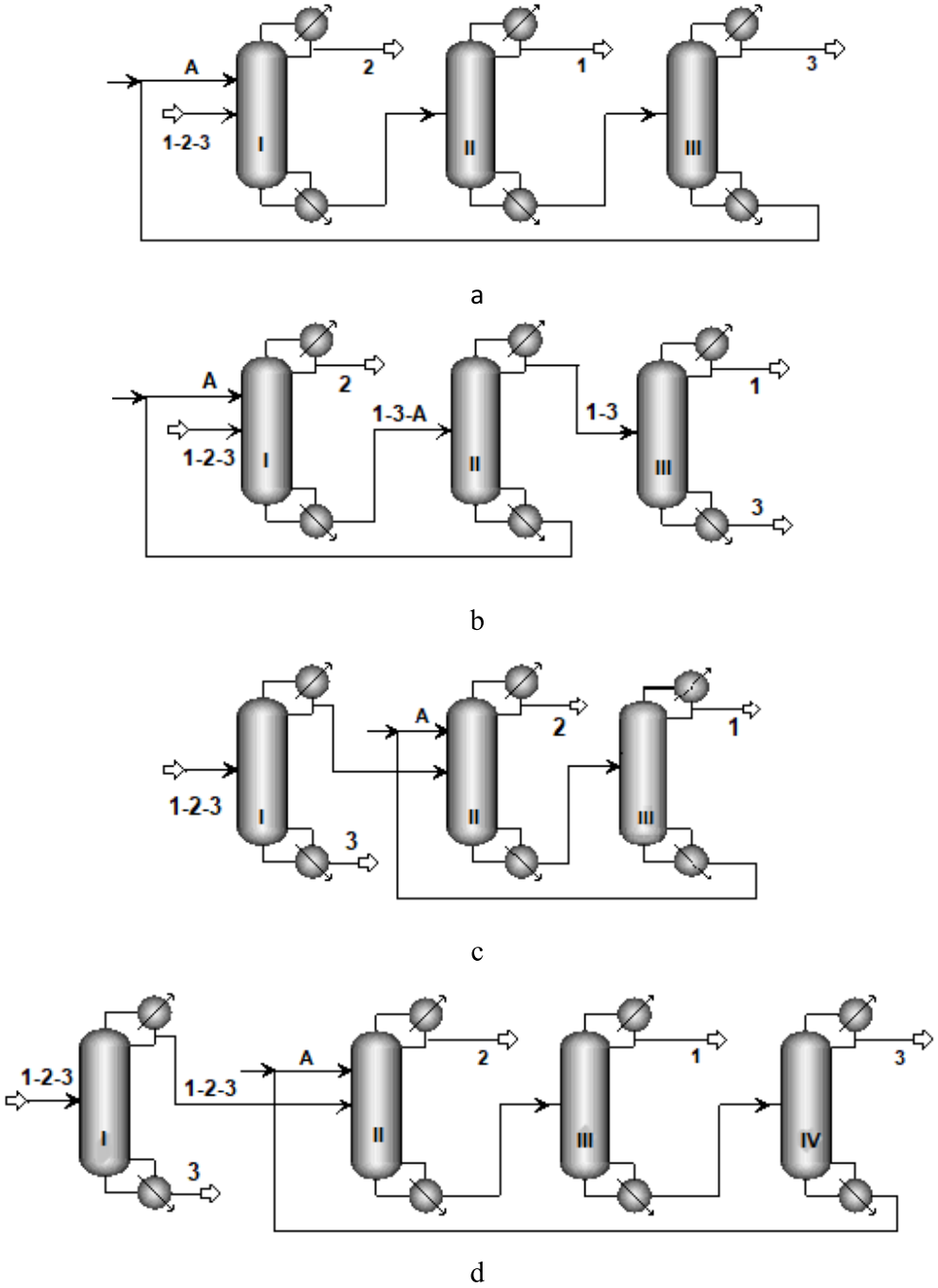

Fig. 4. Principal flowsheets for the extractive distillation of methanol (1)−tetrahydrofuran (2)−water (3) with glycerol (A) (a: scheme I; b: scheme II; c: scheme III; d: scheme IV).

The pressure of all the columns was 101.32 kPa. Tables 4–8 show the parameters of the distillate (D) and bottom (W) flows. The compositions are given sequentially for methanol, tetrahydrofuran, and water in mole fractions; the amount of flows (in kmol/h) and the reboiler duty (in kW) are determined. The flow rate (F) of the basic mixtures was 100 kmol/h.

Scheme I

The calculations were performed for the compositions of the basic methanol(1)–tetrahydrofuran (2)–water (3) mixtures: $x^0_{F\text{-}I}$ (0.392; 0.408; 0.2); $x^0_{F\text{-}II}$ (0.333; 0.333; 0.334); and $x^0_{F\text{-}III}$ (0.049; 0.051; 0.9).

An increase in the water content in the mixtures affects the energy consumption of the distillation columns of scheme I in different ways (Tables 4 and 5). The ED (column I) and methanol-isolation (column II) processes induced a significant reduction in the reboiler loads, while energy consumption, on the contrary, increased with glycerol recovery. The maximum contribution to the energy consumption was made by the methanol-isolation column (compositions $x^0_{F\text{-}I}$ and $x^0_{F\text{-}II}$) and by the agent recovery column ($x^0_{F\text{-}III}$). The total reboiler duty (kW) of the traditional ED flowsheet decreases in the following series: 4778 (x_I: 0.2 mol. fraction water);

Table 4. Static parameters and separation results for the extractive distillation column (schemes I and II)

Basic mixture	N, N_A/N_F	F_A	R	x_D	T_D	x_W	T_W	Q
$x^0_{F\text{-}I}$	30, 2/21	150	1.82	0.0050 0.9950 0 0	338.6	0.1865 0.0007 0.0956 0.7172	375.0	1753
$x^0_{F\text{-}II}$	40, 2/23	110	1.52	0.0050 0.9950 0 0	339.0	0.1855 0.0009 0.1920 0.6215	372.6	1158
$x^0_{F\text{-}III}$	30, 2/21	25	4	0.0039 0.9961 0 0	339.1	0.0407 0 0.7508 0.2085	374.2	442

Table 5. Static parameters and separation results for columns II and III (scheme I)

Basic mixture	No. col.	N, N_F	R	x_D	T_D	x_W	T_W	Q
$x^0_{F\text{-}I}$	II	25, 10	1.27	0.9951 0.0039 0.0010 0	337.3	0.0002 0 0.1174 0.8824	485.0	1966
	III	25, 10	0.12	0.0019 0 0.9950 0.0031	421.5	0 0 0.0004 0.9996	560.1	1059
$x^0_{F\text{-}II}$	II	30, 14	2.97	0.9950 0.0050 0 0	337.6	0 0 0.2361 0.7639	443.0	1783
	III	10, 5	0.2	0 0 0.9999 0.0001	383.5	0 0 0.0001 0.9999	560.8	1310
$x^0_{F\text{-}III}$	II	25, 10	5.66	0 0.9950 0.0050 0	337.5	0 0 0.7825 0.2175	381.0	338
	III	10, 5	0.05	0 0 0.9997 0.0003	390.1	0 0 0.0001 0.9999	560.4	1441

4251 (x_{II}: 0.334 mol. fraction water); 2221 (x_{III}: 0.9 mol. fraction water).

Scheme II

In the traditional ED flowsheet, direct separation is realized. Methanol is isolated in column I, and the agent is regenerated in the last column (direct separation) (Fig. 4). The recovery of the high-boiling point agent in column II, according to the second indirect separation, may reduce the total power consumption of the scheme. In scheme II, with indirect separation, glycerol is the first output; thereafter, the distillation of the zeotropic water–methanol mixture is carried out (indirect separation).

Scheme II was calculated for the basic mixtures of compositions $x^0_{F\text{-}I}$ (0.392; 0.408; 0.200) and $x^0_{F\text{-}III}$ (0.049; 0.051; 0.900). The calculation results for the ED column are given in Table 4; for columns II and III, the results are given in Table 6.

The maximum contribution to the total energy consumption is made by the agent recovery column (column II). The separation of glycerol from the mixtures with methanol and water is more energy-intensive than the recovery of the agent from the aqueous mixtures (column III, scheme I). Scheme II cannot be recommended for separating the basic methanol–tetrahydrofuran–water mixture with a low water content.

The positive effect of diluting the basic mixtures with water in all the columns was noted (Tables 4 and 6). The total energy consumption of scheme II is considerably low: $x^0_{F\text{-}I}$ = 5098, $x^0_{F\text{-}III}$ = 2545 kW.

Scheme III

This separation option caters to the complete dehydration of the basic mixture (Fig. 4). The calculations were carried out only for the equimolar composition, $x^0_{F\text{-}II}$, (Table 7).

Water increases the relative volatility of tetrahydrofuran. Therefore, its removal from mixtures leads to an increase in the glycerol amount: 150 kmol/h of agent per 66.6 kmol/h of methanol—tetrahydrofuran mixture (the ratio is 2.25 : 1) is required. However, in case of the ED of the ternary mixture of the same composition, this ratio is 110 kmol/h per 100 kmol/h (1.1 : 1). The total reboiler duty is 5325 kW, which is 20% higher than that in the case of scheme I (4251 kW). The complete dehydration of the basic mixture is impractical.

Thus, glycerol is not an effective agent for scheme III. The concept of an effective agent considers both the selectivity (effect on the vapor–liquid equilibrium) and the process parameters (reboiler duty) [22]. The energy consumption of the selective glycerol recovery column accounts for more than 51% of the total energy consumption of scheme II. If a more selective agent, with a lower boiling point and enthalpy of vaporization than glycerol (Table 1), which affects the energy consumption of the distillation columns, is used, scheme III may be viable. Such an agent may be, for example, dimethyl sulfoxide [9].

Scheme IV

The calculations of scheme IV were not performed. It can be considered as an intermediate separation option for schemes I and III, without preliminary concentration (partial removal of water) and with complete dehydration of the basic mixtures (Fig. 4). The preliminary concentration is impractical, because it will be inevitably accompanied by an

Table 6. Static parameters and separation results for columns II and III (scheme II)

Basic mixture	No. col.	N, N_F	R	x_D	T_D	x_W	T_W	Q
$x^0_{F\text{-}I}$	II	25, 10	0.5	0.6598 0.0024 0.3378 0	351.8	0 0 0.0003 0.9997	560.7	2813
	III	25, 10	2	0.995 0.0039 0.0011 0	337.7	0.0046 0 0.9954 0	372.3	532
$x^0_{F\text{-}III}$	II	25, 10	0.5	0.0514 0 0.9486 0	371.9	0 0 0.0001 0.9999	560.9	1921
	III	10, 5	2.53	0.9950 0 0.0050 0	337.9	0.0004 0 0.9996 0	373.1	182

Table 7. Static parameters and separation results for scheme III (basic mixture, $x^0_{F\text{-}II}$)

No. col.	N, N_A/N_F	F_A	R	x_D	T_D	x_W	T_W	Q
I	30, 15	–	1.89	0.4995 0.5 0.0005 0	332.9	0.0010 0.9990 0 0	373	1773
II	40, 2/26	150	1.87	0.0035 0.9965 0 0	339.1	0.1795 0.0006 0.0002 0.8197	379.3	810
III	20, 11	–	2	0.9964 0.0036 0 0	339.0	0.0008 0 0.0002 0.9990	374.2	2742

Table 8. Comparison of 1,2-ethanediol and glycerol for scheme I (basic mixture, $x^0_{F\text{-}II}$)

Agent	F_A	No. col.	N, N_A/N_F	R	Product purity		Q
					x	T	
1,2-Ethanediol*	400	I II III	45, 5/30 30,12 13, 6	2.2 1.9 2	$x_2 = 0.9980$ $x_1 = 0.9973$ $x_3 = 0.9991$ $x_A = 0.9999$	339.04 337.65 373.04 470.21	1928 1548 1628
Glycerol	120	I II III	40, 2/23 30, 14 10/5	1.88 3.96 0.1	$x_2 = 0.9980$ $x_1 = 0.9980$ $x_3 = 0.9999$ $x_A = 0.9999$	339.09 337.65 375.31 560.84	1306 2167 1360

* Data [19]: 1,2-ethanediol; in this study: glycerol.

increase in energy consumption due to the introduction of an additional column. A comparison of the energy consumptions for the separation in schemes I and III (Tables 4, 5, and 7) shows that, as the water content in the basic mixtures decreases, glycerol consumption increases due to a decrease in the relative volatility of tetrahydrofuran.

The ED of methanol–tetrahydrofuran–water mixtures can also be carried out using ethylene glycol as the extractive agent [4, 19]. For a correct comparison with the results of [19], additional calculations of scheme I were performed to obtain purer products (Table 8).

Using glycerol reduces the energy consumption of the complex by 5.6%. Therefore, glycerol is an effective agent for scheme I.

CONCLUSIONS

For the separation of mixtures of methanol, tetrahydrofuran, and water, a traditional ED scheme with glycerol is recommended. If it is necessary to separate mixtures with low water contents, a binary agent (water–glycerol) can be introduced into the ED column. In addition to increasing selectivity, this will ensure a decrease in the temperature in the ED column and, consequently, a decrease in the energy consumed for separation in the scheme.

Acknowledgments

This study was supported by a grant from the Russian Science Foundation (project No. 19-19-00620).

The authors declare no conflicts of interest.

REFERENCES

1. Frolkova A.K. Razdelenie azeotropnykh smesei. *Fiziko-khimicheskie osnovy i tekhnologicheskie priemy* (Separation of azeotropic mixtures. Physicochemical fundamentals and technological methods). Moscow: VLADOS; 2010. 192 p. (in Russ.). ISBN 978-5-691-01743-8

2. Hilal N., Yousef G., Langston P. The reduction of extractive agent in extractive distillation and auto-extractive distillation. *Chem. Eng. Process.* 2002;41(8):673-679. https://doi.org/10.1016/S0255-2701(01)00187-8

3. Rodriguez-Donis I., Gerbaud V., Arias-Baretto A., Joulia X. Heterogeneous batch distillation processes for waste solvent recovery in pharmaceutical industry. *Comp. Aid. Chem. Eng.* 2009;27:1119-1124. https://doi.org/10.1016/S1570-7946(09)70407-9

4. Raeva V. M., Sazonova A. Yu. Separation of ternary mixtures by extractive distillation with 1,2-ethandiol and glycerol. *Chem. Eng. Res. Design.* 2015;99:125-131. https://doi.org/10.1016/j.cherd.2015.04.032

5. Zhao L., Lyu X., Wang W., Shan J., Qiu T. Comparison of heterogeneous azeotropic distillation and extractive distillation methods for ternary azeotrope ethanol/toluene/water separation. *Comp. Chem. Eng.* 2017;100:27-37. https://doi.org/10.1016/j.compchemeng.2017.02.007

6. Zhao T., Li M., Yang J., Ma K., Zhu Z., Wang Y. Separation of acetone/isopropyl ether/water ternary mixture via hybrid azeotropic-extractive distillation. *Chem. Eng. Trans.* 2017;61:661-666. https://doi.org/10.3303/CET1761108

7. Wang Y., Bu G., Geng X., Zhu Z., Cui P., Liao Z. Design optimization and operating pressure effects in the separation of acetonitrile/methanol/water mixture by ternary extractive distillation. *J. Clean. Prod.* 2019;218:212-224. https://doi.org/10.1016/j.jclepro.2019.01.324

8. Ivanova L. V., Timoshenko A. V., Timofeev V. S. Synthesis of flowsheets for extractive distillation of azeotropic mixtures. *Theor. Found. Chem. Eng.* 2005;39(1):16-23. https://doi.org/10.1007/s11236-005-0022-7

9. Raeva V.M., Sukhov D.I. Selection of extractive agents for the separation of chloroform – methanol – tetrahydrofuran mixture. *Tonk. Khim. Tekhnol. = Fine Chem. Technol.* 2018;13(3):30-40 (in Russ.). https://doi.org/10.32362/24106593-2018-13-3-30-40

10. Raeva V.M., Gromova O.V. Separation of water – formic acid – acetic acid mixtures in the presence of sulfolane. *Tonk. Khim. Tekhnol. = Fine Chem. Technol.* 2019;14(4):24-32. https://doi.org/10.32362/2410-6593-2019-14-4-24-32

11. Taylor M., Wankat P.C. Increasing the energy efficiency of extractive distillation. *Separ. Sci. Tech.* 2005;39(1):1-7 (in Russ.). https://doi.org/10.1081/SS-120027398

12. Liang K., Li W., Luo H., Xia M., Xu C. Energy-efficient extractive distillation process by combining preconcentration column and entrainer recovery column. *Ind. Eng. Chem. Res.* 2014;53(17):7121-7131. https://doi.org/10.1021/ie5002372

13. An Y., Li W., Ye Li Y., Huang S., Ma J., Shen C., Xu C. Design/optimization of energy-saving extractive distillation process by combining preconcentration column and extractive distillation column. *Chem. Eng. Sci.* 2015;135:166-178. https://doi.org/10.1016/j.ces.2015.05.003

14. Han D., Chen Y. Combining the preconcentration column and recovery column for the extractive distillation of ethanol dehydration with low transition temperature mixtures as entrainers. *Chem. Eng. Proc. - Proc. Intens.* 2018;131:203-214. https://doi.org/10.1016/j.cep.2018.08.005

СПИСОК ЛИТЕРАТУРЫ

1. Фролкова А.К. Разделение азеотропных смесей. Физико-химические основы и технологические приемы. М.: ВЛАДОС; 2010. 192 с. ISBN 978-5-691-01743-8

2. Hilal N., Yousef G., Langston P. The reduction of extractive agent in extractive distillation and auto-extractive distillation. *Chem. Eng. Process.* 2002;41(8):673-679. https://doi.org/10.1016/S0255-2701(01)00187-8

3. Rodriguez-Donis I., Gerbaud V., Arias-Baretto A., Joulia X. Heterogeneous batch distillation processes for waste solvent recovery in pharmaceutical industry. *Comp. Aid. Chem. Eng.* 2009;27:1119-1124. https://doi.org/10.1016/S1570-7946(09)70407-9

4. Raeva V.M., Sazonova A.Yu. Separation of ternary mixtures by extractive distillation with 1,2-ethandiol and glycerol. *Chem. Eng. Res. Design*. 2015;99:125-131. https://doi.org/10.1016/j.cherd.2015.04.032

5. Zhao L., Lyu X., Wang W., Shan J., Qiu T. Comparison of heterogeneous azeotropic distillation and extractive distillation methods for ternary azeotrope ethanol/toluene/water separation. *Comp. Chem. Eng.* 2017;100:27-37. https://doi.org/10.1016/j.compchemeng.2017.02.007

6. Zhao T., Li M., Yang J., Ma K., Zhu Z., Wang Y. Separation of acetone/isopropyl ether/water ternary mixture via hybrid azeotropic-extractive distillation. *Chem. Eng. Trans.* 2017;61:661-666. https://doi.org/10.3303/CET1761108

7. Wang Y., Bu G., Geng X., Zhu Z., Cui P., Liao Z. Design optimization and operating pressure effects in the separation of acetonitrile/methanol/water mixture by ternary extractive distillation. *J. Clean. Prod.* 2019;218:212-224. https://doi.org/10.1016/j.jclepro.2019.01.324

8. Ivanova L.V., Timoshenko A.V., Timofeev V.S. Synthesis of flowsheets for extractive distillation of azeotropic mixtures. *Theor. Found. Chem. Eng.* 2005;39(1):16-23. https://doi.org/10.1007/s11236-005-0022-7

9. Раева В.М., Сухов Д.И. Выбор экстрактивных агентов для разделения смеси хлороформ – метанол – тетрагидрофуран. *Тонкие химические технологии.* 2018;13(3):30-40. https://doi.org/10.32362/24106593-2018-13-3-30-40

10. Раева В.М., Громова О.В. Разделение смеси вода – муравьиная кислота – уксусная кислота в присутствии сульфолана. *Тонкие химические технологии.* 2019;14(4):24-32. https://doi.org/10.32362/2410-6593-2019-14-4-24-32

11. Taylor M., Wankat P.C. Increasing the energy efficiency of extractive distillation. *Separ. Sci. Tech.* 2005;39(1):1-17. https://doi.org/10.1081/SS-120027398

12. Liang K., Li W., Luo H., Xia M., Xu C. Energy-efficient extractive distillation process by combining preconcentration column and entrainer recovery column. *Ind. Eng. Chem. Res.* 2014;53(17):7121-7131. https://doi.org/10.1021/ie5002372

13. An Y., Li W., Ye Li Y., Huang S., Ma J., Shen C., Xu C. Design/optimization of energy-saving extractive distillation process by combining preconcentration column and extractive distillation column. *Chem. Eng. Sci.* 2015;135:166-178. https://doi.org/10.1016/j.ces.2015.05.003

14. Han D., Chen Y. Combining the preconcentration column and recovery column for the extractive distillation of ethanol dehydration with low transition temperature mixtures as entrainers. *Chem. Eng. Proc. - Proc. Intens.* 2018;131:203-214. https://doi.org/10.1016/j.cep.2018.08.005

15. You X., Gu J., Gerbaud V., Peng C., Liu H. Optimization of pre-concentration, entrainer recycle and pressure selection for the extractive distillation of acetonitrile − water with ethylene glycol. *Chem. Eng. Sci.* 2018;177:354-368. https://doi.org/10.1016/j.ces.2017.11.035

16. Lara-Montaño O.D., Melendez-Hernández P.A., Bautista-Ortega R.Y., Hernández S., Delgado L.A. Hernández-Escoto H. Experimental study on the extractive distillation based purification of second-generation bioethanol. *Chem. Eng. Trans.* 2019;74:67-72. https://doi.org/10.3303/CET1974012

17. Sazonova A.Yu., Raeva V.M., Frolkova A.K. The method of separation of solvent mixtures methanol - tetrahydrofuran - acetonitrile - water - pyridine: RF Pat. 2599132. Publ. 10.10.2016. (in Russ). Available from: https://findpatent.ru/patent/259/2599132.html

18. Gómez P., Gil I. Simulation of the tetrahydrofuran dehydration process by extractive distillation in Aspen Plus. *Lat. Am. Appl. Res.* 2009;39(4):275-284.

19. Fan Z., Zhang X., Cai W., Wang F. Design and control of extraction distillation for dehydration of tetrahydrofuran. *Chem. Eng. Technol.* 2013;36(5):829-839. https://doi.org/10.1002/ceat.201200611

20. Sazonova A.Y., Raeva V.M., Frolkova A.K. Design of extractive distillation process with mixed entrainer. *Chem. Pap.* 2016;70(5):594-601. https://doi.org/10.1515/chempap-2015-0247

21. Sazonova A.Yu. The choice of separating agents and patterns of extractive distillation of mixtures of organic products: Dis. Cand. Sci. Moscow; 2015. 225 p. (in Russ.)

22. Raeva V.M., Kapranova A.S. Comparison efficiency of extractive agents at the separation of mixture acetone - methanol. *Khim. Prom. Segodnya = Chem. Ind. Today.* 2015;3:33-46 (in Russ.).

15. You X., Gu J., Gerbaud V., Peng C., Liu H. Optimization of pre-concentration, entrainer recycle and pressure selection for the extractive distillation of acetonitrile − water with ethylene glycol. *Chem. Eng. Sci.* 2018;177:354-368. https://doi.org/10.1016/j.ces.2017.11.035

16. Lara-Montaño O.D., Melendez-Hernández P.A., Bautista-Ortega R.Y., Hernández S., Delgado L.A. Hernández-Escoto H. Experimental study on the extractive distillation based purification of second-generation bioethanol. *Chem. Eng. Trans.* 2019;74:67-72. https://doi.org/10.3303/CET1974012

17. Сазонова А.Ю., Раева В.М., Фролкова А.К. Способ разделения смесей растворителей метанол - тетрагидрофуран - ацетонитрил - вода - пиридин: РФ Пат. 2599132. Заявка № 2015125849/05; заявл. 30.06.2015; опубл. 10.10.2016. URL: https://findpatent.ru/patent/259/2599132.html

18. Gómez P., Gil I. Simulation of the tetrahydrofuran dehydration process by extractive distillation in Aspen Plus. *Lat. Am. Appl. Res.* 2009;39(4):275-284.

19. Fan Z., Zhang X., Cai W., Wang F. Design and control of extraction distillation for dehydration of tetrahydrofuran. *Chem. Eng. Technol.* 2013;36(5):829-839. https://doi.org/10.1002/ceat.201200611

20. Sazonova A.Y., Raeva V.M., Frolkova A.K. Design of extractive distillation process with mixed entrainer. *Chem. Pap.* 2016;70(5):594-601. https://doi.org/10.1515/chempap-2015-0247

21. Сазонова А.Ю. Выбор разделяющих агентов и закономерности экстрактивной ректификации смесей органических продуктов: дис. … канд. техн. наук. М., МИТХТ, 2015. 225 с.

22. Раева В.М., Капранова А.С. Сравнение эффективности экстрактивных агентов при разделении смеси ацетон - метанол. *Хим. пром. сегодня.* 2015;3:33-46.

About authors:

Valentina M. Raeva, Cand. of Sci. (Engineering), Associate Professor, Department of Chemistry and Technology of Basic Organic Synthesis, M.V. Lomonosov Institute of Fine Chemical Technologies, MIREA − Russian Technological University (86, Vernadskogo pr., Moscow, 119571, Russia). E-mail: raevalentina1@gmail.com. Scopus Author ID 6602836975, Researcher ID C-8812-2014, https://orcid.org/0000-0002-5664-4409

Alexey M. Dubrovsky, Engineer, MosFarma JSC (1, Farmatsevticheskii proezd, Moscow, 125239, Russia). Researcher ID Y-7320-2019, https://orcid.org/0000-0002-1178-6104

Об авторах:

Раева Валентина Михайловна, кандидат технических наук, доцент кафедры химии и технологии основного органического синтеза Института тонких химических технологий им. М.В. Ломоносова ФГБОУ ВО «МИРЭА − Российский технологический университет» (119571, Россия, Москва, пр-т Вернадского, д. 86). E-mail: raevalentina1@gmail.com. Scopus Author ID 6602836975, Researcher ID C-8812-2014, https://orcid.org/0000-0002-5664-4409

Дубровский Алексей Михайлович, инженер, ЗАО «МосФарма» (125239, Москва, Фармацевтический проезд, д. 1). Researcher ID Y-7320-2019, https://orcid.org/0000-0002-1178-6104

Submitted: November 16, 2019; Reviewed: April 29, 2020; Accepted: May 11, 2020.

Translated from Russian into English by M. Povorin
Edited for English language and spelling by Enago, an editing brand of Crimson Interactive Inc.

ISSN 2686-7575 (Online)

https://doi.org/10.32362/2410-6593-2020-15-3-31-38

UDC 54.062

An effective method for preparation of high purity oligohexamethylene guanidine salts

Ivan S. Ivanov[1,2,@], Denis O. Shatalov[1,2], Stanislav A. Kedik[1,2], Igor P. Sedishev[1,2], Sergei V. Beliakov[1,2], Kirill N. Trachuk[1], Victoria V. Komarova[1]

[1]MIREA – Russian Technological University (M.V. Lomonosov Institute of Fine Chemical Technologies), Moscow, 119571 Russia
[2]Institute of Pharmaceutical Technologies, Moscow, 121353 Russia
[@]Corresponding author, e-mail: ivan.ivanov1994@gmail.com

Objectives. *Given that microorganisms can become resistant to certain groups of drugs and considering also their ability to form biofilms, the development of new drugs that are active against adapted microflora is required. This study focused on the development of a new method for the synthesis of a promising compound, the branched hydrosuccinate oligohexamethylene guanidine (OHMGsucc), with high purity that meets the standards of the 14th edition State Pharmacopeia of the Russian Federation (SPRF). Previously proposed methods have managed to isolate this product, which, however, complies with the requirements of the outdated SPRF. Therefore, the main aim of this study was to update the regulatory framework for the indicated OHMG salt for its further use in the pharmaceutical industry according to modern standards.*

Methods. *To control the residual impurities of hexamethylenediamine (HMDA) and guanidine hydrochloride (GHC), high-performance liquid chromatography (HPLC) was applied using a Thermo Scientific Dionex UltiMate 3000 chromatograph, and the chromatographic signals of the test solution with those of a standard sample solution obtained by a previously published conventional method were compared.*

Results. *The HPLC experimental data indicated a significant difference in the quantitative content of HMDA and GHC observed for the new and older preparation method of the branched OHMGsucc, suggesting that the method disclosed in this article can be used to obtain highly pure OHMGsucc.*

Conclusions. *The specified compound was standardized with the parameter "related impurities" according to the current (14th) edition of the SPRF. The effectiveness and reproducibility of the proposed method was experimentally confirmed. In addition, a process diagram for the preparation of the indicated OHMG salt was prepared.*

Keywords: *biocide, antibacterial agent, purification, related impurities, oligohexamethylene guanidine salt, disinfectant.*

For citation: Ivanov I.S., Shatalov D.O., Kedik S.A., Sedishev I.P., Beliakov S.V., Trachuk K.N., Komarova V.V. An effective method for preparation of high purity oligohexamethylene guanidine salts. *Tonk. Khim. Tekhnol. = Fine Chem. Technol.* 2020;15(3):31-38. https://doi.org/10.32362/2410-6593-2020-15-3-31-38

Способ получения соли олигогексаметиленгуанидина высокой степени чистоты

И.С. Иванов[1,2,@], Д.О. Шаталов[1,2], С.А. Кедик[1,2], И.П. Седишев[1,2], С.В. Беляков[1,2], К.Н. Трачук[1], В.В. Комарова[1]

[1]МИРЭА – Российский технологический университет (Институт тонких химических технологий имени М.В. Ломоносова), Москва, 119571 Россия
[2]АО «Институт фармацевтических технологий», Москва, 121353 Россия
[@]Автор для переписки, e-mail: ivan.ivanov1994@gmail.com

Цели. *На фоне приобретения микроорганизмами резистентности к определенным группам лекарственных средств, а также способностей образовывать биопленки, требуются новые препараты, активные против адаптированной микрофлоры. Статья посвящена изысканию способа получения перспективного соединения – разветвленного гидросукцината олигогексаметиленгуанидина с высокой степенью чистоты, соответствующей нормам Государственной Фармакопеи 14 издания. Так как предложенные ранее методы позволяли получить продукт, удовлетворяющий требованиям устаревшей Государственной Фармакопеи, то основной целью являлась актуализация нормативной базы в отношении указанной соли олигогексаметиленгуанидина для ее дальнейшего применения в фармацевтической отрасли согласно современным стандартам.*
Методы. *Для контроля примесных соединений – гексаметилендиамина и гуанидина гидрохлорида применяли высокоэффективную жидкостную хроматографию, которую проводили на хроматографе Thermo Scientific Dionex UltiMate 3000 методом внешнего стандарта.*
Результаты. *На основании экспериментальных данных, полученных с помощью высокоэффективной жидкостной хроматографии, отображена разница в количественном содержании остаточных примесей в составе субстанции разветвленного гидросукцината олигогексаметиленгуанидина, полученной двумя разными способами. Отмечено, что способ, предложенный авторами настоящей статьи, позволяет снизить их содержание по сравнению с конвенциональным методом.*
Выводы. *Согласно представленным данным проведена стандартизация указанного соединения по параметру «Родственные примеси» в соответствии с актуальным на данный момент изданием Государственной Фармакопеи. Вследствие того, что эффективность предложенного метода экспериментально подтвердилась, на заключительном этапе работы была составлена технологическая схема получения указанной соли олигогексаметиленгуанидина.*

Ключевые слова: *биоцид, антибактериальный агент, очистка, родственные примеси, соль олигогексаметиленгуанидина, дезинфектант*

Для цитирования: Ivanov I.S., Shatalov D.O., Kedik S.A., Sedishev I.P., Beliakov S.V., Trachuk K.N., Komarova V.V. An effective method for preparation of high purity oligohexamethylene guanidine salts. *Tonk. Khim. Tekhnol. = Fine Chem. Technol.* 2020;15(3):31-38. https://doi.org/10.32362/2410-6593-2020-15-3-31-38

INTRODUCTION

Infectious diseases are one of the most common human pathologies in the modern world. At the beginning of the last century, the fight against this group of diseases was remarkably successful. However, an outbreak of various epidemics is currently being recorded worldwide [1], which is mainly associated with the tendency of microorganisms to form biofilms and their increasing resistance to various drugs [2]. In this regard, there is a need to develop new pharmaceutical agents with a wide spectrum of antimicrobial activity that could serve as a basis for the development of effective drugs against the highly resistant pathogenic microflora. Oligohexamethylene guanidines (OHMG), which are synthetic derivatives of the nitrogenous base guanidine, are an example of such pharmaceutical substances. Oligoguanidines are a class of polymeric biocides that consist of repeating units of the macromolecular chain of a positively charged guanidine moiety and exhibit antimicrobial, antiviral, sporicidal, fungicidal, insecticidal, pesticidal, and algicidal activity. In

addition, they can be used against aerobic and anaerobic microflora [3], while they can also destroy the biofilms formed by pathogenic microflora [4]. It should be noted that the biocidal properties of the OHMG derivatives are significantly determined by their positive charge.

The mechanism of action of the OHMG derivatives is activated after protonation of a guanidine molecule, as shown in Scheme 1, which leads to the uniform distribution of the positive charge throughout the molecule. These polycations are then adsorbed on the cell membrane of the pathogen, which is negatively charged due to the phosphate groups. This, in turn, hinders the respiration and metabolite transfer processes through the bacterial cell wall, while the oligoguanidine macromolecules penetrate into the cell, causing irreversible damage to the cytoplasmic membrane and nucleotide structure, which ultimately leads to cell death (Fig. 1).

Furthermore, the positive charge of the OHMG derivatives enables them to act as organic bases or form salts with various inorganic or organic acids such as hydrochlorides, hydrocyrates, hydrosalicylates, hydrosuccinates, etc. Especially the properties of the branched oligohexamethylene guanidine hydrochloride salt (OHMG-HC) have been earlier established [5, 6], indicating its low toxicity and antibacterial activity against various bacteria and fungi [7]. Therefore, it has been used as an active base for dental gels [8] or for sprays to treat diseases of the oral cavity [9]. Another promising OHMG salt is the branched oligohexamethylene guanidine hydrosuccinate (OHMGsucc), which exhibits modified activity. A study conducted with a compound related to OHMG showed that the succinic acid salt is similar to the hydrochloric acid salt in the spectrum of antimicrobial activities; however, succinate significantly exceeds the hydrochloride in the disintegrating effect on the formed biofilms of the microorganism *P. aeruginosa* [10]. This is the modified activity of this compound. The branched OHMGsucc can be used for the development of various drugs, thus creating new possibilities in the medical field to combat bacterial diseases. This salt has already been synthesized with purity [11] that complied with the earlier (12th) edition of the State Pharmacopeia of the Russian Federation (SPRF). In this study, we aimed to develop a new preparation method of this compound with high purity and adapt its characteristics to the requirements of the current 14th edition of the SPRF.

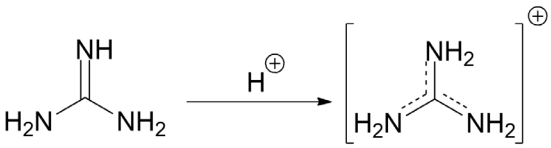

Scheme 1. Protonation of a guanidine molecule.

MATERIALS AND METHODS

Oligo(imnocarbonimidoylimino-1,6-hexanediyl) hydrochloride was obtained from the *Institute of Pharmaceutical Technologies* (Russia). Chloroform (GOST 20015-88), potassium hydroxide (GOST 24363-80), and succinic acid (GOST 6341-75) were obtained from *CHIMMED* (Russia). Ethyl alcohol (95%) was purchased

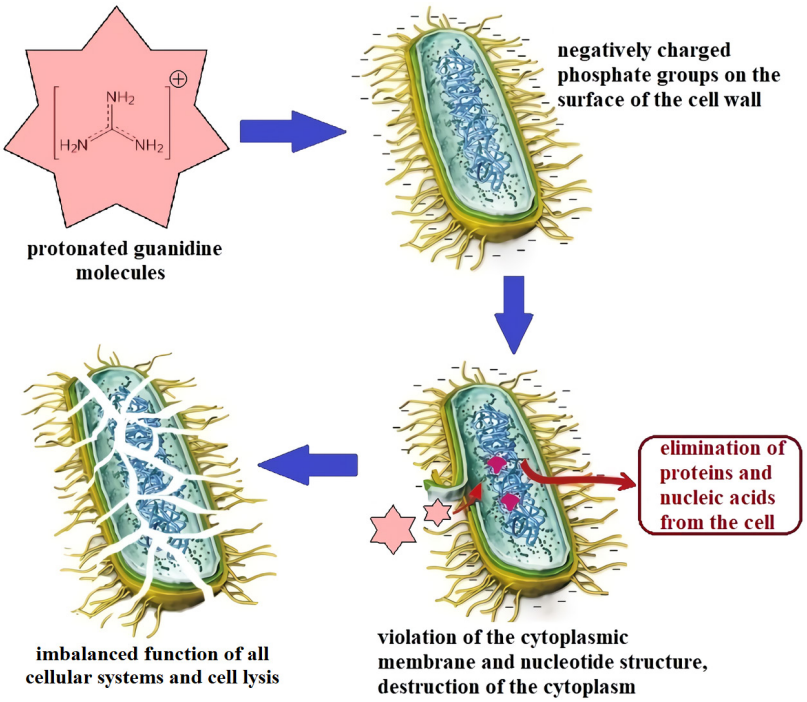

Fig. 1. Effect of OHMG on a bacterial cell.

from *Flora Kavkaza* (Russia), hexamethylenediamine (1,6-diaminohexane) from *Acros Organics* (Belgium), and guanidine hydrochloride from *Sigma-Aldrich* (USA).

The OHMGsucc samples were obtained using a conventional (Method 1) and a novel (Method 2) method, as described below.

Method 1. The conventional synthetic methodology has been in detail described in ref. [11], where carbon dioxide was used to fully saturate the solution for the preparation of the OHMG base.

Method 2. For the preparation of the base, a solution of potassium hydroxide (60 ml of 5-M KOH solution) was prepared in ethyl alcohol, followed by the addition of technical OHMG-HC (1 eq. per 1–4 eq. of solution). The resulting mixture was then added upon stirring to 1 volume part of an aqueous solution (40–60%) of OHMG-HC and the mixture was allowed to stand for about 16 h, until the phases separated. Afterward, 1–3 eq. of potassium hydroxide per 1 eq. of OHMG-HC were added to the phase with the highest OHMG base content. The resulting mixture was stirred for 3–4 h and then was allowed to stand for 16 h until phase separation. A portion of succinic acid was subsequently added to the phase with the highest OHMG base content until the precipitation stopped. The precipitate was separated by filtration, the filtrate was evaporated, and the dry residue of OHMGsucc was dissolved in 1 mass part of water. Ethyl alcohol and chloroform in a 2 : 1 ratio were then added to the aqueous solution, followed by stirring for 1 h. After phase separation, the lower phase, which contained the purified OHMGsucc, was collected and evaporated to afford the desired analogue as a solid salt. Its content in impurities, i.e., hexamethylenediamine (HMDA) and guanidine hydrochloride (GHC), was determined by high-performance liquid chromatography (HPLC) using a Thermo Scientific Dionex UltiMate 3000 chromatograph (USA), and the chromatographic peaks of the test solution were compared with those of the standard sample solution obtained by the conventional Method 1.

RESULTS AND DISCUSSION

In this study, it was expected that the application of Method 2 will provide better results and overcome the significant disadvantages of the previously developed Method 1 [11]. In order to confirm the effectiveness of the proposed method, the OHMGsucc salt was synthesized both by the conventional method and the currently described method, which has not been previously used in practice. Thus, a comparative analysis of the amount of residual impurities contained in the OHMGsucc salt was performed. More specifically, the chromatograms of HMDA (Fig. 2) and GHC (Fig. 3) were recorded to identify the effectiveness of the proposed method (Method 2) compared to the conventional process (Method 1). As observed in Figs. 2 and 3, irrespective of the applied method, the peaks of HMDA and GHC could be detected at retention time ranges of 14.0–15.0 and 4.0–4.5 min, respectively. However, it is clear that

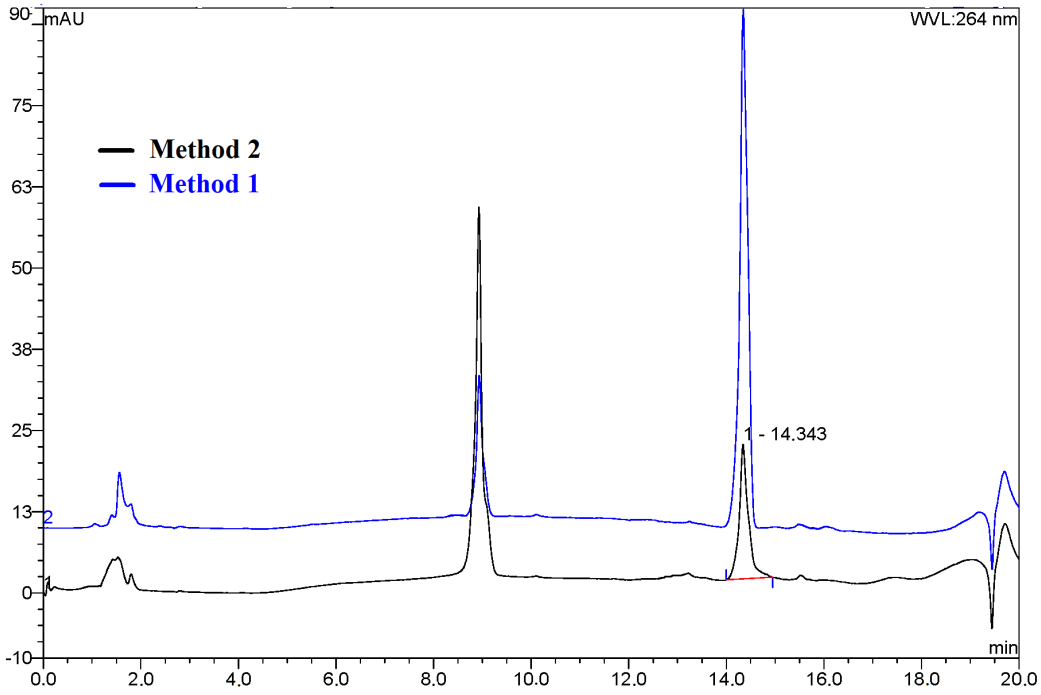

Fig. 2. Chromatogram of the quantitative content of HMDA in OHMGsucc samples purified by Methods 1 and 2.

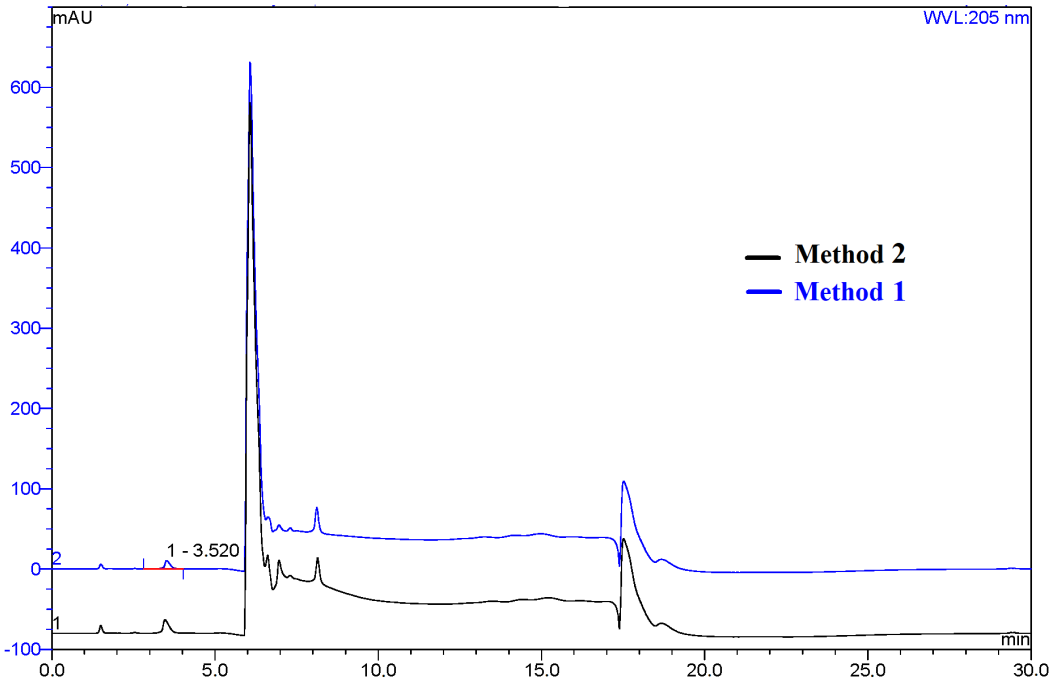

Fig. 3. Chromatogram of the quantitative GHC content in OHMGsucc samples purified by Methods 1 and 2.

Method 2 was more efficient than Method 1, as the respective HPLC peaks of the residual impurities were lower in both cases.

Furthermore, to confirm the reproducibility of the results, each purification process was performed in triplicate, resulting in six batches. It is clear from the data in table that the results of both methods were reproducible, while the higher efficiency of Method 2 in purifying OHMGsucc compared to that of Method 1 was again indicated by the lower mol % values of the residual impurities.

A process diagram of the proposed method was also created, which shows in detail all the necessary steps required for the implementation of Method 2 and the acquisition of high purity OHMGsucc (Fig. 4). This scheme clearly demonstrates the simplicity of the proposed technology for obtaining compounds of high purity.

Content of HMDA and GHC impurities obtained after purification of OHMGsucc with Methods 1 and 2.

Batch	Method	HMDA, mol %	GHC, mol %
1.1	Method 1 according to ref. [10]	0.076	0.18
1.2		0.071	0.17
1.3		0.077	0.16
2.1	Method 2	0.048	0.14
2.2		0.049	0.14
2.3		0.046	0.15

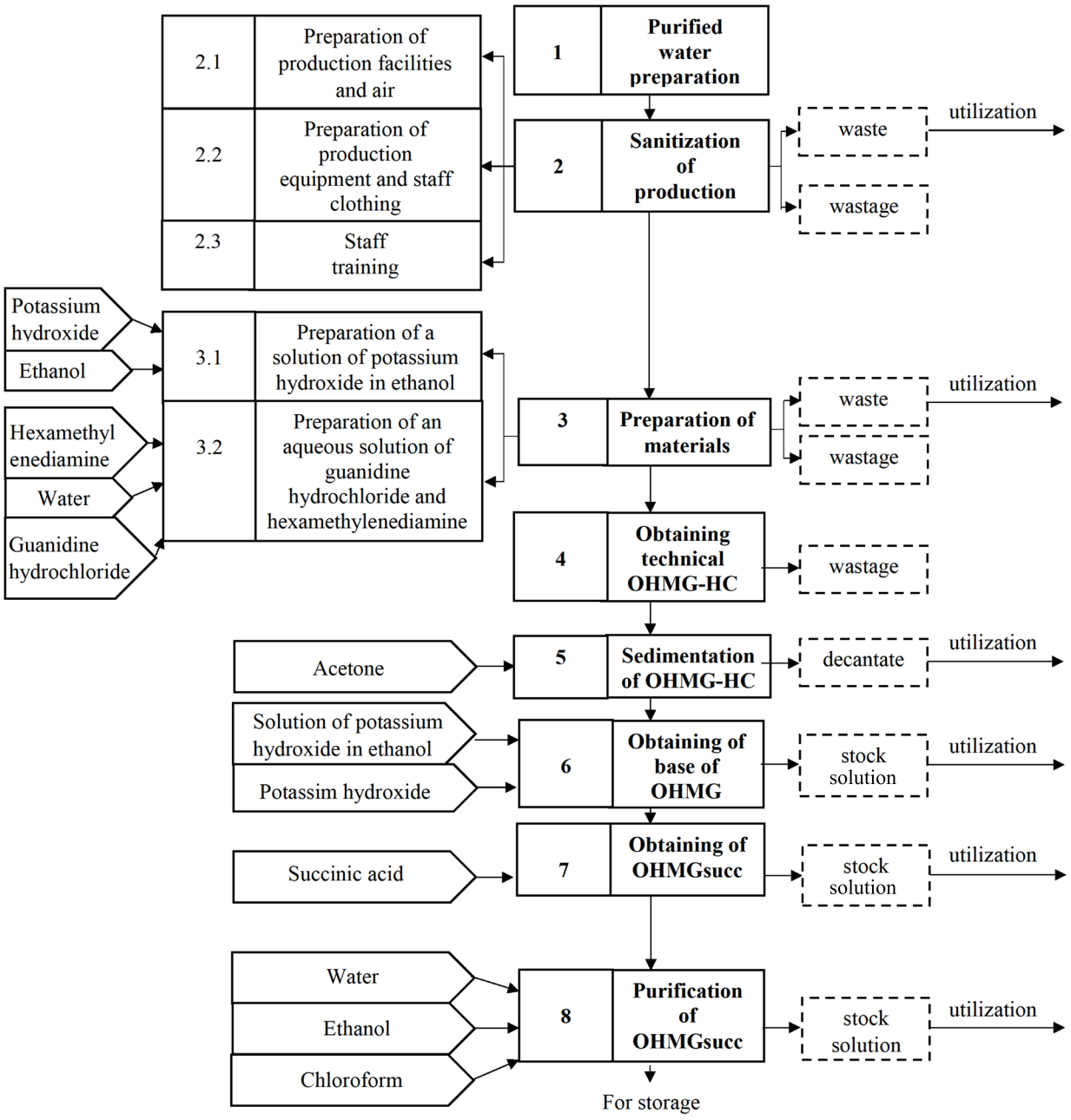

Fig. 4. Process diagram of Method 2 for the preparation and isolation of high purity OHMGsucc.

CONCLUSIONS

A new synthesis and purification method was developed to obtain the branched OHMGsucc salt with high purity by limiting the content of HMDA and GHC residues. The described method also proved to be more efficient than an earlier reported conventional method, as it can reduce the number of toxic impurities in the composition of the target compound, while complying with the requirements of the most recent 14th edition of the SPRF. Therefore, the suggested preparation process would be useful for the effective production of highly pure OHMGsucc, so that it can be further used in the pharmaceutical industry to develop new drugs that can fight the resistant harmful microorganisms.

The authors certify that they have no commercial or associative interest that represents a conflict of interest in connection with the manuscript.

REFERENCES

1. Dieleman J.L., Schneider M.T., Singh L., Sadat N., Birger M., Reynolds A., Templin T., Hamavid H., Chapin A., Murray C.J.L., Haakenstad A. Development assistance for health: past trends, associations, and the future of international financial flows for health. *The Lancet.* 2016;387(10037):2536-2544. https://doi.org/10.1016/S0140-6736(16)30168-4

2. Sadekuzzaman M., Yang S., Mizan M.F.R., Ha S.D. Current and recent advanced strategies for combating biofilms. *Compr. Rev. Food Sci. F.* 2015;14(4):491-509. https://doi.org/10.1111/1541-4337.12144

3. Vointseva I.I., Gembitsky P.A. *Poliguanidiny - dezinfektsionnye sredstva i polifunktsional'nye dobavki v kompozitsionnye materialy* (Polyguanidines - disinfectants and multifunctional additives in composite materials). Moscow: LKM-Press Publishing House, 2009; 304 p. (in Russ). ISBN 978-5-9901286-2-0

4. Zhou Z.X., Wei D.F., Guan Y., Zheng A.N., Zhong J.J. Damage of Escherichia coli membrane by bactericidal agent polyhexamethylene guanidine hydrochloride: Micrographic evidences. *J. Appl. Microbiol.* 2010;108(3):898-907. http://dx.doi.org/10.1111/j.1365-2672.2009.04482.x

5. Kedik S.A., Sedishev I.P., Panov A.V., Zhavoronok E.S., Kha K.A. Branched oligomers based on a guanidine derivative and a disinfectant containing them: RF Pat. 2443684. Publ. 27.02.2012 (in Russ.).

6. Rodlovskaya E.N., Izmailov B.A., Vasnev V.A., Mishina E.S. Protection of Textile Materials against Biodamage. Immobilization of Oligohexamethylene Guanidine Hydrochloride on the Surface of Fiber. *International Polymer Science and Technology.* 2013;40(6):39-42. https://doi.org/10.1177/0307174X1304000608

7. Garcia I.M., Rodrigues S.B., Leitune C.B., Collares F.M. Antibacterial, chemical and physical properties of sealants with polyhexamethylene guanidinehydrochloride. *Braz. Oral Res.* 2019;33(0). https://doi.org/10.1590/1807-3107bor-2019.vol33.0019

8. Shatalov D.O., Kedik S.A., Aidakova A.V., Krupenchenkova N.V., Kovalenko A.V., Ivanov I.S. Current approaches to the development of dosage forms for the treatment of diseases of the oral cavity (review). *Biofarmatsevticheskii Zhurnal = Russian Journal of Biopharmaceuticals.* 2019;11(4):15-28 (in Russ.).

9. Shatalov D.O., Kedik S.A., Panov A.V., Aidakova A.V., Ivanov I.S., Belyakov S.V. The combined drug in the form of a solution for obtaining a spray for the treatment of diseases of the oral cavity: RF Pat. 2687745. Publ. 16.05.2019 (in Russ.).

10. Kha K.A., Grammatikova N.E., Vasilenko I.A., Kedik S.A. Comparative *in vitro* Antibacterial Activity of Polyhexamethylene Guanidine Hydrochloride and Polyhexamethylene Guanidine Succinate. *Antibiotics and Chemotherapy*. 2013;(58):3-7. PMID: 24640138.

11. Kha K.A. Development of a technology for producing a substance of oligoghexamethylene guanidine hydrosuccinate and eye drops based on it: Dis. Cand. Sci. Farm. Moscow, 2013. 131 p. (in Russ.).

About the authors:

Ivan S. Ivanov, Postgraduate Student, Department of Biotechnology and Industrial Pharmacy, M.V. Lomonosov Institute of Fine Chemical Technologies, MIREA – Russian Technological University (86, Vernadskogo pr., Moscow, 119571, Russia); Researcher, Institute of Pharmaceutical Technologies JSC (86, Vernadskogo pr., Moscow, 119571, Russia). E-mail: ivan.ivanov1994@gmail.com. https://orcid.org/0000-0002-1346-7588

Denis O. Shatalov, Cand. of Sci. (Pharmaceutical Science), Associate Professor, Department of Biotechnology and Industrial Pharmacy, M.V. Lomonosov Institute of Fine Chemical Technologies, MIREA – Russian Technological University (86, Vernadskogo pr., Moscow, 119571, Russia); Researcher, Institute of Pharmaceutical Technologies JSC (86, Vernadskogo pr., Moscow, 119571, Russia). E-mail: shat-05@mail.ru. https://orcid.org/0000-0003-4510-1721

Stanislav A. Kedik, Dr. of Sci. (Engineering), Professor, Head of the Department of Biotechnology and Industrial Pharmacy, M.V. Lomonosov Institute of Fine Chemical Technologies, MIREA – Russian Technological University (86, Vernadskogo pr., Moscow 119571, Russia); General Director of the Institute of Pharmaceutical Technologies JSC (86, Vernadskogo pr., Moscow, 119571, Russia). E-mail: doctorkedik@yandex.ru. https://orcid.org/0000-0003-2610-8493

Igor P. Sedishev, Cand. of Sci. (Chemistry), Associate Professor, Department of Biotechnology and Industrial Pharmacy, M.V. Lomonosov Institute of Fine Chemical Technologies, MIREA – Russian Technological University (86, Vernadskogo pr., Moscow, 119571, Russia); Researcher, Institute of Pharmaceutical Technologies JSC (86, Vernadskogo pr., Moscow, 119571, Russia). E-mail: sedipa@list.ru, https://orcid.org/0000-0002-1348-4126

Sergei V. Beliakov, Postgraduate Student, Department of Biotechnology and Industrial Pharmacy, M.V. Lomonosov Institute of Fine Chemical Technologies, MIREA – Russian Technological University (86, Vernadskogo pr., Moscow, 119571, Russia); Researcher, Institute of Pharmaceutical Technologies JSC (86, Vernadskogo pr., Moscow, 119571, Russia). E-mail: s.v_belyakov@mail.ru. https://orcid.org/0000-0002-0957-4268

Kirill N. Trachuk, Student, Department of Biotechnology and Industrial Pharmacy, M.V. Lomonosov Institute of Fine Chemical Technologies, MIREA – Russian Technological University (86, Vernadskogo pr., Moscow, 119571, Russia). E-mail: trachuk98@yandex.ru. https://orcid.org/0000-0002-2061-0274

Victoria V. Komarova, Student, Department of Biotechnology and Industrial Pharmacy, M.V. Lomonosov Institute of Fine Chemical Technologies, MIREA – Russian Technological University (86, Vernadskogo pr., Moscow, 119571, Russia). E-mail: murzilka991@gmail.com. https://orcid.org/0000-0002-2701-3309

Сведения об авторах:

Иванов Иван Сергеевич, аспирант кафедры биотехнологии и промышленной фармации Института тонких химических технологий им. М.В. Ломоносова ФГБОУ ВО «МИРЭА – Российский технологический университет» (119571, Россия, Москва, пр-т Вернадского, д. 86); сотрудник АО «Институт фармацевтических технологий» (119571, Россия, Москва, пр-т Вернадского, д. 86). E-mail: ivan.ivanov1994@gmail.com. https://orcid.org/0000-0002-1346-7588

Шаталов Денис Олегович, кандидат фармацевтических наук, доцент кафедры биотехнологии и промышленной фармации Института тонких химических технологий им. М.В. Ломоносова ФГБОУ ВО «МИРЭА – Российский технологический университет» (119571, Россия, Москва, пр-т Вернадского, д. 86); сотрудник АО «Институт фармацевтических технологий» (119571, Россия, Москва, пр-т Вернадского, д. 86). E-mail: shat-05@mail.ru. https://orcid.org/0000-0003-4510-1721

Кедик Станислав Анатольевич, доктор технических наук, профессор, заведующий кафедрой биотехнологии и промышленной фармации Института тонких химических технологий им. М.В. Ломоносова ФГБОУ ВО «МИРЭА – Российский технологический университет» (119571, Россия, Москва, пр-т Вернадского, д. 86), генеральный директор АО «Институт фармацевтических технологий» (119571, Россия, Москва, пр-т Вернадского, д. 86). E-mail: doctorkedik@yandex.ru. https://orcid.org/0000-0003-2610-8493

Седишев Игорь Павлович, кандидат химических наук, доцент кафедры биотехнологии и промышленной фармации Института тонких химических технологий им. М.В. Ломоносова ФГБОУ ВО «МИРЭА – Российский технологический университет» (119571, Россия, Москва, пр-т Вернадского, д. 86); сотрудник АО «Институт фармацевтических технологий» (119571, Россия, Москва, пр-т Вернадского, д. 86). E-mail: sedipa@list.ru. https://orcid.org/0000-0002-1348-4126

Беляков Сергей Вячеславович, аспирант кафедры биотехнологии и промышленной фармации Института тонких химических технологий им. М.В. Ломоносова ФГБОУ ВО «МИРЭА – Российский технологический университет» (119571, Россия, Москва, пр-т Вернадского, д. 86); сотрудник АО «Институт фармацевтических технологий» (119571, Россия, Москва, пр-т Вернадского, д. 86). E-mail: s.v_belyakov@mail.ru. https://orcid.org/0000-0002-0957-4268

Трачук Кирилл Николаевич, студент кафедры биотехнологии и промышленной фармации Института тонких химических технологий им. М.В. Ломоносова ФГБОУ ВО «МИРЭА – Российский технологический университет» (119571, Россия, Москва, пр-т Вернадского, д. 86). E-mail: trachuk98@yandex.ru. https://orcid.org/0000-0002-2061-0274

Комарова Виктория Вадимовна, студент кафедры биотехнологии и промышленной фармации Института тонких химических технологий им. М.В. Ломоносова ФГБОУ ВО «МИРЭА – Российский технологический университет» (119571, Россия, Москва, пр-т Вернадского, д. 86). E-mail: murzilka991@gmail.com. https://orcid.org/0000-0002-2701-3309

Submitted: November 19, 2019; Reviewed: December 15, 2019; Accepted: May 28, 2020.

The text was submitted by the author in English.
Edited for English language and spelling by Enago, an editing brand of Crimson Interactive Inc.

ISSN 2686-7575 (Online)

https://doi.org/10.32362/2410-6593-2020-15-3-39-46

UDC 615.322

Flavonoid-profile determination for a hypoglycemic collection by high-performance liquid chromatography

Angelina M. Kutovaya[1], Valentina N. Davydova[1], Irina B. Perova[2], Konstantin I. Eller[2,@]

[1]All-Russian Scientific Research Institute of Medicinal and Aromatic Plants (VILAR), Moscow, 117216 Russia
[2]Federal Research Center of Nutrition, Biotechnology and Food Safety, Moscow, 109240 Russia
[@]Corresponding author, e-mail: ellki42@yandex.ru

Objectives. *Herbal hypoglycemic drugs complement the conventional approach to the treatment of type-2 diabetes based on the use of synthetic prescription drugs. However, their scientifically based application and standardization are limited due to inadequate and often outdated information on their chemical composition. Accordingly, we have developed a hypoglycemic collection (HGC) consisting of common bean pods (Phaseolus vulgaris L.), bilberry shoots (Vaccinium myrtillus L.), galega herb (Gallega officinalis L.), common knotgrass herb (Polygonum aviculare L.), burdock roots (Arctium lappa L.), and cinnamon rose hips (Rosa cinnamomea L.). According to a number of researchers, the antidiabetic properties of these herbs are largely due to the presence of polyphenolic compounds, especially flavonoids. The aim of this study was to determine the profile of flavonoids in the HGC and in its total dry extract (TDE).*

Methods. *The study was performed by reverse-phase high-performance liquid chromatography with diode array and mass spectrometric detection.*

Results. *Nine individual flavonol glycosides—derivatives of myricetin, quercetin, kaempferol and kaempferide—were identified in the HGC and the TDE. The main flavonol glycosides in the studied objects were robinin and kaempferol-3-glucuronide, the contents of which in the HGC were 2.09 and 2.22 mg/g, in the TDE 4.85 and 3.84 mg/g, respectively. The other flavonol glycosides were determined in the HGC and its TDE at significantly lower concentrations.*

Conclusions. *The method developed in the study can be used to standardize HGCs and estimate their pharmacological activities.*

Keywords: *flavonoids, hypoglycemic collection, total dry extract, high-performance liquid chromatography, diode array detection, mass spectrometric detection.*

For citation: Kutovaya A.M., Davydova V.N., Perova I.B., Eller K.I. Flavonoid-profile determination for a hypoglycemic collection by high-performance liquid chromatography. *Tonk. Khim. Tekhnol. = Fine Chem. Technol.* 2020;15(3):39-46. https://doi.org/10.32362/2410-6593-2020-15-3-39-46

Определение профиля флавоноидов в гипогликемическом сборе методом высокоэффективной жидкостной хроматографии

А.М. Кутовая[1], В.Н. Давыдова[1], И.Б. Перова[2], К.И. Эллер[2,@]

[1]Всероссийский научно-исследовательский институт лекарственных и ароматических растений (ВИЛАР), Москва, 117216 Россия
[2]Федеральный исследовательский центр питания, биотехнологии и безопасности пищи, Москва, 109240 Россия
[@]Автор для переписки, e-mail: ellki42@yandex.ru

Цели. *Гипогликемические препараты растительного происхождения успешно дополняют синтетические рецептурные лекарства, использующиеся в традиционном подходе к лечению сахарного диабета 2 типа. Однако научно обоснованное применение и стандартизация таких препаратов ограничены из-за неадекватной и часто устаревшей информации об их химическом составе. Нами был разработан гипогликемический сбор (ГГС), состоящий из створок фасоли обыкновенной (Phaseolus vulgaris L.), побегов черники обыкновенной (Vaccinium myrtillus L.), травы галеги лекарственной (Gallega officinalis L.), травы горца птичьего (спорыша) (Polygonum aviculare L.), корней лопуха большого (Arctium lappa L.), плодов шиповника коричного (Rosa cinnamomea L.). По мнению ряда исследователей, антидиабетические свойства вышеупомянутых растений во многом обусловлены присутствием в них полифенольных соединений, особенно флавоноидов. Цель данного исследования – определение профиля флавоноидов в ГГС и в суммарном сухом экстракте (ССЭ) на основе ГГС.*
Методы. *Исследование проводили методом обращено-фазовой высокоэффективной жидкостной хроматографии с диодно-матричным и масс-спектрометрическим детектированием.*
Результаты. *В ГГС и ССЭ было идентифицировано девять индивидуальных флавонолгликозидов – производных мирицетина, кверцетина, кемпферола и кемпферида. Основными флавонолгликозидами в исследуемых объектах были робинин и кемпферол-3-глюкуронид, содержание которых в ГГС составило 2.09 и 2.22 мг/г, в ССЭ – 4.85 и 3.84 мг/г, соответственно. Остальные флавонолгликозиды были обнаружены в ГГС и ССЭ в существенно более низких концентрациях.*
Выводы. *Результаты работы могут быть использованы при стандартизации ГГС и оценке его фармакологической активности.*

Ключевые слова: *флавоноиды, сбор гипогликемический, суммарный сухой экстракт, высокоэффективная жидкостная хроматография, диодно-матричное детектирование, масс-спектрометрическое детектирование.*

Для цитирования: Кутовая А.М., Давыдова В.Н., Перова И.Б., Эллер К.И. Определение профиля флавоноидов в гипогликемическом сборе методом высокоэффективной жидкостной хроматографии. *Тонкие химические технологии.* 2020;15(3):39-46. https://doi.org/10.32362/2410-6593-2020-15-3-39-46

In recent years, diabetes has become a serious global public health problem, affecting people of all ages, genders, and ethnicities. A close relationship has been established between type 2 diabetes and lack of physical activity, excessive body weight, and poor diet. To ameliorate the negative effects of diabetes, a number of synthetic antidiabetic drugs have been developed that lower blood glucose levels by various mechanisms. These include, but are not restricted to, sulfonylureas, biguanidines, and α-glucosidase inhibitors. The use of herbal pharmaceuticals and nutraceuticals can complement that of conventional synthetic prescription drugs in the treatment of this disease. Due to the lower probability of side effects and lower cost, herbal medicines are often used in the treatment of patients with type 2 diabetes [1, 2]. Such herbal collections are a valuable source of biologically active substances (BASs). However, their science-based application and standardization are limited due to inadequate and often outdated information on their chemical composition.

Informed by literature data on the antidiabetic properties of medicinal plants, we have developed a herb collection with hypoglycemic effects. The collection includes common bilberry shoots (*Vaccinium myrtillus* L.) [3, 4], common bean pods (*Phaseolus vulgaris* L.) [4], galega herb (*Gallega officinalis* L.) [5, 6], burdock roots (*Arctium lappa* L.) [7], common knotgrass herb (*Polygonum aviculare* L.) [8], and cinnamon rose hips (*Rosa cinnamomea* L.) [9, 10]. According to a number of researchers, the antidiabetic properties of these herbs are largely due to the presence of polyphenolic compounds, especially flavonoids. [11, 12].

The aim of the work was to determine the flavonoid profile of this herb collection and its total dry extract (TDE) using reverse-phase high-performance liquid chromatography (HPLC) fitted with an online diode array detector (DAD) and mass spectrometer (MS).

MATERIALS AND METHODS

Objects. The hypoglycemic collection (HGC) was obtained from plant materials produced by *Fitofarm* (Anapa, Krasnodar krai, Russia) [13, 14]. The TDE based on the collection was obtained according to the following technological scheme: extraction of the herb collection with purified water; filtering the extract; concentrating the extract; drying; and sieving the finished product.

Standards and solvents. Commercially available standard samples were used: rutin (≥94%, *Sigma-Aldrich*, USA), hyperoside (≥95%, *HWI ANALYTIK GMBH*, Germany), isoquercitrin (≥94%, *HWI ANALYTIK GMBH*, Germany), avicularin (*ChromaDex*, USA), kaempferol-3-glucoside (≥95%, *PhytoLab*, Germany), myricetin (appr. 85%, *Sigma-Aldrich*, USA), quercetin (≥98%, *Sigma-Aldrich*, USA), and kaempferol (≥99%, *Extrasynthese*, France). The following solvents and reagents were used: ultrapure water (Milli-Q® Advantage A10, *Merck*, Germany), acetonitrile UPLC/HPLC grade *AppliChem PanReac* production (Darmstadt, Germany), methanol UPLC/HPLC grade *J.T. Baker* production (*Avantor Performance Materials*, *Inc.,* Palo Alto, USA), and formic acid 98–100% *Merck* production (Darmstadt, Germany).

Sample preparation. HGC: approximately 2.0 g (exact weight) was transferred to a 100-mL round-bottom flask, and 50 mL of 60% aqueous methanol was added. The mixture was heated in a boiling water bath under reflux for 1 h. Then, the flask was allowed to cool to room temperature, placed in an ultrasonic bath for 5 min, and the extract was transferred to a 50-mL volumetric flask, made up to the mark with 60% aqueous methanol, and stirred. An aliquot was then transferred to a 1.5-mL centrifuge tube, centrifuged at 15000 rpm, and the supernatant transferred to an autosampler vial. The TDE (approximately 0.5 g accurately weighed) was transferred to a 50-mL volumetric flask, and 30 mL of 60% aqueous methanol was added. The mixture was placed in an ultrasonic bath for 10 min then made to the mark with 60% aqueous methanol and stirred. An aliquot was transferred to a 1.5-mL centrifuge tube, centrifuged at 15000 rpm, the supernatant transferred to an autosampler vial.

Equipment. The analysis was performed using an Ultimate 3000 liquid chromatography system equipped with a degasser, a three-channel pump, a column thermostat, a thermostatically controlled autosampler, a DAD, and an TSQ Endura triple-quadrupole mass spectrometer (MS) (*Thermo Scientific*, USA).

HPLC conditions: stationary phase: Waters NovaPak® C18 ID 4 μм 4.6 × 150 mm column; mobile phase A: 0.1% aqueous solution of formic acid, mobile phase B: acetonitrile; flow rate: 0.5 mL/min; gradient elution: 0–30 min 10–25% B, 30–40 min 25–50% B; column regeneration: 40–45 min 50–10% B, 45–50 min 10% B; column temperature: 25°C; sample volume: 10 μL; autosampler temperature: 20°C; detection was performed at four different analytical wavelengths: 70, 350, 338, and 290 nm. Spectra were recorded in the wavelength range 190–400 nm.

MS conditions: heated electrospray ionization in positive ion detection mode (HESI-MS+) was performed over the m/z range 100–1000 Da. Scanning speed: 100 Da/s; Q1 quadrupole resolution: 0.7. Operating parameters of the ionization source: capillary voltage: 3500 V, fragmentation voltage: 5 V, desiccant gas (N_2) flow: 50 arbitrary units; auxiliary gas flow: 15 arbitrary units; purge gas flow: 2 arbitrary units; ion transfer tube temperature: 325°C, evaporator temperature: 350°C.

Data processing was carried out using the Thermo Xcalibur 3.0.63 Qual browser program.

RESULTS AND DISCUSSION

The peaks in the chromatograms were identified by comparing their retention times and ultraviolet and mass spectra with those of standards as well as on the basis of published data on the flavonoid profiles of the constituent plants.

Chromatograms of the HGC extract and the TDE are presented in Fig. 1 and Fig. 2.

Nine individual flavonol glycosides—derivatives of myricetin, quercetin, kaempferol, and kaempferid—were identified in the HGC and TDE (Table 1). According to published data, robinin, 3-glucuronides

of quercetin, and kaempferol are characteristic of common beans [15]. We have previously identified 3-glucuronides of myricetin, quercetin, kaempferol and kaempferide as well as 3-arabinoside kaempferol in common knotgrass (*Polygonum aviculare*). In addition, according to the results of our previous studies, quercetin and kaempferol 3-glucuronides are present in blueberry shoots. With a high degree of probability, quercetin-3-robinoside-7-rhamnoside and quercetin-3-pentosyl glucuronide are flavonol glycosides of common beans, the contents of which have not been previously reported in the literature.

The quantitative contents of the flavonoids identified were determined by an external standard method: quercetin tri- and diglycosides are expressed in terms of rutin, myricetin- and quercetin-3-glucuronides are expressed in terms of isoquercitrin, and kaempferol glycosides are expressed in terms of keampferol-3-glucoside (Table 2).

As can be seen from Table 2, the main flavonoids in the studied objects are robinin and kaempferol-3-glucuronide, the contents of which in the HGC are 2.09 and 2.22 mg/g, and in the TDE are 4.85 and 3.84 mg/g, respectively. Quercetin-3-robinoside-7-rhamnoside, campferol-3-robinoside, quercetin-3-glucuronide, campferid-3-glucuronide, and campferol-3-arabinoside were detected in HGC and TDE at significantly lower concentrations than those of the main flavonoids

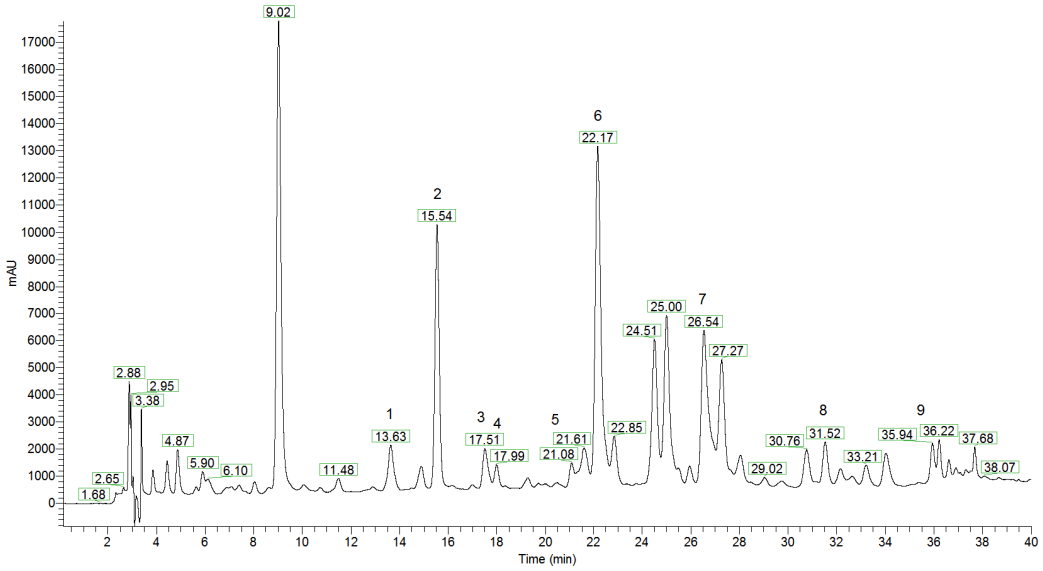

Fig. 1. Chromatogram of the HGC extract at λ = 350 nm.
The peak numbers correspond to the flavonoid numbers in Tables 1 and 2.

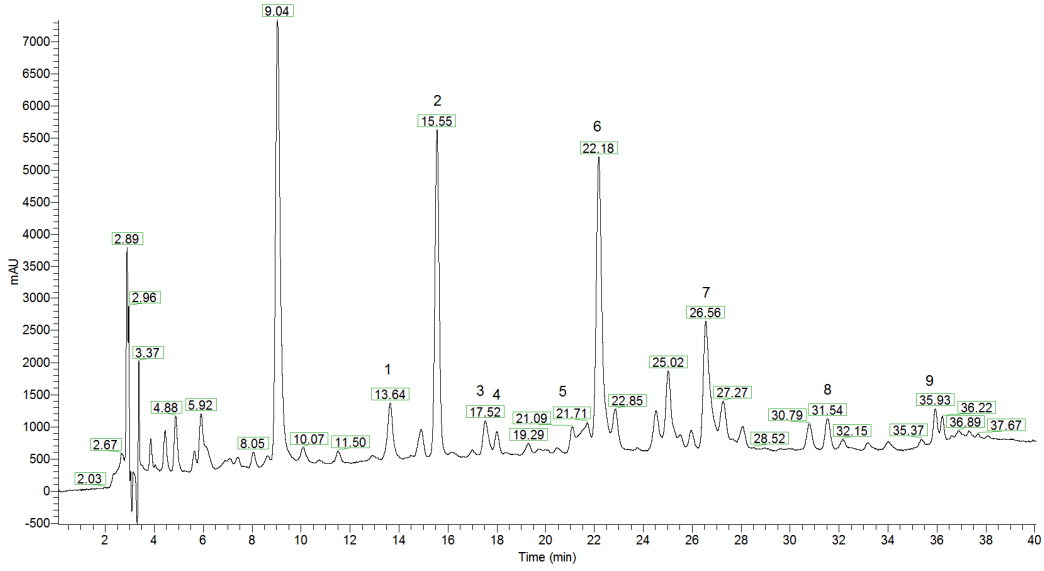

Fig. 2. Chromatogram of the TDE at λ = 350 nm.
The peak numbers correspond to the flavonoid numbers in Tables 1 and 2.

Table 1. HPLC-DAD-MS results for the HGC and its extract

No.	Flavonoid	R_t, min	λ_{max}, nm	m/z	Ion detected
1	Quercetin-3-robinoside-7-rhamnoside	13.6	255, 265, 355	757 611 449 303	$[M + H]^+$ [M – rhamnose* + H]$^+$ [M – robinose + H]$^+$ [M – rhamnose – robinose + H]$^+$
2	Kaempferol-3-robinoside-7-rhamnoside (Robinin)	15.5	265, 350	741 595 433 287	$[M + H]^+$ [M – rhamnose + H]$^+$ [M – robinose + H]$^+$ [M – rhamnose – robinose + H]$^+$
3	Myricetin-3-glucuronide	17.5	255, 270, 355	495 319	$[M + H]^+$ [M – glucuronic acid + H]$^+$
4	Quercetin-3-pentosylglucuronide	18.0	255, 270, 355	611 435 303	$[M + H]^+$ [M – glucuronic acid + H]$^+$ [M – pentose + H]$^+$
5	Kaempferol-3-robinoside	21.0	270, 345	595 433 287	$[M + H]^+$ [M – rhamnose + H]$^+$ [M – robinose + H]$^+$
6	Quercetin-3-glucuronide	22.1	255, 265, 355	479 303	$[M + H]^+$ [M – glucuronic acid + H]+
7	Kaempferol-3-glucuronide	26.5	265, 345	463 287	$[M + H]^+$ [M – glucuronic acid + H]$^+$
8	Kaempferol-3-arabinoside	31.5	265, 245	419 287	$[M + H]^+$ [M – arabinose + H]$^+$
9	Kaempferide-3-glucuronide	35.9	270, 345	477 301	[M + H]+ [M – glucuronic acid + H]$^+$

**Hereinafter:* for dehydrated carbohydrate or glucuronic acid ($–H_2O$), water is lost upon forming a glycosidic bond.

Table 2. Flavonoids content in HGC and TDE

No.	Flavonoid	Content, mg/g	
		HGC	TDE
1	Quercetin-3-robinoside-7-rhamnoside	0.10	0.31
2	Robinin	2.09	4.85
3	Myricetin-3-glucuronide	0.07	0.16
4	Quercetin-3-pentosylglucuronide	0.05	0.15
5	Kaempferol-3-robinoside	0.33	0.93
6	Quercetin-3-glucuronide	0.43	0.72
7	Kaempferol-3-glucuronide	2.22	3.84
8	Kaempferol-3-arabinoside	0.64	1.63
9	Kaempferide-3-glucuronide	0.53	1.37
	Total flavonoids	**6.46**	**13.96**

(0.10–0.64 and 0.31–1.63 mg/g, respectively). The contents of minor flavonol glycosides, which include quercetin-3-pentosyl glucuronide and myricetin-3-glucuronide, are less than 0.10 mg/g in the collection and less than 0.20 mg/g in the extract. The total content of flavonoids in the collection is 6.46 mg/g (or 0.646%) and that in the extract is 13.96 mg/g (or 1.396%).

CONCLUSIONS

The flavonoid profiles of HGC and its TDE were determined by HPLC-DAD-MS. Nine individual flavonol glycosides were identified, and these were found to be derivatives of myricetin, quercetin, kaempferol and kaempferide, which are characteristic for common bean pods (*Phaseolus vulgaris*), common knotgrass (*Polygonum aviculare*), and bilberry shoots. Robinin and kaempferol-3-glucuronide predominated in HGC and TDE. Quercetin-3-robinoside-7-rhamnoside and quercetin-3-pentosyl glucuronide were identified for the first time and assigned as bean flavonoids. The total flavonoid content in the HGC was 6.46 mg/g (or 0.646%) and that in the TDE was 13.96 mg/g (or 1.396%).

This method and its results can be used to standardize hypoglycemic collections and evaluate their pharmacological activities.

The authors declare no conflicts of interest.

REFERENCES

1. Williamson E.M. Synergy and other interactions in phytomedicines. *Phytomedicine.* 2001;8(5):401-409. https://doi.org/10.1078/0944-7113-00060

2. Prabhakar P.K., Doble M. A target based therapeutic approach towards diabetes mellitus using medicinal plants. *Curr. Diabetes Rev.* 2008;4(4):291-308. https://doi.org/10.2174/157339908786241124

3. Stargrove M.B., Treasure J., McKee D.L. Herb, Nutrient, and Drug Interactions: Clinical Implications and Therapeutic Strategies. Missouri: Mosby Elsevier; 2007. P. 9-11. ISBN 978 0 323 02964 3

4. Sidorova Y., Shipelin V., Mazo V., Zorin S., Petrov N., Kochetkova A. Hypoglycemic and hypolipidemic effect of *Vaccinium myrtillus* L. leaf and *Phaseolus vulgaris* L. seed coat extracts in diabetic rats. *Nutrition.* 2017;41:107-112. https://doi.org/10.1016/j.nut.2017.04.010

5. Martinchik I.A., Trumpe T.E., Gurin A.V. Hypoglycemic properties of some plants from family *Fabaceae*. Collection of Scientific Papers of the Sixth Scientific Conference with International Participation "Young Scientists and Pharmacy of the 21st Century." 2018. P. 271-276 (in Russ.).

6. Yakimova T.V., Nasanova O.N., Vengerovsky A.I., Burkova V.N. Influence of Galega extracts on lipids metabolism in experimental diabetes mellitus. *Sibirskii meditsinskii zhurnal = The Siberian Medical Journal.* 2011;26(4-2):98-102 (in Russ.).

7. Assessment report on *Arctium lappa* L., radix. European Medicines Agency, 2011. Available from: https://www.ema.europa.eu/en/documents/herbal-report/final-assessment-report-arctium-lappa-l-radix_en.pdf (Accessed July 3, 2019)

8. Assessment report on *Polygonum aviculare* L., herba. European Medicines Agency, 2016. Available from: https://www.ema.europa.eu/en/documents/herbal-report/final-assessment-report-polygonum-aviculare-l-herba_en.pdf (Accessed July 3, 2019).

СПИСОК ЛИТЕРАТУРЫ

1. Williamson E.M. Synergy and other interactions in phytomedicines. *Phytomedicine.* 2001;8(5):401-409. https://doi.org/10.1078/0944-7113-00060

2. Prabhakar P.K., Doble M. A target based therapeutic approach towards diabetes mellitus using medicinal plants. *Curr. Diabetes Rev.* 2008;4(4):291-308. https://doi.org/10.2174/157339908786241124

3. Stargrove M.B., Treasure J., McKee D.L. Herb, Nutrient, and Drug Interactions: Clinical Implications and Therapeutic Strategies. Missouri: Mosby Elsevier; 2007. P. 9-11. ISBN 978 0 323 02964 3

4. Sidorova Y., Shipelin V., Mazo V., Zorin S., Petrov N., Kochetkova A. Hypoglycemic and hypolipidemic effect of *Vaccinium myrtillus* L. leaf and *Phaseolus vulgaris* L. seed coat extracts in diabetic rats. *Nutrition.* 2017;41:107-112. https://doi.org/10.1016/j.nut.2017.04.010

5. Мартынчик И.А., Трумпе Т.Е., Гурин А.В. Гипогликемические свойства некоторых растений семейства Бобовые (*Fabaceae*). Сборник трудов шестой научной конференции с международным участием «Молодые ученые и фармация XXI века». 2018. С. 271-276.

6. Якимова Т.В., Насанова О.Н., Венгеровский А.И., Буркова В.Н. Влияние экстракта галеги лекарственной на метаболизм липидов при экспериментальном сахарном диабете. *Сибирский медицинский журнал.* 2011;26(4-2):98-102.

7. Assessment report on *Arctium lappa* L., radix. European Medicines Agency, 2011. URL: https://www.ema.europa.eu/en/documents/herbal-report/final-assessment-report-arctium-lappa-l-radix_en.pdf (дата обращения: 03.07.2019).

8. Assessment report on *Polygonum aviculare* L., herba. European Medicines Agency, 2016. URL: https://www.ema.europa.eu/en/documents/herbal-report/final-assessment-report-polygonum-aviculare-l-herba_en.pdf (дата обращения 03.07.2019).

9. Chrubasik C., Duke R.K., Chrubasik S. The evidence for clinical efficacy of rose hip and seed: a systematic review. *Phytother. Res.* 2006;20(1):1-3. https://doi.org/10.1002/ptr.1729

10. Andersson U., Berger K., Högberg A., Landin-Olsson M., Holm C. Effects of rose hip intake on risk markers of type 2 diabetes and cardiovascular disease: a randomized, double-blind, cross-over investigation in obese persons. *Eur. J. Clin. Nutr.* 2012;66(5):585-590. https://doi.org/10.1038/ejcn.2011.203

11. Benzie I.F.F., Wachter-Galor S. (Eds.). Herbal Medicine. Biomolecular and Clinical Aspects. Second Edition. Boca Raton, Fla.: CRC Press; 2011. 472 p.

12. Ferlemi A.V., Lamari F.N. Berry leaves: an alternative source of bioactive natural products of nutritional and medicinal value. *Antioxidants.* 2016;5(2):17. https://doi.org/10.3390/antiox5020017

13. Kutovaya A.M., Davydova V.N., Mizina P.G. Prospects for the development of the herbal mix containing hypoglycemic effect in the complex therapy of patients with diabetes. *Voprosy biologicheskoi, meditsinskoi i farmatsevticheskoi khimii = Problems of Biological, Medical and Pharmaceutical Chemistry.* 2016;6:40-43 (in Russ.).

14. Kutovaya A.M., Martinchik I.A., Trumpe T.E., Ferubko E.V., Davydova V.N. Development and experimental study of hypoglycemic composition prepared from medicinal plants. *Razrabotka i registratsiya lekarstvennykh sredstv = Drug Development & Registration.* 2018;(4):78-81 (in Russ.).

15. Onyilagha J.C., Islam S. Flavonoids and other polyphenols of the cultivated species of the genus. *Phaseolus. Int. J. Agric. Biol.* 2009;11(3):231-234.

9. Chrubasik C., Duke R.K., Chrubasik S. The evidence for clinical efficacy of rose hip and seed: a systematic review. *Phytother. Res.* 2006;20(1):1-3. https://doi.org/10.1002/ptr.1729

10. Andersson U., Berger K., Högberg A., Landin-Olsson M., Holm C. Effects of rose hip intake on risk markers of type 2 diabetes and cardiovascular disease: a randomized, double-blind, cross-over investigation in obese persons. *Eur. J. Clin. Nutr.* 2012;66(5):585-590. https://doi.org/10.1038/ejcn.2011.203

11. Benzie I.F.F., Wachter-Galor S. (Eds.). Herbal Medicine. Biomolecular and Clinical Aspects. Second Edition. Boca Raton, Fla.: CRC Press; 2011. 472 p.

12. Ferlemi A.V., Lamari F.N. Berry leaves: an alternative source of bioactive natural products of nutritional and medicinal value. *Antioxidants.* 2016;5(2):17. https://doi.org/10.3390/antiox5020017

13. Кутовая А.М., Давыдова В.Н., Мизина П.Г. Перспективы разработки сбора гипогликемического действия в комплексной терапии больных диабетом. *Вопросы биологической, медицинской и фармацевтической химии.* 2016;6:40-43.

14. Кутовая А.М., Мартынчик И.А., Трумпе Т.Е., Ферубко Е.В., Давыдова В.Н. Разработка и экспериментальное изучение гипогликемического сбора из лекарственных растений. *Разработка и регистрация лекарственных средств.* 2018;(4):78-81.

15. Onyilagha J.C., Islam S. Flavonoids and other polyphenols of the cultivated species of the genus. *Phaseolus. Int. J. Agric. Biol.* 2009;11(3):231-234.

About the authors:

Angelina M. Kutovaya, Postgraduate Student, Federal State Budgetary Scientific Institution "All-Russian Scientific Research Institute of Medicinal and Aromatic Plants" (VILAR) (7, ul. Grina, Moscow, 117216, Russia). E-mail: linia25@mail.ru. ResearcherID AAK-6219-2020, https://orcid.org/0000-0001-9513-9272

Valentina N. Davydova, Dr. of Sci. (Pharm.), Chief Researcher, Pharmaceutical Technology Department, Federal State Budgetary Scientific Institution "All-Russian Scientific Research Institute of Medicinal and Aromatic Plants" (VILAR) (7, ul. Grina, Moscow, 117216, Russia). E-mail: davydova.vn@gmail.com. Scopus Author ID 57195220369

Irina B. Perova, Cand. of Sci. (Pharm.), Senior Researcher, Laboratory of Metabolomic and Proteomic Analysis, Federal State Budgetary Scientific Institution "Federal Research Center of Nutrition, Biotechnology and Food Safety" (2/14, Ust'inskii proezd, Moscow, 109240, Russia). E-mail: Erin.Feather@yandex.ru. ResearcherID K-6257-2018, Scopus Author ID 56403250700, https://orcid.org/0000-0001-5975-1376

Konstantin I. Eller, Dr. of Sci. (Chemistry), Professor, Head of the Laboratory of Metabolomic and Proteomic Analysis, Federal State Budgetary Scientific Institution "Federal Research Center of Nutrition, Biotechnology and Food Safety" (2/14, Ust'inskii proezd, Moscow, 109240, Moscow, Russia). E-mail: ellki42@yandex.ru. Researcher ID K-6408-2018, Scopus Author ID 7003969952, https://orcid.org/0000-0003-1046-4442

Об авторах:

Кутовая Ангелина Михайловна, аспирант ФГБНУ «Всероссийский научно-исследовательский институт лекарственных и ароматических растений» (ВИЛАР) (Россия, 117216, Москва, ул. Грина, д. 7). E-mail: linia25@mail.ru. Researcher ID AAK-6219-2020, https://orcid.org/0000-0001-9513-9272

Давыдова Валентина Николаевна, доктор фармацевтических наук, главный научный сотрудник отдела фармацевтической технологии ФГБНУ «Всероссийский научно-исследовательский институт лекарственных и ароматических растений» (ВИЛАР) (Россия, 117216, Москва, ул. Грина, д. 7). E-mail: davydova.vn@gmail.com. Scopus Author ID 57195220369

Перова Ирина Борисовна, кандидат фармацевтических наук, старший научный сотрудник лаборатории метаболомного и протеомного анализа ФГБУН «Федеральный исследовательский центр питания, биотехнологии и безопасности пищи» (Россия, 109240, Москва, Устьинский проезд, д. 2/14). E-mail: Erin.Feather@yandex.ru. Researcher ID K-6257-2018, Scopus Author ID 56403250700, https://orcid.org/0000-0001-5975-1376

Эллер Константин Исаакович, доктор химических наук, профессор, заведующий лабораторией метаболомного и протеомного анализа ФГБУН «Федеральный исследовательский центр питания, биотехнологии и безопасности пищи» (Россия, 109240, Москва, Устьинский проезд, д. 2/14). E-mail: ellki42@yandex.ru. ResearcherID K-6408-2018, Scopus Author ID 7003969952, https://orcid.org/0000-0003-1046-4442

Submitted: February 27, 2020; Reviewed: April 17, 2020; Accepted: May 11, 2020.

Translated from Russian into English by S. Durakov
Edited for English language and spelling by Enago, an editing brand of Crimson Interactive Inc.

ISSN 2686-7575 (Online)
https://doi.org/10.32362/2410-6593-2020-15-3-47-57
UDC 678.026

Investigation of surface tension and contact angles for effective polymer binders based on epoxy oligomers and active diluents

Angelina D. Bresskaya[1,@], Dmitry A. Trofimov[1], Igor D. Simonov-Emel'yanov[1], Sergey I. Shalgunov[2], Vladimir I. Sokolov[2]

[1]MIREA – Russian Technological University (M.V. Lomonosov Institute of Fine Chemical Technologies), Moscow, 119571 Russia
[2]NPO Stekloplastic, Andreevka, Moscow oblast, 141551 Russia
[@]Corresponding author, e-mail: angelinabresskaya@gmail.com

Objectives. *This study focused on the quantification of the surface tension and the static and dynamic contact angles of epoxy oligomers, active diluents, and their mixtures of various compositions at different temperatures. The active diluents were aliphatic compounds based on glycidyl ethers, namely laproxides and a laprolate of different structure, functionality, molecular weight, and viscosity. Moreover, the preparation of effective polymer binders (matrices) for composites was explored.*

Methods. *In this study, the epoxy oligomers ED-20 and DER-330, laproxides 201B, DEG-1, E-181, and 703, laprolate 301, and their mixtures in various compositions were investigated. Their surface tension and the static and dynamic contact angles were determined by the Wilhelmy plate and ring methods on a semiautomatic tensiometer at different temperatures (20–60°C). The static contact angle was measured on a thin aluminum borosilicate glass plate, and the dynamic contact angles were determined using an installation for measuring surface tension developed by NPO Stekloplastik.*

Results. *The surface tension and static and dynamic contact angles were obtained for all epoxy oligomers and active diluents, as well as for their mixtures at 20–60°C. For binders based on systems of epoxy oligomers and active diluents, the impregnation rate of fiber reinforcement was also calculated. The introduction of laproxides or laprolates into the epoxy oligomers led to a decrease in surface tension and contact angles, while the increase in temperature increased the impregnation rate by 10–20 times.*

Conclusions. *The temperature increase from 20 to 60°C resulted in a decrease in the surface tension of mixed systems of epoxy oligomers and active diluents by almost two times. In addition, the contact angles changed by only 4°–7°, while the impregnation was significantly improved and the corresponding rate increased by 10–20 times.*

Keywords: *epoxy oligomers, active diluents, glycidyl ether-based aliphatic compounds, laproxides, laprolate, surface tension, static and dynamic contact angles, impregnation of fiber reinforcement.*

For citation: Bresskaya A.D., Trofimov D.A., Simonov-Emel'yanov I.D., Shalgunov S.I., Sokolov V.I. Investigation of surface tension and contact angles for effective polymer binders based on epoxy oligomers and active diluents. *Tonk. Khim. Tekhnol. = Fine Chem. Technol.* 2020;15(3):47-57. https://doi.org/10.32362/2410-6593-2020-15-3-47-57

Исследование поверхностного натяжения и углов смачивания для создания эффективных полимерных связующих на основе эпоксидных олигомеров с активными разбавителями

А.Д. Бресская[1,@], Д.А. Трофимов[1], И.Д. Симонов-Емельянов[1], С.И. Шалгунов[2], В.И. Соколов[2]

[1]МИРЭА – Российский технологический университет (Институт тонких химических технологий имени М.В. Ломоносова), Москва, 119571 Россия
[2]АО «НПО Стеклопластик», Московская область, Андреевка, 141551 Россия
[@]Автор для переписки, e-mail: angelinabresskaya@gmail.com

Цели. *Определение поверхностного натяжения, статического и динамического углов смачивания при разных температурах для эпоксидных олигомеров марок ЭД-20 и DER-330; для активных разбавителей – алифатических соединений на основе глицидиловых эфиров – Лапроксидов и Лапролата разной структуры, функциональности, молекулярной массы, вязкости; а также для систем, состоящих из эпоксидных олигомеров и активных разбавителей разного состава. Также целью являлось создание эффективных полимерных связующих (матриц) для композитов.*

Методы. *В качестве объектов исследования использовали эпоксидные олигомеры марок ЭД-20 и DER-330; активные разбавители – Лапроксиды (201Б, ДЭГ-1, Э-181, 703) и Лапролат 301; а также системы эпоксидный олигомер + Лапроксид (Лапролат) разных составов. Поверхностное натяжение, статический и динамический углы смачивания определяли методом Вильгельми и методом отрыва кольца на полуавтоматическом тензиометре при разных температурах (20–60 °С). Статический угол смачивания измеряли на тонкой пластине из алюмоборосиликатного стекла. Значения динамического угла смачивания определяли на установке для измерения поверхностного натяжения, разработанной АО «НПО Стеклопластик».*

Результаты. *Определены значения поверхностного натяжения, углов статического и динамического смачивания для эпоксидных олигомеров ЭД-20 и DER-330, Лапроксидов 201Б, ДЭГ-1, Э-181, 703 и Лапролата 301, а также для смешанных систем при температурах от 20 до 60 °С. Рассчитаны скорости пропитки армирующих волокнистых наполнителей эффективными связующими на основе смешанных систем. Показано, что при введении в эпоксидные олигомеры Лапроксидов (Лапролата), поверхностное натяжение снижается, углы смачивания уменьшаются, температура повышается, в результате чего скорость пропитки возрастает в 10–20 раз.*

Выводы. *Повышение температуры от 20 до 60 °С приводит к снижению поверхностного натяжения систем, состоящих из эпоксидных олигомеров и активных разбавителей, практически в 2 раза. Углы смачивания изменяются всего на 4°–7°, существенно улучшается качество пропитки, скорость пропитки увеличивается в 10–20 раз.*

Ключевые слова: *эпоксидные олигомеры, активные разбавители, алифатические соединения на основе глицидиловых эфиров, Лапроксиды, Лапролат, поверхностное натяжение, статический и динамический углы смачивания, пропитка армирующих волокнистых наполнителей.*

Для цитирования: Бресская А.Д., Трофимов Д.А., Симонов-Емельянов И.Д., Шалгунов С.И., Соколов В.И. Исследование поверхностного натяжения и углов смачивания для создания эффективных полимерных связующих на основе эпоксидных олигомеров с активными разбавителями. *Тонкие химические технологии.* 2020;15(3):47-57. https://doi.org/10.32362/2410-6593-2020-15-3-47-57

INTRODUCTION

During the production of fiberglass for several purposes, various modifiers are introduced to regulate the physical, chemical, technological, and operational characteristics of epoxy binders [1, 2]. The use of glycidyl ester-based aliphatic compounds that contain epoxy groups as modifiers of epoxy oligomers (EO) is of particular interest. These compounds are also known as laproxides and laprolates[1] and can be efficiently combined with EO [3, 4]. More specifically, laproxides and laprolates act as active diluents (AD) and are embedded in the three-dimensional structure of the epoxy polymer during curing [5, 6], thus eliminating the solvent removal (drying) stage in the fiberglass manufacturing. Their effect on the kinetics of bulk shrinkage and stress during curing, as well as on the physical properties, deformation behavior, and molecular structure of epoxy matrices has already been investigated [7–10].

Although it is known that determining the composition of epoxy binders and the impregnation rate of reinforcing fiber fillers requires additional data on the contact angles and surface tension [11], there are no relevant literature reports on the surface tension and static contact angle of various AD surfaces and systems that are based on an epoxy oligomer and an AD (EO–AD). Moreover, data on the dynamic contact angle of polymer epoxy binders, EO, AD and EO–AD systems are also not available in the literature.

Therefore, the aim of this work is to study the surface tension (σ) and the static (θ_{st}) and dynamic (θ_{dyn}) contact angles of laproxides, laprolates, and EO–AD systems of different compositions at temperatures 20–60°C for the preparation of effective polymer binders based on the EO ED-20 and DER-330 and various AD with high impregnation rate of reinforcing fiberglass systems.

MATERIALS AND METHODS

For this study, EO ED-20 (*Ya.M. Sverdlov plant*, Russia) and DER-330 (*DOW Chemicals*, CAS Number 25036-25-3/1330-20-7 (100-41-4), USA), laproxides 201B (L-201B), DEG-1 (L-DEG-1), E-181 (L-E-181), and 703 (L-703) with different structures, functionalities, molecular weights, and viscosities, and laprolate 301 (LT-301) (*V.S. Lebedev NPP Makromer*, Russia) were used. Their main characteristics are provided in Table 1. Moreover, a series of EO–laproxide (or laprolate) systems of different compositions were used.

Table 1. Characteristics of EO and AD

Brand of EO or AD[2]	M_w, g/mol	ρ, g/cm^3	Functionality N, units	Epoxy content, wt %	Viscocity η at 25°C, mPa·s
Epoxy oligomer DER-330	340	1.16	2	23.2–24.4	5–7*
Epoxy oligomer ED-20 (GOST 10587-84[3])	410	1.17	2	20.0–22.5	20–25*
Laproxide 201 B (TU 2225-037-10488057-2007)	130	1.01	1	≥25.0	≤2.5
Laproxide DEG-1 (TU 2225-053-10488057-2010)	218	1.02	2	≥24.0	≤70
Laproxide E-181 (TU 2225-058-10488057-2010)	222.5	1.25	2	25.0–30.0	≤80
Laproxide 703 (TU 2226-029-10488057-98)	434	1.09	3	13.6–16.5	90–160
Laprolate 301 (TU 2226-303-10488057-94)	230	1.04	3	~2.5	≤30

* viscosity in Pa·s.

[1] Catalogue of products. NPP Makromer. Available from: http://www.macromer.ru/product/him/komponenty-dlya-lakokrasochnoj-promyshlennosti/aktivnye-razbaviteli-marki-laproksid/ (Accessed May 26, 2019) (in Russ.).
[2] Catalogue of products. NPP Makromer. Available from: http://www.macromer.ru/product/him/komponenty-dlya-lakokrasochnoj-promyshlennosti/aktivnye-razbaviteli-marki-laproksid/ (Accessed May 26, 2019) (in Russ.).
[3] GOST 10587-84. Uncured epoxy resins. Specifications (amended). Moscow: Standard Publishing, 1989 (in Russ.).

The surface tension (σ) of the EO, laproxides, laprolate, and EO–AD systems was determined by the Wilhelmy and ring separation methods using a semiautomatic tensiometer at different temperatures according to GOST R 50003-92 (ISO 304-85)[4]. The static contact angle (θ_{st}) was measured according to GOST 7934.2-74[5]. A thin plate of aluminum borosilicate glass was used as contact surface, which fully corresponded to the composition of glass fibers used in the production of fiberglass. Furthermore, the dynamic contact angles (θ_{dyn}) for the EO, AD, and EO–AD systems were calculated from the surface tension measurement data that were obtained using an installation developed by *NPO Stekloplastik* [12].

RESULTS AND DISCUSSION

The main aim of this study was to determine the surface tension (σ) and the static (θ_{st}) and dynamic (θ_{dyn}) contact angles for the indicated EO and AD (Table 2) and their mixed systems. It is worth noting that the θ_{dyn} values of the analyzed substances were identified for the first time and allowed the calculation of the impregnation rate of fibrous fillers, packages, and frames during a dynamic movement of the polymer binder, e.g., by infusion.

It is clear from Table 2 that the physical and chemical characteristics (σ, θ_{st}, and θ_{dyn}) of the indicated laproxides with various structures, LT-301, and the EO ED-20 and DER-330 were significantly different. Thus, these distinct variations were exploited to prepare a series of EO–AD systems with different compositions and characteristics and optimize the impregnation process of fibrous fillers within a wide range.

According to the σ values obtained after combining different EO–AD systems (Table 3), an increase in the content of AD to 40 vol % led to a significant decrease in the surface tension value of DER-330 and ED-20 by 1.5–4 times, i.e., from 37.2 and 43.0 mN/m, respectively, to a range of 11.6–25.6 mN/m depending on the AD brand. The greatest reduction was achieved for the DER-330–L-201B and ED-20–L-201B systems when 40 vol % L-201B was added, mainly due to the low surface tension of L-201B. However, the introduction of 40 vol % L-DEG-1 in each EO led to a less significant decrease in surface tension, while L-181 and L-703 led to a reduction in the surface tension of ED-20 and DER-330 by about 1.5 times. Instead, the introduction of LT-301 (40 vol %) in the EO was more effective, as the σ value of the corresponding ED-20–AD and DER-330–AD systems was reduced to 14.5 and 13.1 mN/m, respectively.

It should also be noted that reducing the surface tension can improve the impregnation of fiber fillers with an EO–AD-based polymer binder. Thus, the dependence of the surface tension on the AD content for the ED-20–AD systems and a semilogarithmic version of this dependence were plotted as depicted in Fig. 1. Based on Fig. 1a, the most effective reduction in the EO σ value was achieved when 25–40 vol % AD was added. However, it is known that the introduction of more than 20 vol % of a laproxide or a laprolate in EO is impractical, since there is a sharp decrease in the glass transition temperature of cured epoxy systems [8].

Furthermore, the linear dependence of lnσ on the AD content (Fig. 1b) allowed the application of the semilogarithmic additivity rule:

$$\ln \sigma = \varphi_{EO} \ln \sigma_{EO} + \varphi_{AD} \ln \sigma_{AD}, \quad (1)$$

where φ_{EO} and φ_{AD} are the volume fractions of the EO and AD contents, respectively, in the EO–AD system. Thus, the compositions of the EO–AD

Table 2. Surface tension and contact angles for the EO and AD at 20°C

Parameters	Epoxy oligomers		Laproxides				Laprolate
	DER-330	ED-20	L-201B	L-DEG-1	L-181	L-703	LT-301
σ, mN/m	37.2	43.0	9.4	18.7	14.5	13.8	10.0
θ_{st}, °	37.0	38.0	7.0	21.0	20.0	18.0	11.0
θ_{dyn}, °	57.8	58.7	27.0	39.8	36.5	33.0	31.4

[4] GOST P 50003-92 (ISO 304-85). Surface active agents. Determination of surface tension by drawing up liquid films. Moscow: Standard Publishing; 1992 (in Russ.).
[5] GOST 7934.2-74 Watch oils. Method for the determination of regional wetting angle (amended). Collection of Standards. Moscow: Standartinform; 2006 (in Russ.).

Table 3. Surface tension of the studied EO–AD systems at 20°C*

AD content, vol %	Surface tension (σ), mN/m				
	L-201B	L-DEG-1	L-181	L-703	LT-301
10	24.0/16.0	34.7/24.8	31.3/29.1	28.3/22.4	26.4/19.5
20	16.0/13.3	29.8/21.9	26.0/27.6	21.2/18.2	19.5/14.5
30	13.1/12.8	26.0/21.0	22.5/26.8	18.0/15.9	16.3/13.7
40	11.6/12.0	23.4/20.7	20.0/25.6	16.0/13.8	14.5/13.1

*The numerator in the σ values indicates the σ value obtained for the ED-20–AD systems, and the denominator indicates the σ value obtained for the DER-330–AD systems.

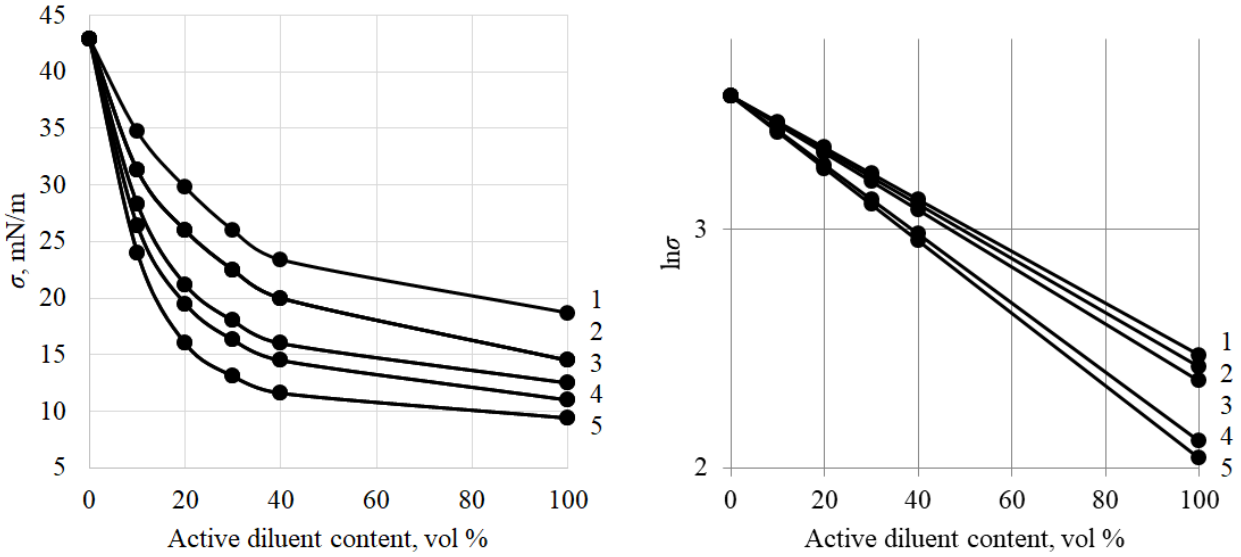

a b

Fig. 1. Dependence of the (a) σ and (b) lnσ parameters of the ED-20–AD systems on the content of 1) L-E-181, 2) L-DEG-1, 3) LT-301, 4) L-703, and 5) L-201B at 20°C.

systems could be calculated based on Eq. (1) with a given value of surface tension.

In addition to the reduction of the σ value, the decrease in θ_{st} could also improve the impregnation of fiber fillers with an EO–AD-based polymer binder. According to the data obtained for the EO-20–AD and DER-330–AD systems with different AD contents (Table 4), the initial θ_{st} values (Table 2) of EO-20 and DER-330 were significantly reduced.

The results of Table 4 were further confirmed by exploring the dependence of θ_{st} and lnθ_{st} on the AD content for ED-20–AD systems. In particular, based on Fig. 2a, the introduction of different AD contents in ED-20 reduced the static contact angle by a range of 7°–21°, while the most effective decrease (by 3.5 times) was achieved for the ED-20–L-201B system, when 40 vol % L-201B was used.

Moreover, the linear dependence of lnθ_{st} on the AD content (Fig. 2b) allowed the application of the semilogarithmic additivity rule, which could be also used to calculate the composition of the EO–AD systems with a given θst value, as with Eq. (1):

$$\ln\theta_{st} = \varphi_{EO}\ln\theta_{EO}^{st} + \varphi_{AD}\ln\theta_{AD}^{st}, \quad (2)$$

where φ_{EO} and φ_{AD} are the volume fractions of the EO and AD contents, respectively, in the EO–AD system.

Another important parameter for the investigated substances is the dynamic contact angle (θ_{dyn}), which can significantly affect their impregnation in reinforcing systems. The θ_{dyn} values obtained for the EO–AD systems with different AD contents (Table 5) indicated that the introduction of various AD in the EO can decrease the θ_{dyn} value.

These results were further confirmed by the investigation of the dependence of θ_{dyn} and $\ln\theta_{dyn}$ on the AD content of the ED-20–AD systems (Fig. 3). However, the introduction of the laproxides and laprolate in EO reduced the θ_{dyn} value only by 15°–20° (Fig. 3a).

As for the other factors, the linear dependence of $\ln\theta_{dyn}$ on the AD content (Fig. 3b) allowed the application of the semilogarithmic additivity rule:

Table 4. Static contact angle (θ_{st}) of the studied EO–AD systems at 20°C*

AD content, vol %	Static contact angle θ_{st}, °				
	L-201B	L-DEG-1	L-181	L-703	LT-301
10	27/27	32/32	32/31	31/31	30/30
20	20/20	28/28	27/27	26/26	24/24
30	14/14	25/25	24/24	23/23	20/18
40	11/11	23/23	22/22	21/21	15/17

*The numerator in the θ_{st} values indicates the θ_{st} value obtained for the ED-20–AD systems, and the denominator indicates the θ_{st} value obtained for the DER-330–AD systems.

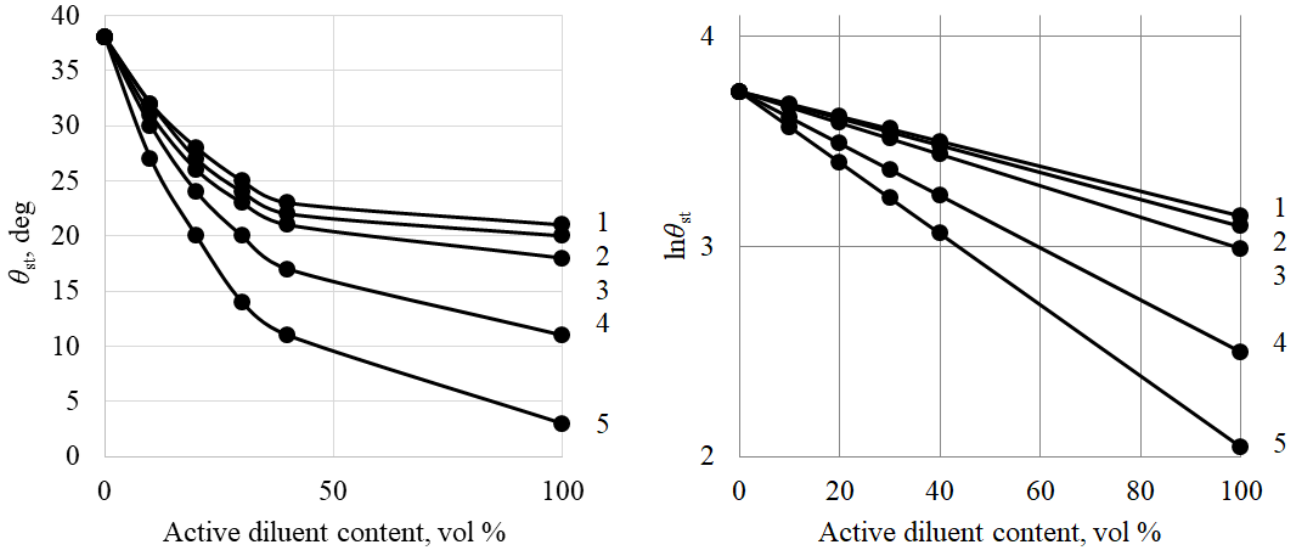

a b

Fig. 2. Dependence of the (a) θ_{st} and (b) $\ln\theta_{st}$ parameters of the ED-20–AD systems on the content of 1) L-DEG-1, 2) L-E-181; 3) L-703, 4) LT-301, and 5) L-201B at 20°C.

$$\ln\theta_{dyn} = \varphi_{EO}\ln\theta_{EO}^{dyn} + \varphi_{AD}\ln\theta_{AD}^{dyn} \quad (3)$$

In summary, based on the obtained results, the effectiveness of the studied AD substances on the σ, θ_{st}, and θ_{dyn} values of the EO–AD systems increased in the order L-DEG-1 → L-E-181 → L-703 → LT-301 → L-201B.

Furthermore, the molecular mobility of EO and AD increased with increasing temperature, leading to changes in the physical and chemical characteristics (σ, θ_{st}, and θ_{dyn}) of EO, laproxides, laprolate, and EO–AD systems. Thus, these values were measured for the ED-20–AD system at 20 and 60°C with 20 vol % AD content (Table 6). These temperatures were selected taking into account the technological impregnation modes of fibrous fillers with epoxy binders [11].

An increase in temperature from 20 to 60°C led to a decrease in the surface tension of the studied EO–AD systems by 4–14 mN/m. However, the θ_{st} and θ_{dyn} parameters were not significantly affected by the temperature increase, as they were reduced by only 2°–7°.

Table 5. Dynamic contact angle (θ_{dyn}) of the studied EO–AD systems at 20°C*

AD content, vol %	Dynamic contact angle θ_{dyn}, °				
	L-201B	L-DEG-1	L-181	L-703	LT-301
10	51.1/50.0	55.7/55.0	54.0/54.0	53.2/53.0	52.0/52.0
20	43.5/43.0	52.2/51.5	50.0/49.9	48.9/48.6	47.0/46.6
30	39.0/38.0	48.7/48.0	46.8/46.0	44.7/44.2	42.0/41.3
40	36.0/35.0	46.3/45.4	44.0/43.1	41.0/40.4	39.0/38.0

*The numerator in the θ_{dyn} values indicates the θ_{dyn} value obtained for the ED-20–AD systems, and the denominator indicates the θ_{dyn} value obtained for the DER-330–AD systems.

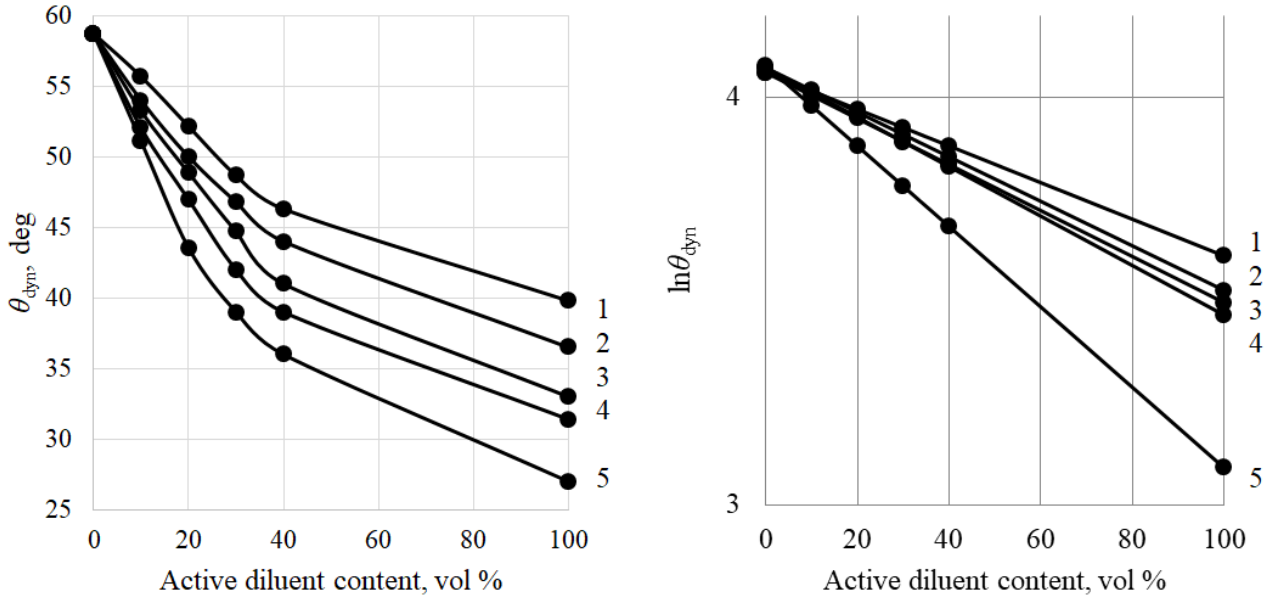

a b

Fig. 3. Dependence of (a) θ_{dyn} and (b) $\ln\theta_{dyn}$ for the ED-20–AD systems on the content of 1) L-DEG-1, 2) L-E-181, 3) L-703, 4) LT-301, and 5) L-201B at 20°C.

Table 6. Surface tension and contact angles of the ED-20–AD systems at 20 and 60°C*

Parameters	ED-20–AD				
	L-201B	L-DEG-1	L-181	L-703	LT-301
σ, mN/m	16.0/12.3	29.8/16.0	26.0/15.0	21.2/13.8	19.5/11.8
θ_{st}, °	20/18	28/24	27/24	26/23	24/21
θ_{dyn}, °	43.5/39.7	52.2/47.5	50.0/46.6	48.9/42.7	47.0/40.0

*The numerators and denominators indicate the obtained values at 20 and 60°C, respectively.

To evaluate the effectiveness of AD in the preparation of new epoxy binders using EO–AD systems for the impregnation of reinforcing fillers used in the production of fiberglass, the optimal impregnation rate was calculated using the prediction method for the impregnation rate of frame fillers with epoxy binders during injection molding. The calculation formula [Eq. (4)] of the optimal impregnation rate (W_{opt} in m/s) involved the Deryagin criterion (De), which establishes a relationship between W_{opt} and the parameters of the polymer binder, i.e., σ, η, θ_{st}, and θ_{dyn}. Therefore, the optimal impregnation rate of a glass fiber filler with an EO–AD-based polymer binder could be calculated using the formula:

$$De = W_{opt} \times \eta / \sigma = 0.045 \times \left(\frac{\theta_{dyn} - \theta_{st}}{180 - \theta_{dyn}} \right)^{\frac{2}{1-\theta_{st}/180}} = 0.045 \times \left(\frac{60 - \theta_{st}}{120} \right)^{\frac{2}{1-\theta_{st}/180}} \quad (4)$$

The θ_{dyn} parameter was assumed to be 60°, as it should not exceed this value when impregnating the fibrous filler [11]. Moreover, from the graphs in Figs. 4 and 5, it is clear that the impregnation rate of the ED-20–L-201B and ED-20–L-DEG-1 systems was highly dependent on surface tension

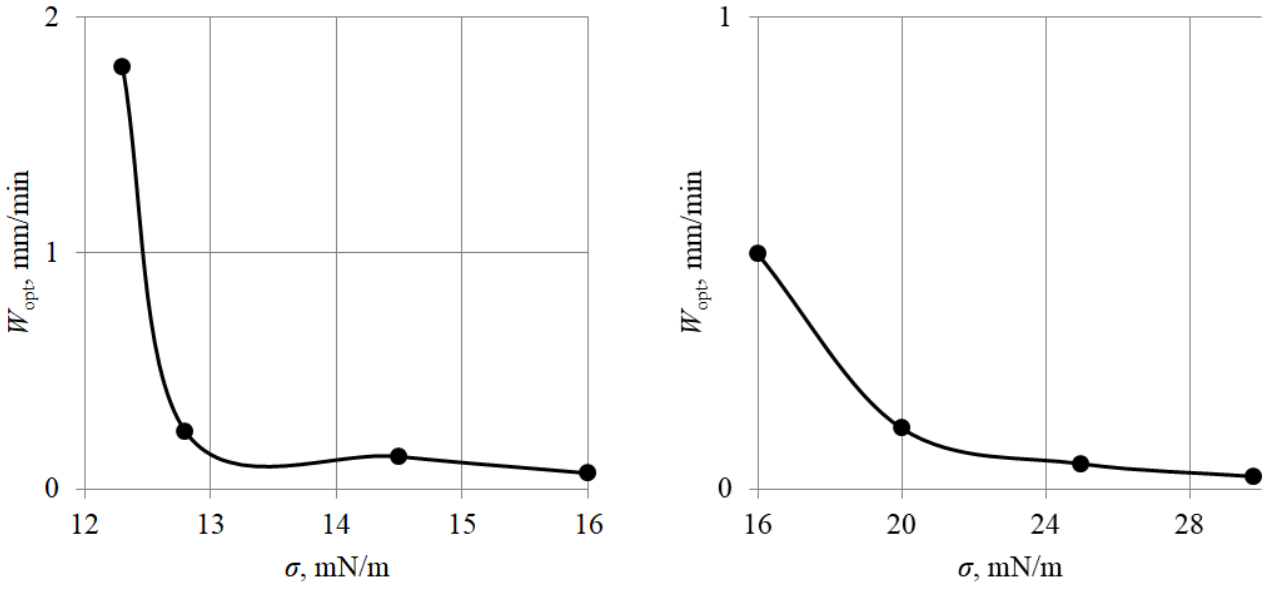

a b

Fig. 4. Dependence of W_{opt} on surface tension for the (a) ED-20–L-201B and (b) ED-20–L-DEG-1 systems with an AD content of 20 vol % and known η and θ values.

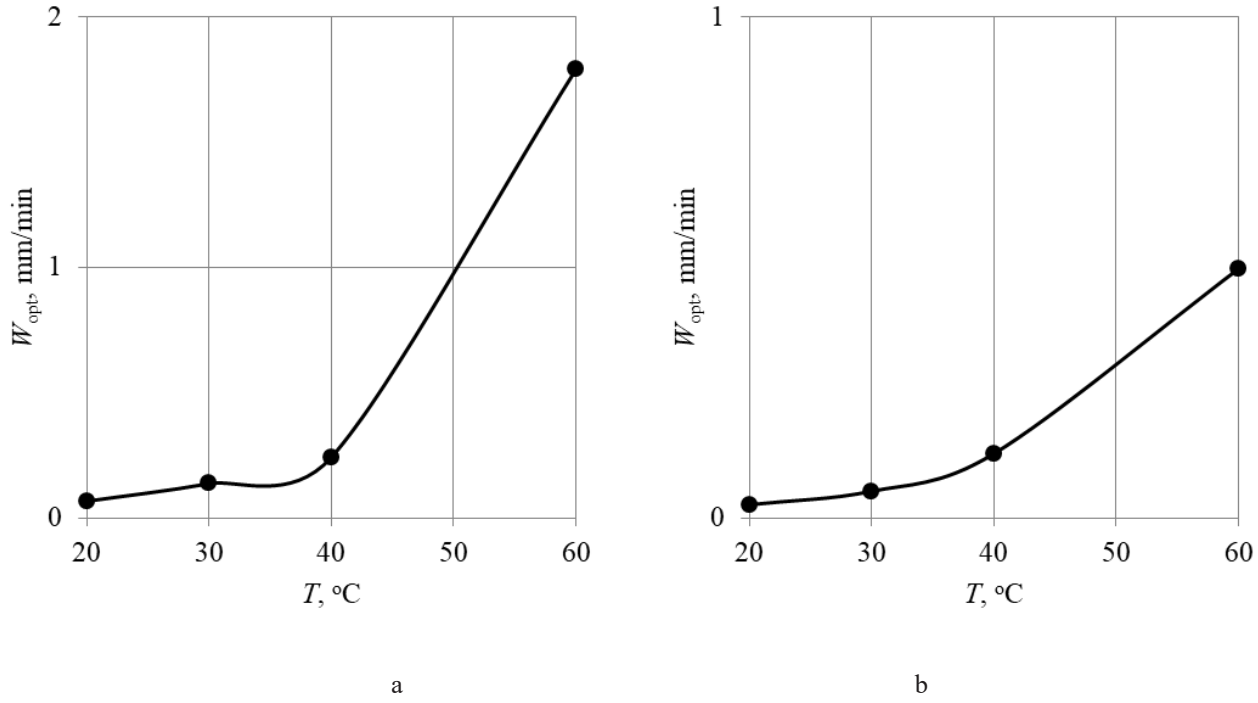

a b

Fig. 5. Dependence of W_{opt} on the temperature for the (a) ED-20–L-201B and (b) ED-20–L-DEG-1 with an AD content of 20 vol % and η values of 0.03–0.9 and 0.9–2.4, respectively.

and temperature. In particular, the impregnation rate was significantly reduced as σ increased, whereas the temperature increase from 20 to 60°C increased the optimal W_{opt} by 10–20 times for optimal binder compositions. Moreover, according to the data of Table 6 and Fig. 5, it was revealed that the surface tension decreased at a higher temperature, which in turn led to an increase in the optimal impregnation rate.

Thus, it was concluded that increasing the temperature of optimal binder compositions based on EO–AD systems using active diluents of different nature, functionality, and molecular weight, allows the regulation of the technological characteristics of polymer binders, i.e., the surface tension, while increasing the impregnation rate of reinforcing systems by 10–20 times.

CONCLUSIONS

The surface tension and the static and dynamic contact angles of the EO, laproxides, laprolate, and EO–AD systems were obtained. These data allowed the variation of the generated systems' properties within a wide range and the regulation of the compositions and technological properties of epoxy binders and the impregnation parameters of fibrous fillers. Increasing the impregnation temperature from 20 to 60°C reduced the surface tension of the EO–AD systems by about two times, thus significantly improving the impregnation quality of fiber and frame fillers and increasing the impregnation speed by 10–20 times.

The authors declare no conflicts of interest.

REFERENCES

1. Deberdeev T.R., Garipov R.M., Sychova M.V., Ulitin N.V., Fomin A.A., Irzhak V.I. Description of the topological structure of cyclocarbonate-modified epoxyamine systems. *Vestnik Kazanskogo tekhnologicheskogo universiteta = Herald of Kazan Technological University.* 2008;(5):112-118 (in Russ.).

2. Antipova E.A., Korotkova N.P., Lebedev V.S. Modern polyurethane, epoxy, PU acrylate and epoxy acrylate binders for industrial coatings manufactured by NPP Macromer LLC. *Russian Coatings Journal (Lakokrasochnye materialy i ikh primenenie)* 2012;(9):14-21 (in Russ.).

СПИСОК ЛИТЕРАТУРЫ

1. Дебердеев Т.Р., Гарипов Р.М., Сычова М.В., Улитин Н.В., Фомин А.А., Иржак В.И. Описание топологической структуры модифицированных циклокарбонатом эпоксиаминных систем. *Вестник Казанского технологического университета.* 2008;(5):112-118.

2. Антипова Е.А., Короткова Н.П., Лебедев В.С. Современные полиуретановые, эпоксидные, ПУ- акрилатные и эпоксиакрилатные связующие для индустриальных ЛКМ производства ООО «НПП Макромер». *Лакокрасочные материалы и их применение.* 2012;(9):14-21.

3. Shode L.G., Sorokin M.F., Kuzmin A.I. Glycidyl esters of carboxylic acids and their use. *Russian Coatings Journal (Lakokrasochnye materialy i ikh primenenie)* 1982;(4):20-23 (in Russ.).

4. Osipchik V.S., Smotrova S.A. Tomilchik A.Ya. Investigation of the properties of modified epoxy-containing oligomers. *Plasticheskie Massy.* 2011;(2):4-7. (in Russ.).

5. Zhavoronok E.S., Senchikhin I.N., Vysotskii V.V. *et al.* Effect of the nature and associate structure of an epoxy oligomer on the rate of its curing with diamine. *Polym. Sci. Ser. B.* 2017;(59):421-429.
https://doi.org/10.1134/S1560090417040121

6. Sidorov O.I., Dubkov K.A., Semikolenov S.V. *et al.* A Study of the Properties of Unsaturated Polyketone as a Representative of New-Type Reactive Oligomers for the Development of an Adhesive Composition on Its Basis. *Polym. Sci. Ser. D.* 2018;(11):215-224.
https://doi.org/10.1134/S199542121802017X

7. Kryzhanovsky V.K., Burlov V.V., Semenova A.D., Zhorova Yu.V. Study of the effect of laproxides on the physical properties and deformation behavior of epoxy-dianic polymers. *Plasticheskie Massy.* 2011;(9):29-32 (in Russ.).

8. Trofimov A.N., Apeksimov N.V., Simonov-Emelyanov I.D., Prokhorova Yu.S. Influence of diluents on the kinetics of volumetric shrinkage and stresses during curing of epoxydian oligomers. *Tonk. Khim. Tekhnol. = Fine Chem. Technol.* 2016;11(6):103-107 (in Russ.).
https://doi.org/10.32362/2410-6593-2016-11-6-103-107

9. Senchikhin I.N, Sotnikova E.F, Zhavoronok E.S, Kiselev M.R, Chalykh A.E. Study of the curing of epoxyamine mixtures in the presence of an active diluent by DSC. *Uspekhi v Khimii i Khimicheskoi Tekhnologii.* 2007;3(71):77-81 (in Russ.).

10. Mezhikovsky S.M., Irzhak V.I. *Khimicheskaya fizika otverzhdeniya oligomerov* (Chemical physics of curing oligomers). Moscow: Nauka; 2008. 269 p. (in Russ.).

11. Kanovich M.Z., Trofimov N.N. Soprotivlenie kompozitsionnykh materialov Resistance of composite materials. Moscow: Mir; 2004. 504 p. (in Russ.).

12. Kiselev V.I., Sokolov V.I., Shalgunov S.I. Method for measuring the surface tension coefficient and static and dynamic contact angles of wetting: RF Pat. 2 244 288 C1, 2004.04.01 (in Russ.).

3. Шодэ Л.Г., Сорокин М.Ф., Кузьмин А.И. Глицидиловые эфиры карбоновых кислот и их применение. *Лакокрасочные материалы и их применение.* 1982;(4):20-23.

4. Осипов П.В., Осипчик В.С., Смотрова С.А., Томильчик А.Я. Исследование свойств модифицированных эпоксисодержащих олигомеров. *Пластические массы.* 2011;(2):4-7.

5. Zhavoronok E.S., Senchikhin I.N., Vysotskii V.V. *et al.* Effect of the nature and associate structure of an epoxy oligomer on the rate of its curing with diamine. *Polym. Sci. Ser. B.* 2017;(59):421-429.
https://doi.org/10.1134/S1560090417040121

6. Sidorov O.I., Dubkov K.A., Semikolenov S.V. *et al.* A Study of the Properties of Unsaturated Polyketone as a Representative of New-Type Reactive Oligomers for the Development of an Adhesive Composition on Its Basis. *Polym. Sci. Ser. D.* 2018;(11):215-224.
https://doi.org/10.1134/S199542121802017X

7. Крыжановский В.К., Бурлов В.В., Семенова А.Д., Жорова Ю.В. Изучение влияния лапроксидов на физические свойства и деформационное поведение эпоксидно-диановых полимеров. *Пластические массы.* 2011;(9):29-32.

8. Трофимов А.Н., Апексимов Н.В., Симонов-Емельянов И.Д., Прохорова Ю.С. Влияние разбавителей на кинетику объемной усадки и напряжений при отверждении эпоксидиановых олигомеров. *Тонкие химические технологии.* 2016;11(6):103-107.
https://doi.org/10.32362/2410-6593-2016-11-6-103-107

9. Сенчихин И.Н., Сотникова Е.Ф., Жаворонок Е.С., Киселев М.Р., Чалых А.Е. Исследование отверждения эпоксиаминных смесей в присутствии активного разбавителя методом ДСК. *Успехи в химии и химической технологии.* 2007;3(71):77-81.

10. Межиковский С.М., Иржак В.И. Химическая физика отверждения олигомеров. М.: Наука; 2008. 269 с.

11. Канович М.З., Трофимов Н.Н. Сопротивление композиционных материалов. М.: Мир; 2004. 504 с.

12. Киселёв В.И., Соколов В.И., Шалгунов С.И. Способ измерения коэффициента поверхностного натяжения и статического и динамического краевых углов смачивания: Патент РФ 2 244 288 C1, 2004.04.01.

About the authors:

Angelina D. Bresskaya, Master Student, Department of Chemistry and Technology of Plastic Processing and Polymer Composites, M.V. Lomonosov Institute of Fine Chemical Technologies, MIREA – Russian Technological University (86, Vernadskogo pr., Moscow, 119571, Russia). E-mail: angelinabresskaya@gmail.com. https://orcid.org/0000-0002-4941-2036

Dmitry A. Trofimov, Postgraduate Student, Department of Chemistry and Technology of Plastic Processing and Polymer Composites, M.V. Lomonosov Institute of Fine Chemical Technologies, MIREA – Russian Technological University (86, Vernadskogo pr., Moscow, 119571, Russia). E-mail: trofimov_d_a95@mail.ru. https://orcid.org/0000-0002-8458-3690

Igor D. Simonov-Emel'yanov, Dr. of Sci. (Engineering), Professor, Head of the Department of Chemistry and Technology of Plastic Processing and Polymer Composites, M.V. Lomonosov Institute of Fine Chemical Technologies, MIREA – Russian Technological University (86, Vernadskogo pr., Moscow, 119571, Russia). E-mail: simonov@mitht.ru. Scopus Author ID 6603181099

Sergey I. Shalgunov, Cand. of Sci. (Chemistry), Director of VNIISPV, NPO Stekloplastic (3-A, Andreevka, Solnechnogorsk district, Moscow oblast, 141551, Russia). E-mail: shsi@aha.ru. https://orcid.org/0000-0001-5893-6811

Vladimir I. Sokolov, Deputy Director of VNIISPV, NPO Stekloplastic (3-A, Andreevka, Solnechnogorsk district, Moscow oblast, 141551, Russia). E-mail: v.sokolov45@mail.ru. https://orcid.org/0000-0002-3104-3770

Об авторах:

Бресская Ангелина Дмитриевна, магистрант кафедры «Химия и технология переработки пластмасс и полимерных композитов» Института тонких химических технологий им. М.В. Ломоносова ФГБОУ ВО «МИРЭА – Российский технологический университет» (119571, Россия, Москва, пр-т Вернадского, д. 86). E-mail: angelinabresskaya@gmail.com. https://orcid.org/0000-0002-4941-2036

Трофимов Дмитрий Александрович, аспирант кафедры «Химия и технология переработки пластмасс и полимерных композитов» Института тонких химических технологий им. М.В. Ломоносова ФГБОУ ВО «МИРЭА – Российский технологический университет» (119571, Россия, Москва, пр-т Вернадского, д. 86). E-mail: trofimov_d_a95@mail.ru. https://orcid.org/0000-0002-8458-3690

Симонов-Емельянов Игорь Дмитриевич, профессор, доктор технических наук, заведующий кафедрой «Химия и технология переработки пластмасс и полимерных композитов» Института тонких химических технологий им. М.В. Ломоносова ФГБОУ ВО «МИРЭА – Российский технологический университет» (119571, Россия, Москва, пр-т Вернадского, д. 86). E-mail: simonov@mitht.ru. Scopus Author ID 6603181099

Шалгунов Сергей Иосифович, кандидат химических наук, директор ВНИИ стеклопластиков и стекловолокна (ВНИИСПВ) АО «НПО Стеклопластик» (141551, Россия, Московская область, Солнечногорский р-н, пос. Андреевка, стр. 3-А). E-mail: shsi@aha.ru. https://orcid.org/0000-0001-5893-6811

Соколов Владимир Иванович, заместитель директора ВНИИ стеклопластиков и стекловолокна (ВНИИСПВ) АО «НПО Стеклопластик» (141551, Россия, Московская область, Солнечногорский р-н, пос. Андреевка, стр. 3-А). E-mail: v.sokolov45@mail.ru. https://orcid.org/0000-0002-3104-3770

Submitted: November 13, 2019; Reviewed: April 13, 2020; Accepted: May 25, 2020.

Translated from Russian into English by N. Isaeva
Edited for English language and spelling by Enago, an editing brand of Crimson Interactive Inc.

ISSN 2686-7575 (Online)

https://doi.org/10.32362/2410-6593-2020-15-3-58-69

UDC 665.656.2

Aluminum oxide carrier for a catalyst for low-temperature isomerization of hydrocarbons

Nurjahan Tagandurdyyeva[@], Natalya V. Maltseva, Tatyana A. Vishnevskaya, Vyacheslav N. Narayev, Arkady Yu. Postnov

Saint-Petersburg State Institute of Technology, St. Petersburg, 190013 Russia
[@]Corresponding author, e-mail: jahana_18101993@mail.ru

Objectives. *Determine the necessary conditions for obtaining a granulated η-Al_2O_3 carrier, investigate its structural and strength properties, and evaluate its activity for the model n-butane isomerization reaction.*

Methods. *Samples containing bayerite structure aluminum trihydroxide were synthesized by precipitation from aqueous solutions of aluminum nitrate with ammonia under isothermal conditions at a constant pH value. The samples of the granulated carrier were obtained using an extrusion method when the composition of molding pastes was varied by tuning the ratio of bayerite- and η-Al_2O_3-containing components and introducing polyvinyl alcohol.*

Results. *The influence of the preparation conditions on the structural and strength properties of the active Al_2O_3 granules is evaluated. Samples of the aluminum oxide carrier were tested for a model reaction of low-temperature isomerization of n-butane, demonstrating a sufficiently high selectivity and reasonable prospects for use as catalysts for low-temperature isomerization of hydrocarbons.*

Conclusions. *Increasing the content of the polyvinyl alcohol in the molding paste from 0.4 to 1.8 wt % is accompanied by an increase in the predominant sizes of the mesopores in the range of 10–50 nm and pores in the range of 50–80 nm, explaining the high values of all recorded parameters for the process of isomerization of n-butane.*

Keywords: *isomerization, n-alkanes, the carrier of the catalyst for isomerization, aluminum oxide, bayerite.*

For citation: Tagandurdyyeva N., Maltseva N.V., Vishnevskaya T.A., Narayev V.N., Postnov A.Yu. Aluminum oxide carrier for a catalyst for low-temperature isomerization of hydrocarbons. *Tonk. Khim. Tekhnol. = Fine Chem. Technol.* 2020;15(3):58-69. https://doi.org/10.32362/2410-6593-2020-15-3-58-69

Алюмооксидный носитель для катализатора низкотемпературной изомеризации углеводородов

Н. Тагандурдыева[@], Н.В. Мальцева, Т.А. Вишневская, В.Н. Нараев, А.Ю. Постнов

Санкт-Петербургский государственный технологический институт (технический университет), Санкт-Петербург, 190013 Россия
[@]Автор для переписки, e-mail: jahana_18101993@mail.ru

Цели. *Определение условий получения гранулированного η-Al_2O_3-носителя, исследование его структурно-прочностных свойств и оценка активности в модельном процессе изомеризации н-бутана.*

Методы. *Образцы, содержащие тригидроксид алюминия байеритной структуры, синтезированы осаждением из водных растворов нитрата алюминия аммиаком в изотермических условиях при постоянном значении pH. Экструзионным методом получены образцы гранулированного носителя при варьировании состава формовочных паст: соотношения количеств байерит- и η-Al_2O_3-содержащих компонентов и введения поливинилового спирта.*

Результаты. *Оценено влияние условий приготовления на структурно-прочностные свойства гранул активного Al_2O_3. Образцы алюмооксидного носителя испытаны в модельной реакции низкотемпературной изомеризации н-бутана, показана их достаточно высокая селективность и перспективность при получении катализаторов низкотемпературной изомеризации углеводородов.*

Выводы. *Увеличение содержания поливинилового спирта в формовочной пасте от 0.4 до 1.8 масс. % сопровождается смещением преобладающих размеров мезопор в интервале 10–50 нм и пор в интервале 50–80 нм в большую сторону, что объясняет высокие значения всех регистрируемых показателей процесса изомеризации н-бутана.*

Ключевые слова: *изомеризация, н-алканы, носитель катализатора изомеризации, оксид алюминия, байерит.*

Для цитирования: Тагандурдыева Н., Мальцева Н.В., Вишневская Т.А., Нараев В.Н., Постнов А.Ю. Алюмооксидный носитель для катализатора низкотемпературной изомеризации углеводородов. *Тонкие химические технологии.* 2020;15(3):58-69. https://doi.org/10.32362/2410-6593-2020-15-3-58-69

INTRODUCTION

The process of isomerization of linear alkanes to produce automobile fuels is a key stage for ensuring the conversion of low-octane unbranched paraffins to high-octane branched molecules. This process can be considered an effective and economically viable way to increase the octane number of motor gasoline without forming significant quantities of aromatic compounds [1].

The isomerization process occurs on acid catalysts and can be initiated by strong Lewis acids, Friedel–Crafts catalysts, at relatively low temperatures but with the significant disadvantages of instability and highly corrosive nature [2, 3]. In industrial isomerization processes, solid acids with platinum deposits are usually used as catalysts, of which platinum deposited on chlorinated aluminum oxide or zeolites are the most commonly used catalytic systems [4–6]. Zeolites are less acidic than chlorinated aluminum oxides, thus requiring higher temperatures (250–400°C) for isomerization to occur, resulting in the lower production of branched isomers [3, 7].

The most active catalysts currently used for the isomerization process are chlorinated aluminum-platinum catalysts (Pt/Al_2O_3-Cl). The increased activity of these catalysts allows isomerization at low temperatures of 120–180°C, with high degrees of conversion (X = 28%) and selectivity (S = 98%) for the target product [7, 8].

Aluminum oxide is widely used as a carrier for aluminum-platinum catalysts, in particular the γ- and η-Al_2O_3 forms. However, the η-Al_2O_3 oxide demonstrates advantages over γ-Al_2O_3 in some cases, as granulated η-Al_2O_3 is characterized by both a high specific surface area (S_{sp} = 300–400 m^2/g) and the presence of large mesopores with a size of more than 25 nm ($V_{mesopores}$ = 0.10–0.25 cm^3/g), as well as increased Lewis acidity [2].

η-Al_2O_3 oxide is primarily obtained by the heat treatment of bayerite structure aluminum trihydroxide. The most common method for obtaining bayerite is via precipitation from aqueous solutions of aluminum salts with solutions of ammonia or alkalis [9]. The precipitation of aluminum hydroxide is generally conducted at pH values of 10–11, at which bayerite falls out as large, poorly hydrated, and loosely packed crystals with gaps filled with colloid-bound water. However, the link of water in bayerite, unlike pseudoboehmite, is not durable. Therefore, bayerite precipitates are considerably more thixotropic and under the influence of the shear loads that occur during the preparation of the molding pastes and their extrusion, sharply liquefy. When the shear loads are reduced, they become sharply structured, significantly complicating the process of forming the trihydroxide [10]. Researchers found that this property occurs in a much greater extent in molding pastes made of bayerite precipitated from aluminum salts by ammonia, compared to those obtained using sodium hydroxide as the precipitator [11]. In the latter case, careful washing of the precipitate is required, as strict restrictions exist on the levels of sodium (no more than 0.02 wt %) in carriers for isomerization catalysts [11]. This leads to prioritizing precipitating bayerite with ammonia, as the high structuring of the pastes obtained from hydroxide complicates their extrusion and requires finding conditions for the preparation of granulated oxide η-Al_2O_3 that meet the suitability requirements for a hydrocarbon isomerization catalyst.

A promising method of regulating the properties of aluminum oxide-based molding pastes is changing the properties of the dispersed phase by introducing aluminum oxide powder as a heterogeneous additive [12] and the dispersion medium by introducing a water-soluble organic polymer, polyvinyl alcohol (PVA), as a surfactant. The content of the dispersed phase plays an important role in the system [13].

The objective of this work was to determine conditions for obtaining a granular η-Al_2O_3 carrier, study its structural and strength properties, and evaluate its activity for *n*-butane isomerization.

MATERIALS AND METHODS

Obtaining experimental bayerite-containing samples by deposition

Samples containing bayerite structure aluminum trihydroxide were obtained by precipitation of an aluminum salt solution with an ammonia solution. Nonahydrate aluminum nitrate $Al(NO_3)_3 \cdot 9H_2O$ (GOST 3757-75, batch 25, *NevaReaktiv*, Russia, purity 97%) was used as the initial reagent for preparing a 5 mol/L salt solution. A 25% solution of ammonia $NH_3 \cdot H_2O$ (GOST 3760-79, batch 49, *NevaReaktiv*, Russia, purity 25%) was diluted to give a 5 mol/L ammonia solution. The following conditions for the preparation of bayerite-containing samples were based on prior literature results [14].

The solutions were mixed in a glass reactor containing an ammonia buffer solution of pH = 10.3–10.5 with constant stirring (the speed of rotation of the agitator is ~300 rpm). Simultaneous supply of the solutions of aluminum nitrate and ammonia to the reactor was performed using a peristaltic pump with a flow rate of 1 and 5 mL/min, respectively. The reaction medium was maintained at a constant pH value of 10.5 ± 0.1, which was monitored at 30 min intervals. The set pH value was created by a 5-fold excess of ammonia relative to the stoichiometry of the reaction:

$$Al(NO_3)_3 + 3NH_4OH = Al(OH)_3 \downarrow + 3NH_4NO_3$$

Using a thermostat, the temperature of the reaction medium was maintained at 20 ± 1°C. Under isothermal conditions, the duration of the deposition process was 2 h, and the duration of the aging process of the resulting sediment was 24 h.

The resulting precipitate was separated using a Buchner funnel and washed a neutral reaction pH. The precipitate was dried at a temperature of 100–110°C to a constant mass. The content of bayerite in the synthesized hydroxide precipitate was 85 ± 2 wt % [14].

Obtaining systems containing η-Al_2O_3

During this work, a series of carriers were obtained by the extrusion method (Table 1), differing in their ratios of the amounts of introduced bayerite- and η-Al_2O_3-containing components.

For the production of carrier granules, molding pastes were prepared using powdered components: bayerite-containing hydroxide (hereinafter bayerite), dried at 110°C and η-Al_2O_3-containing aluminum oxide (hereinafter η-Al_2O_3), obtained by the calcination of synthesized hydroxide at 500°C.

When mixed with distilled water, bayerite powder or its mixtures with 20–80 wt % oxide powder undergo further homogenization with the application of shear loads. However, pastes suitable for extrusion could not be obtained.

Using a five percent polyvinyl alcohol/distilled water solution as a plasticizer allowed the homogenized pastes to be formed in a screw granulator through a 2-mm-diameter die.

Extrudates, after "drying" at 20 ± 2°C for 16–18 h and drying at 100–110°C to constant mass, were heat-treated at 280–290°C and 500–510°C for 4 h at each temperature (temperature rise rate of 10°C/min).

Table 1. Compositions of molding pastes

Sample No.	Bayerite	η-Al_2O_3	Humidity,* wt %	PVA**, wt % (in relation to bayerite)
	wt % (according to Al_2O_3)			
1	20	80	49.5	2.7
2	40	60	51	
3	60	40	52	
4	80	20	55	
5	100	0	56	

*ratio of the total mass of water contained in each component to the total mass of all components;
**PVA—polyvinyl alcohol.

Sample characterization methods

Differential thermal (DTA) and thermogravimetric analysis of synthesized bayerite samples were performed in an air atmosphere on a SHIMADZU DTG-60H derivatograph at a heating rate of 10°C/min from room temperature to 800°C. The mass of per sample was ≈ 15–50 mg. The temperature was determined with an accuracy of 1°C and the mass change with an accuracy up to 0.1%. Quantitatively, the phase composition of the samples was determined based on the observed mass loss as a result of thermolysis. The phase composition of the dried bayerite samples was studied by X-ray phase analysis, using a multifunctional X-ray diffractometer "RigakuSmartLab 3" (*RigakuCorporation*, Tokyo, Japan) with CuKα-monochromatic radiation in the range of angles 2Θ = 10°–80° with a scanning speed of 10 °C/min. The volume of the loaded sample was no less than 0.1 cm^3, and the angular resolution of the reflections was up to 0.01°. Transcription of the radiographs was performed using Crystallographica Search-Match V. 2,0,3,1 Oxford Cryosystems, and the standard database was used for decryption.

The fractional composition of powders of the synthesized samples of bayerite and η-Al_2O_3 used for the preparation of molding pastes was determined by laser scattering using the SALD-2201 Laser Diffraction Particle Size Analyzer (*SHIMADZU*, Japan).

The surface acidity function (H_0) of the carrier samples was determined by pH-metry, using a pH meter-millivoltmeter pH-673.M with a glass electrode EVL-1M3 in an aqueous medium exhibiting pH_{H2O} in the range 6.4–6.6, according literature methods [15].

The specific surface area (S_{sp}) of granulated experimental samples was determined by the thermal desorption of nitrogen, using the single-point Bruner-Emmet-Teller method.

Tests of granulated sample strength during crushing "on the end" ($P_{□}$) were conducted using a MP-2C extensometer device according to prior literature [17].

The determination of the total pore volume (V_{Σ}) of granular samples by moisture capacity was performed, using water as a pycnometric liquid [18].

Studies of the distribution of pore volume by size were carried out using nitrogen porometry. Nitrogen adsorption/desorption isotherms were determined using a "Autosorb 6iSA" facility (*Quantachrome Instruments*, USA) after degassing the samples in a vacuum oven at 250℃ for 1 h. The specific surface area, specific pore volume (pore filling with adsorbate at its relative pressure ≈ 1), and average effective pore size were determined using density functional theory [16].

To determine the relative activity of carrier samples to evaluate their prospects as effective acid isomerization catalysts, tests were performed for the *n*-butane isomerization reaction, using the method of *NPF OLKAT* company in accordance with established recommendations [19]. The tests were performed while loading the catalyst carrier, 3.0 cm^3, under the following conditions: reactor inlet temperature was 75°C, the volume flow rate of *n*-butane (per liquid) was 1 h^{-1}, and the molar ratio of H_2 : *n*-butane was maintained at 1 : 1. Analysis for the content of isomerizate in the gas mixture at the reactor exit was performed by gas chromatography [19].

The research was carried out on research equipment provided by the Engineering Center of the Saint-Petersburg State Technological Institute (Technical University) and *NPF OLKAT*.

RESULTS AND DISCUSSION

Figure 1 presents the results of the phase composition study on the synthesized samples of aluminum hydroxide by X-ray phase analysis. The diffraction maxima, which are characteristic for aluminum hydroxides of bayerite and boehmite structures, are determined based on the given X-ray pattern.

The study of the aluminum hydroxide samples by DTA allowed us to quantify the content of bayerite structure aluminum trihydroxide in the samples. According to calculations based on mass loss, deposition under experimental conditions (for 2 h of deposition and 24 h of aging) leads to the formation of 85 ± 2 wt % bayerite. Figure 2 shows the derivatogram of the resulting sediments.

When heated, two endoeffects can be observed on the DTA curve with minimums at 63°C and 278°C. The first is related to the removal of physically adsorbed water. Literature data [9, 10, 20] show that the phase transition of bayerite to η-Al_2O_3 occurs in the temperature range of 250–350°C, the cause of the second endothermic effect.

The quantitative evaluation of the phase composition of the calcination product of the synthesized bayerite powder at 500°C shows a content of 80 wt % η-Al_2O_3 and 20 wt % γ-Al_2O_3 [14].

The fractional compositions of the powders of the synthesized sample of bayerite and η-Al_2O_3 used for the preparation of molding pastes are shown in Fig. 3, 4 and in Table 2.

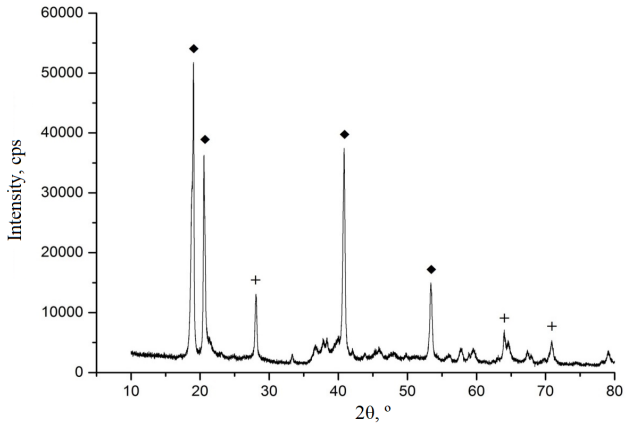

Fig. 1. X-ray diffraction pattern of the synthesized bayerite sample (♦ – bayerite; + – boehmite).

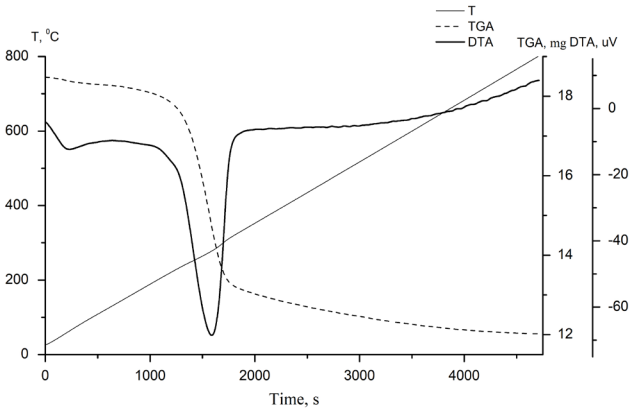

Fig. 2. Derivatogram of a synthesized bayerite sample.

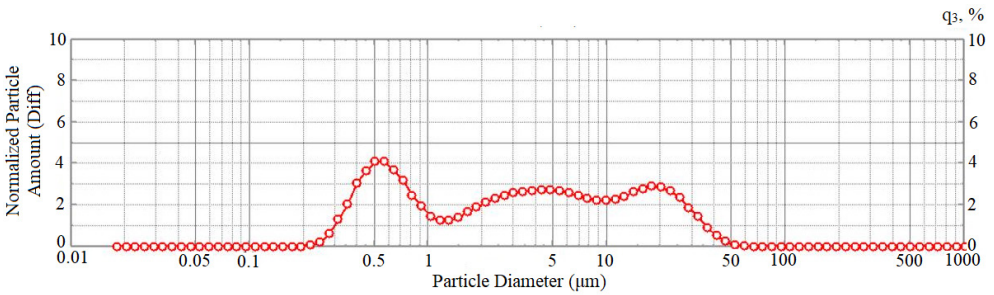

Fig. 3. Differential particle size distribution curve of bayerite powder.

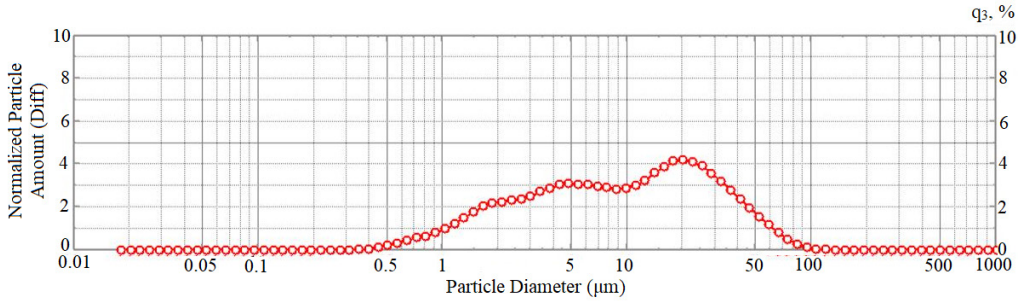

Fig. 4. Differential particle size distribution curve of η-Al_2O_3 powder.

Table 2. Fractional composition of bayerite and η-Al_2O_3 powders used for the preparation of molding pastes

Sample	Fraction, μm	Content, wt %	Prevailing size,* μm
Bayerite	0.2–1	30.6	0.5
	1–10	42.0	5
	10–50	27.4	19
η-Al_2O_3	0.5–3	21.5	2
	3–10	30.4	5
	10–100	48.1	20

*equivalent diameter

Based on the obtained results, a bayerite precipitate with particles ranging in size from 0.2 to 50 μm is formed during deposition under the experimental conditions with particles of around 1 to 10 μm (42 wt %) predominating. Heat treatment of this sample at 500°C to produce η-Al_2O_3 leads to an increase in the particle size to 100 μm. At the same time, a decrease in the number of particles of the 0.5–3-μm fraction occurs.

The results of measurements of the surface acidity function, specific surface area, porous structure parameters, the crushing strength of granules, as well as the total pore volume of granular carrier samples are presented in Table 3.

The determination of the acid-base properties of the various carriers indicates that the studied conditions of their preparation do not affect the value of the Gammet function, $H_0 = 7.1 \pm 0.1$.

An increase in the proportion of bayerite powder in the molding paste (from sample 1 to sample 5) corresponds to an increase in the values of the following textural characteristics of the carrier granules: S_{sp} from 285 to 365 m^2/g, V_Σ from 0.68 to 0.76 cm^3/g, and $P_{\square}$ from 0.6 to 2.0 MPa.

These trends can be explained by the cumulative effect of changes that occur when particles are packed in pastes or granules, as well as the formation of interparticle contacts that ensure the strength of the porous body on the secondary porous structure and strength of granules. First, from sample 1 to sample 5, the proportion of smaller particles increases, increasing the number of single contacts per unit contact section and the proportion of reactive particles (hydroxide compared to oxide). Thus, the number of higher strength contacts increases, contributing to an increase in strength and a decrease in pore size. Second, an increase in the content of a burnout additive-PVA leads to the formation of an additional volume of secondary pores, increasing the total volume of pores V_Σ and decreasing the overall strength.

Data on the distribution of pore volume based on size, calculated from the integral and differential curves obtained from the results of the azotoporometry, are shown in Table 4.

According to the results shown in Table 4, an increase in the share of bayerite in the molding paste leads to a shift in the prevailing d_{max} pore size in the range of 3–10 nm from 4.6 to 3.7 nm and an increase in their volume from 0.12 to 0.14 cm^3/g. The change in these parameters is accompanied by an increase in the pore surface area in the range of 3–10 nm, as well as the "total" S_{sp} of carrier samples (see Tables 3 and 5). At the same time, (Table 4) a slight increase occurs in the prevailing pore sizes and volumes of larger pores, producing mesopores in the range of 10–50 nm (d_{max} from 27.4 to 31.5 nm and $V_{pores\ (10–50)}$ from 0.16 to 0.24 cm^3/g) and pores in the range of 50–80 nm (d_{max} from 65.2 to 77.8 nm and $V_{pores\ (50–80)}$ from 0.08 to 0.16 cm^3/g). This reflects changes in the secondary porous structure of the granules and may be due to the influence of the burning additive-PVA (see Tables 3 and 5).

The nitrogen adsorption-desorption isotherms of the synthesized carriers are shown in Fig. 5.

The sorption isotherms of all carrier samples, with some quantitative differences in the adsorption values at certain relative pressure values P/P_0, where P and P_0 are the equilibrium pressure and the saturated vapor pressure of the adsorbate at the adsorption temperature, respectively, exhibit the same shape. Hysteresis of all samples is H3 type, usually characterized by slit-like pores with almost flat-parallel walls. The adsorption branches of these isotherms exhibit the form typical of type II from the Brunauer classification, indicating the presence of polymolecular adsorption. No horizontal

Table 3. Properties of carrier samples

Characteristics	Sample No.				
	1	2	3	4	5
Surface acidity function H_0	7.1	7.1	7.1	7.0	7.2
Specific surface S_{sp}, m^2/g	285	290	300	310	365
Total pore volume V_Σ, cm^3/g	0.68	0.70	0.70	0.74	0.76
Maximum volume of sorption space W_S, cm^3/g	0.24	0.25	0.26	0.32	0.37
Macropore volume $V_{macro} = V_\Sigma - W_S$, cm^3/g	0.44	0.45	0.44	0.42	0.39
Strength $P_□$, MPa	0.6	0.7	1.6	2.0	2.0
Bulk density Δ, g/cm^3	0.57	0.57	0.54	0.54	0.53

*The composition of the molding pastes differs for the samples presented in Table 3: from sample 1 to 5, the content of hydroxide powder increases from 20 to 100 wt % (with regards to $A1_2O_3$) and the amount of polyvinyl alcohol (depending on the content of hydroxide powder) increases from 0.0054 to 0.027 g of PVA per 1 g Al_2O_3, corresponding to a PVA content of 0.4 to 1.8 wt %.

sections exist on the desorption branches and the position of the lower point of the hysteresis loop, which depends on the nature of the adsorbent rather than the texture of the sample, corresponds to the value P/P_0 = 0.40 [16]. The textural characteristics of the synthesized carriers are shown in Table 5.

Based on the observations during the extrusion of molding pastes, it can be concluded that the use of PVA as a component of the dispersion medium leads to a decrease in the degree of liquefaction of the molding paste during extrusion by enveloping the bayerite particles, thereby preventing the release of colloid-bound water and allowing the production of granules of the η-$A1_2O_3$ carrier. The use of aluminum oxide powder in the preparation of molding pastes can, within certain limits, helps regulate the porous structure of the obtained carriers.

The results of carrier sample testing for the low-temperature isomerization of *n*-butane are presented in Table 6. A carrier based on η-$A1_2O_3$ obtained from a powder of bayerite structure aluminum hydroxide produced by Pural BT (*Sasol*, Germany) was used as a comparison control sample.

The test results of the carrier samples show that, regardless of the ratio of bayerite- and Al_2O_3-containing components used, the samples demonstrate comparable selectivity with the reference model.

An increase in the proportion of bayerite in the molding paste leads to an increase in all monitored indicators of the *n*-butane isomerization process. This may be due to the noted increase in the specific surface area of the carrier samples and the volume of large mesopores in the range of 20–40 nm. Thus, sample 5 provides the highest selectivity and conversion values in the process.

CONCLUSIONS

The influence of forming conditions on the textural characteristics and catalytic activity of the low-temperature isomerization catalyst η-aluminum oxide carriers were studied.

We determined that during the deposition of bayerite from an aluminum nitrate solution with ammonia under literature conditions [14], a precipitate with particle sizes from 0.2 to 50 μm was formed, with further heat treatment of the sample at 500°C leading to an increase in the particle size to 100 μm.

We found that using PVA as a component of the dispersion medium of the forming pastes from bayerite powder led to a decrease in the degree of separation of colloid-bound water from the interlayer space of bayerite, providing the capability of obtaining granules of η-Al_2O_3 by screw extrusion.

The granules of the η-Al_2O_3 carrier obtained by the screw extrusion of pastes of bayerite powder with PVA were characterized by the following textural characteristics: S_{sp} = 365 m_2/g, V_Σ = 0.76 cm^3/g, W_s = 0.37 cm^3/g, V_{macro} = 0.39 cm^3/g, mechanical strength $P_□$ = 2.0 MPa. The introduction of the η-Al_2O_3 powder as a heterogeneous additive in the bayerite molding paste, plasticized by PVA, allowed us to regulate the porous structure of the resulting carriers. Their textural characteristics changed.

Table 4. Size distribution of the volumes and surface areas of pores

Sample No.	Characteristic	Range of pore size, nm		
		3–10	10–50	50–80
1	d_{max}, nm	4.6	27.4	65.2
	Pore volume, cm^3/g	0.12	0.16	0.08
	Surface area, m^2/g	130	90	5
2	d_{max}, nm	4.4	30.5	67.2
	Pore volume, cm^3/g	0.12	0.16	0.08
	Surface area, m^2/g	130	95	5
3	d_{max}, nm	3.9	31.5	69.2
	Pore volume, cm^3/g	0.12	0.18	0.14
	Surface area, m^2/g	100	125	10
4	d_{max}, nm	3.9	31.5	71.3
	Pore volume, cm^3/g	0.13	0.21	0.15
	Surface area, m^2/g	110	150	10
5	d_{max}, nm	3.7	31.5	77.8
	Pore volume, cm^3/g	0.14	0.24	0.16
	Surface area, m^2/g	215	155	10

Table 5. Summary data table of the porous structure of synthesized carriers studied by nitrogen porosimetry at 77 K using an Autosorb 6iSA unit

Defined parameter	Sample No.				
	1	2	3	4	5
Specific surface, m^2/g	230	240	250	275	380
Pore volume, cm^3/g	0.39	0.48	0.38	0.54	0.53

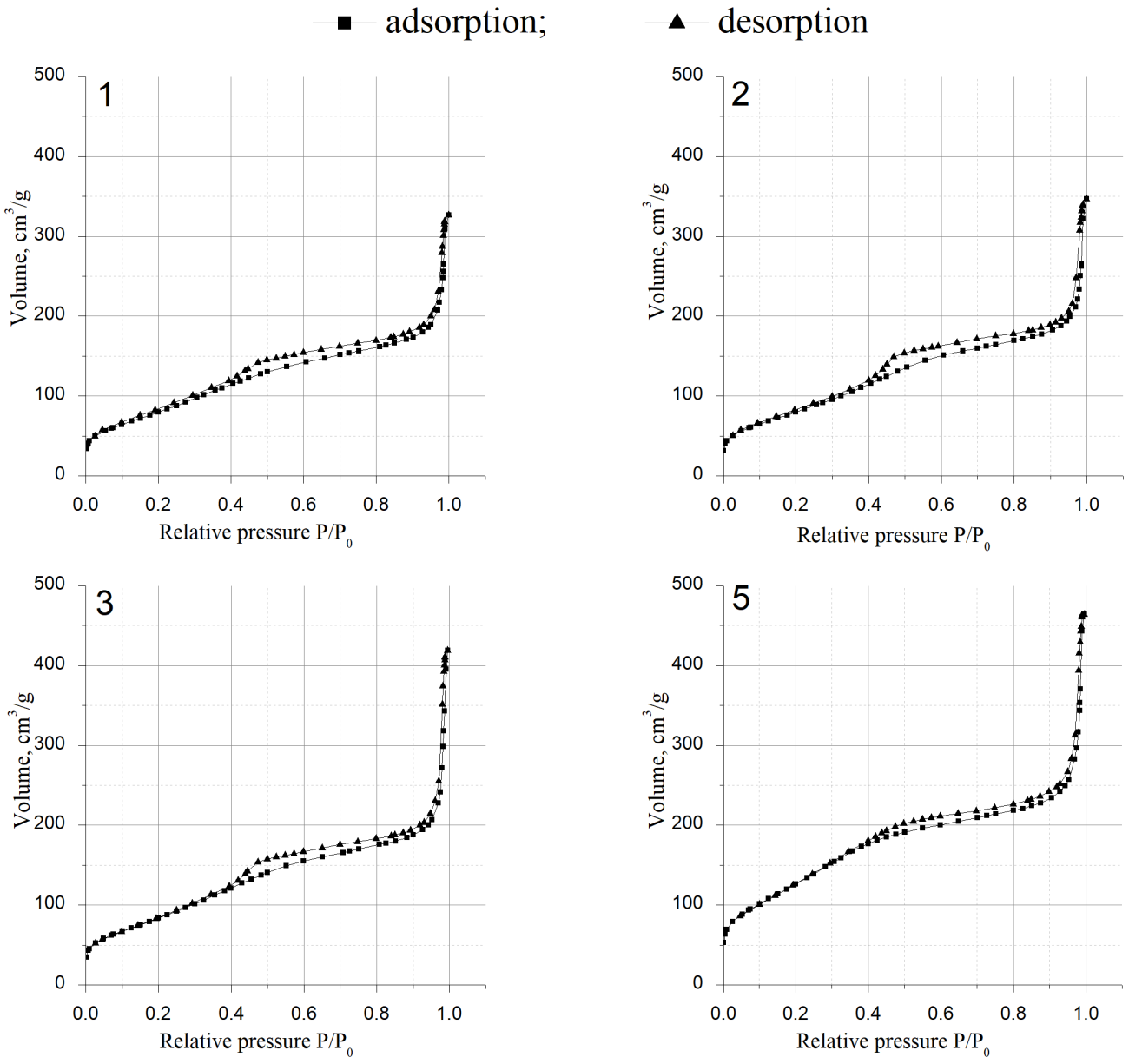

Fig. 5. Nitrogen adsorption-desorption isotherms at 77 K for synthesized carrier samples (the numbers on the graph corresponds to the sample number).

Table 6. Test results of the carrier samples for the low-temperature isomerization reaction of *n*-butane

Activity indicator	Sample No.					*Sasol*
	1	2	3	4	5	
Depth of isomerization *I*, %	17.0	20.5	20.9	21.3	21.4	21.8
Conversion of *n*-butane *K*, %	17.5	21.2	21.6	22	22.1	24.3
Selectivity *S*, %	94.5	94.8	95.3	95.3	95.6	94.4

Increasing the mass fraction of the powder in a mixture with bayerite to 80 mass % led to a decrease in the S_{sp} to 285 m^2/g, V_{Σ} to 0.68 cm^3/g, W_s to 0.24 cm^3/g, and an increase in the V_{macro} to 0.44 cm^3/g, with an unfortunately noticeable decrease in the mechanical strength of the $P_{\square}$ to 0.6 MPa. Increasing the PVA content in the molding paste from 0.4 to 1.8 wt % accompanied an increase in the ranges of the prevailing size of the secondary pores to values of 10–50 and 50–80 nm.

Tests of the carriers for catalytic isomerization of *n*-butane revealed that the samples, which are different in the ratio of the initial bayerite and Al_2O_3-containing components, have approximately equal and sufficiently high selectivity and are promising materials as catalysts for low-temperature isomerization of hydrocarbons.

The authors declare no conflicts of interest.

REFERENCES

1. Valavarasu G., Sairam B. Light Naphta Isomerization Process: A Review. *Petrol. Sci. Technol.* 2013;31(6):580-595. https://doi.org/10.1080/10916466.2010.504931

2. Borutsky P.N. Catalytic processes for the production of branched hydrocarbons. St. Petersburg: NPO Professional; 2010. 724 p. (in Russ.).

3. Ono Y. A survey of the mechanism in catalytic isomerization of alkanes. *Catal. Today.* 2003; 81(1):3-16. https://doi.org/10.1016/S0920-5861(03)00097-X

4. Smolikov M., Dzhikiya O., Zatolokina E., Kiryanov D., Belyi A. Isomerization of *n*-hexane over bifunctional $Pt/SO_4/ZrO_2$ catalysts. *Petrol. Chem.* 2009;49(473):473-480. https://doi.org/10.1134/S096554410906005X

5. Yasakova E.A., Sitdikova A.V., Akhmetov A.F. Trends in the development of the isomerization process in Russia and abroad. *Neftegazovoe delo = Electronic scientific journal Oil and Gas Business.* 2010;1:1-19 (in Russ.). Available from: http://ogbus.ru/files/ogbus/authors/Yasakova/Yasakova_1.pdf

6. Sousa B.V., Brito K.D., Alves J.J.N., Rodrigues M.G.F., Yoshioka C.M.N., Caardoso D. *n*-Hexane Isomerization on Pt/HMOR: Effect of Platinum Content. *Reaction Kinetics, Mechenisms and Catalysis.* 2011;102(2):473-485. https://doi.org/10.1007/s11144-010-0273-0

7. Hidalgo J.M., Zbuzek M., Černý R., Jíša P. Current uses and trends in catalytic isomerization, alkylation and etherification processes to improve gasoline quality. *Cent. Eur. J. Chem.* 2014; 12(1):1-13. https://doi.org/10.2478/s11532-013-0365-6

8. Borutsky P.N., Podkletnova N.M. Catalytic processes of isomerization and dehydrogenation of hydrocarbons for the production of gasoline isocomponents. *Kataliz v promyshlennosti (Catalysis in Industry).* 2003;2:86-88 (in Russ.).

9. Ivanova A.S. Alumina: application, production methods, structure and acid-base properties. *Promyshlennyi kataliz v lektsiyakh = Industrial Catalysis in Lectures.* 2009;8:7-61 (in Russ.).

10. Chukin G.D. *Stroenie oksida alyuminiya i katalizatorov gidroobesserivaniya. Mekhanizmy reaktsii* (The structure of alumina and hydrodesulfurization catalysts. Reaction mechanisms). Moscow: Printa; 2012. 288 p. ISBN 5-93969-036-X (in Russ.).

11. Kinyakin A.S., Glushachenkova E.A., Borutskii P.N., Shuvalov A.S., Pisarenko Yu.A. Kinetics of the low-temperature isomerization of *n*-hexane on the NIP-3A catalyst in an isothermal flow reactor. *Theor. Found. Chem. Eng.* 2008;42(6):815-821. https://doi.org/10.1134/S0040579508060031

СПИСОК ЛИТЕРАТУРЫ

1. Valavarasu G., Sairam B. Light Naphta Isomerization Process: A Review. *Petrol. Sci. Technol.* 2013;31(6):580-595. https://doi.org/10.1080/10916466.2010.504931

2. Боруцкий П.Н. Каталитическиепроцессы получения углеводородов разветвленного строения. СПб.: НПО «Профессионал»; 2010. 724 с.

3. Ono Y. A survey of the mechanism in catalytic isomerization of alkanes. *Catal. Today.* 2003; 81(1):3-16. https://doi.org/10.1016/S0920-5861(03)00097-X

4. Smolikov M., Dzhikiya O., Zatolokina E., Kiryanov D., Belyi A. Isomerization of *n*-hexane over bifunctional $Pt/SO_4/ZrO_2$ catalysts. *Petrol. Chem.* 2009;49(473):473-480. https://doi.org/10.1134/S096554410906005X

5. Ясакова Е.А., Ситдикова А.В., Ахметов А.Ф. Тенденции развития процесса изомеризации в России и за рубежом. *Электронный научный журнал Нефтегазовое дело.* 2010;1:1-19. URL: http://ogbus.ru/files/ogbus/authors/Yasakova/Yasakova_1.pdf

6. Sousa B.V., Brito K.D., Alves J.J.N., Rodrigues M.G.F., Yoshioka C.M.N., Caardoso D. *n*-Hexane Isomerization on Pt/HMOR: Effect of Platinum Content. *Reaction Kinetics, Mechanisms and Catalysis.* 2011;102(2):473-485. https://doi.org/10.1007/s11144-010-0273-0

7. Hidalgo J.M., Zbuzek M., Černý R., Jíša P. Current uses and trends in catalytic isomerization, alkylation and etherification processes to improve gasoline quality. *Cent. Eur. J. Chem.* 2014;12(1):1-13. https://doi.org/10.2478/s11532-013-0365-6

8. Боруцкий П.Н., Подкетнова Н.М. Каталитические процессы изомеризации и дегидрирования углеводородов для производства изокомпонентов бензинов. *Катализ в промышленности.* 2003;2:86-88.

9. Иванова А.С. Оксид алюминия: применение, способы получения, структура и кислотно-основные свойства. *Промышленный катализ в лекциях*. 2009;8:7-61.

10. Чукин Г.Д. Строение оксида алюминия и катализаторов гидрообессеривания. Механизмы реакций. М.: Принта; 2012. 288 с. ISBN 5-93969-036-X

11. Kinyakin A.S., Glushachenkova E.A., Borutskii P.N., Shuvalov A.S., Pisarenko Yu.A. Kinetics of the low-temperature isomerization of *n*-hexane on the NIP-3A catalyst in an isothermal flow reactor. *Theor. Found. Chem. Eng.* 2008;42(6):815-821. https://doi.org/10.1134/S0040579508060031

12. Seliverstova M.B., Vlasov E.A., Deryuzhkina V.I. Investigation of the rheological properties of peptized pastes of aluminum hydroxide. *Zhurnal Prikladnoi Khimii = J. Appl. Chem.* 1981;54:2307-2310 (in Russ.).

13. Il'in A.P., Prokof'ev V.Ju. *Fiziko-khimicheskaya mekhanika v tekhnologii katalizatorov i sorbentov* (Physical and chemical mechanics in the technology of catalysts and sorbent). Ivanovo: Ivanovo State University of Chemistry and Technology; 2004. 315 p. ISBN 5-9616-0049-1 (in Russ.).

14. Tagandurdyyeva N., Burlutskaya L.P. Development of a method for the synthesis of a bayerite-containing catalyst for the isomerization of hydrocarbons. In: *Innovative materials and technologies in design: abstracts of the IV All-Russian scientific and practical conference with the participation of young scientists, March 22*, *23*. 2018:17-18 (in Russ.).

15. Nechiporenko A.P., Kudryashova A.I., Koltsov S.I. The method for determining the surface acidity of solids: USSR Pat. 4036187. Publ. 28.02.1988 (in Russ.).

16. Greg S., Sing K. *Adsorbtsiya. Udel'naya poverkhnost'. Poristost'* (Adsorption, Specific Surface Area, Porosity). Moscow: Mir; 1984. 306 p. (in Russ.).

17. Muhlenov I.P. *Issledovanie mekhanicheskoi prochnosti katalizatorov* (The study of the mechanical strength of the catalysts). Leningrad: LTI im. Lensoveta; 1981. 27 p. (in Russ.).

18. Deryuzhkina V.I. *Metody issledovaniya poristoi struktury katalizatorov* (Methods of studying the porous structure of catalysts). Leningrad: LTI im. Lensoveta; 1981. 27 p. (in Russ.).

19. Borutskiy P.N. Sal'nikov V.A., Nikul'shin P.A., Aleksandrova Yu.V., Kuzichkin N.V. *Konversiya n-butana – metod testirovaniya tverdokislotnykh katalizatorov i ikh nositelei dlya protsessov neftepererabotki* (Conversion of *n*-butane – a test method for solid acid catalysts and their carriers for oil refining processes). St. Petersburg: SPbGTI (TU); 2017. 94 p. (in Russ.).

20. Busca G. Structural, Surface, and Catalytic Properties of Aluminas. *Adv. Catal.* 2014;57(3):319-404. https://doi.org/10.1016/B978-0-12-800127-1.00003-5

12. Селиверстова М.Б., Власов Е.А., Дерюжкина В.И. Исследование реологических свойств пептизированных паст гидроокиси алюминия. *Журн. Прикладной Химии.* 1981;54(1):2307-2310.

13. Ильин А.П., Прокофьев В.Ю. Физико-химическая механика в технологии катализаторов и сорбентов: Монография. Иваново: Ивановский государственный химико-технологический университет; 2004. 315 с. ISBN 5-9616-0049-1

14. Тагандурдыева Н., Бурлуцкая Л.П. Разработка метода синтеза байеритсодержащего носителя катализатора изомеризации углеводородов. Инновационные материалы и технологии в дизайне: тезисы докладов IV Всероссийской научно-практической конференции с участием молодых ученых, 22, 23 марта 2018 г. 2018; 17-18.

15. Нечипоренко А.П., Кудряшова А.И., Кольцов С.И. Способ определения кислотности поверхности твердых веществ: SU 1377709 A1 А.с. СССР. Заявка № 4036187; заявл. 10.03.1986; опубл. 29.02.1988; Бюл. № 8.

16. Грег С., Синг К. Адсорбция. Удельная поверхность. Пористость. 2-е изд. М.: МИР; 1984. 306 с.

17. Мухленов И.П. Исследование механической прочности катализаторов. Л.: ЛТИ им. Ленсовета; 1981. 27 с.

18. Дерюжкина В. И. Методы исследования пористой структуры катализаторов. Л.: ЛТИ им. Ленсовета; 1981. 27 с.

19. Боруцкий П.Н. Сальников В.А., Никульшин П.А., Александрова Ю.В., Кузичкин Н.В. Конверсия *н*-бутана – метод тестирования твердокислотных катализаторов и их носителей для процессов нефтепереработки. СПб.: СПбГТИ(ТУ); 2017. 94 с.

20. Busca G. Structural, Surface, and Catalytic Properties of Aluminas. *Adv. Catal.* 2014;57(3):319-404. https://doi.org/10.1016/B978-0-12-800127-1.00003-5

About the authors:

Nurjahan Tagandurdyyeva, Postgraduate Student, Department of General Chemical Technology and Catalysis, Saint-Petersburg State Institute of Technology (26, Moskovsky pr., St. Petersburg, 190013, Russia). E-mail: jahana_18101993@mail.ru. https://orcid.org/0000-0001-7560-3605

Natalya V. Maltseva, Cand. of Sci. (Engineering), Associate Professor of the Department of General Chemical Technology and Catalysis, Saint-Petersburg State Institute of Technology (26, Moskovsky pr., St. Petersburg, 190013, Russia). E-mail: maltzeva.nv@yandex.ru. https://orcid.org/0000-0001-5978-5189

Tatyana A. Vishnevskaya, Engineer, Department of General Chemical Technology and Catalysis, Saint-Petersburg State Institute of Technology (26, Moskovsky pr., St. Petersburg, 190013, Russia).

Vyacheslav N. Narayev, Dr. of Sci. (Chemistry), Professor, Department of General Chemical Technology and Catalysis, Saint-Petersburg State Institute of Technology (26, Moskovsky pr., St. Petersburg, 190013, Russia). E-mail: naraev@lti-gti.ru. https://orcid.org/0000-0003-0276-8593

Arkady Yu. Postnov, Cand. of Sci. (Engineering), Associate Professor, Head of the Department of General Chemical Technology and Catalysis, Saint-Petersburg State Institute of Technology (26, Moskovsky pr., St. Petersburg, 190013, Russia). E-mail: ap1804@yandex.ru. https://orcid.org/0000-0003-2302-0103

Об авторах:

Тагандурдыева Нурджахан, аспирант кафедры общей химической технологии и катализа Санкт-Петербургского государственного технологического института (технический университет) (190013, Россия, Санкт-Петербург, Московский пр-т, д. 26). E-mail: jahana_18101993@mail.ru. https://orcid.org/0000-0001-7560-3605

Мальцева Наталья Васильевна, кандидат технических наук, доцент кафедры общей химической технологии и катализа Санкт-Петербургского государственного технологического института (технический университет) (190013, Россия, Санкт-Петербург, Московский пр-т, д. 26). E-mail: maltzeva.nv@yandex.ru. https://orcid.org/0000-0001-5978-5189

Вишневская Татьяна Алексеевна, инженер кафедры общей химической технологии и катализа Санкт-Петербургского государственного технологического института (технический университет) (190013, Россия, Санкт-Петербург, Московский пр-т, д. 26).

Нараев Вячеслав Николаевич, доктор химических наук, профессор кафедры общей химической технологии и катализа Санкт-Петербургского государственного технологического института (технический университет) (190013, Россия, Санкт-Петербург, Московский пр-т, д. 26). E-mail: naraev@lti-gti.ru. https://orcid.org/0000-0003-0276-8593

Постнов Аркадий Юрьевич, кандидат технических наук, доцент, заведующий кафедрой общей химической технологии и катализа Санкт-Петербургского государственного технологического института (технический университет) (190013, Россия, Санкт-Петербург, Московский пр-т, д. 26). E-mail: ap1804@yandex.ru. https://orcid.org/0000-0003-2302-0103

Submitted: January 16, 2020; Reviewed: February 18, 2020; Accepted: May 19, 2020.

Translated from Russian into English by N. Isaeva
Edited for English language and spelling by Enago, an editing brand of Crimson Interactive Inc.

ISSN 2686-7575 (Online)

https://doi.org/10.32362/2410-6593-2020-15-3-70-77

UDC 543.066

Quantification of polysorbate 80 in biopharmaceutical formulations implementing an optimized colorimetric approach

Aleksandr S. Seregin[1], Natalya V. Orlova[1], Aleksandr D. Askretkov[2,@], Dmitry I. Zybin[2], Yuri A. Seregin[1]

[1]Scientific Center "Kurchatov Institute," Research Institute for Genetics and Selection of Industrial Microorganisms, Moscow, 117545 Russia
[2]PHARMAPARK, Moscow, 117246 Russia
[@]Автор для переписки, e-mail: askretkov.a.d@gmail.com

Objectives. *We hereby describe an improvement of a previously developed quantification technique for polysorbate 80 in biopharmaceutical formulations (darbepoetin alfa and eculizumab) and report the validation of the new approach.*
Methods. *Polysorbate was isolated from analyte samples by protein precipitation using an organic solvent, followed by supernatant evaporation in vacuum. Polysorbate was derivatized using a ferric thiocyanate reagent and extracted into an organic phase; the relevant optical density measurements were performed.*
Results. *We established the optimal conditions for each step of the analysis procedure. The accuracy was 97–102% in the tested analytical range, the relative standard deviation did not exceed 5%, and the limit of quantification was 0.01 mg/mL.*
Conclusions. *The reported approach is highly sensitive; polysorbate isolation and quantification do not depend on the matrix or, most importantly, the protein.*

Keywords: *validation, darbepoetin alfa, eculizumab, polysorbate, precipitation, ferric thiocyanate.*

For citation: Seregin A.S., Orlova N.V., Askretkov A.D., Zybin D.I., Seregin Yu.A. Quantification of polysorbate 80 in biopharmaceutical formulations implementing an optimized colorimetric approach. *Tonk. Khim. Tekhnol. = Fine Chem. Technol.* 2020;15(3):70-77. https://doi.org/10.32362/2410-6593-2020-15-3-70-77

Определение полисорбата 80 в биофармацевтических препаратах с помощью оптимизированной колориметрической методики

А.С. Серегин[1], Н.В. Орлова[1], А.Д. Аскретков[2,@], Д.И. Зыбин[2], Ю.А. Серегин[1]

[1]Национальный исследовательский центр «Курчатовский институт» – ГосНИИгенетика, Москва, 117545 Россия
[2]ООО «ФАРМАПАРК», Москва, 117246 Россия
[@]Corresponding author, e-mail: askretkov.a.d@gmail.com

Цели. *В данной работе была усовершенствована ранее разработанная методика определения полисорбата 80 в биотехнологических препаратах (дарбэпоэтин альфа, экулизумаб), а также проведена ее валидация.*
Методы. *Полисорбат извлекали из пробы осаждением белка органическим растворителем, затем выпаривали супернатант в вакууме. Полисорбат дериватизировали оптимизированным железо–тиоцианатным реагентом; дериват экстрагировали в слой органического растворителя и измеряли оптическую плотность.*
Результаты. *Были установлены оптимальные условия для каждой стадии методики. Правильность находится в диапазоне степени извлечения 97–102%, относительное стандартное отклонение составляет не более 5%, предел количественного определения методики 0.01 мг/мл.*
Выводы. *Представленная методика имеет высокую чувствительность. Извлечение и определение полисорбата не зависят от матрикса пробы – прежде всего, от присутствующего белка.*

Ключевые слова: *валидация, дарбэпоэтин альфа, экулизумаб, полисорбат, осаждение, тиоцианат железа.*

Для цитирования: Seregin A.S., Orlova N.V., Askretkov A.D., Zybin D.I., Seregin Yu.A. Quantification of polysorbate 80 in biopharmaceutical formulations implementing an optimized colorimetric approach. *Tonk. Khim. Tekhnol. = Fine Chem. Technol.* 2020;15(3):70-77. https://doi.org/10.32362/2410-6593-2020-15-3-70-77

INTRODUCTION

Polysorbates (PSs), especially polysorbate 20 (PS20) and polysorbate 80 (PS80), are very common surfactants in biopharmaceutical formulations, due to their low toxicity, reasonably low cost, and high efficacy at low concentrations. The addition of PSs to biopharmaceuticals affords a mitigation of protein adsorption, denaturation, degradation [2], and aggregation [3, 4] that may occur in stress conditions, such as agitation [5], freeze–thaw cycling [6], and contact with an air–water interface in the course of downstream purification and storage [7]. In the course of biopharmaceutical downstream production and storage, PS concentration can significantly change because they tend to be adsorbed onto surfaces and filter membranes, so the target PS concentration, which ensures protein stability, in intermediate downstream products, drug substances, and drug dosage forms must always be maintained. Therefore, in this context, access to a simple and relatively fast method for PS quantification is a necessity.

PSs are characterized by heterogeneous structures, a lack of chromophoric groups, and a low tendency to bind proteins [8, 9], so PS analysis is not a very straightforward proposition. Numerous analytical methods have been developed, including high-performance liquid chromatography relying on spectrophotometry [10, 11], mass-spectrometry [12], evaporative light scattering [9], fluorometry [13], or gas chromatography [14] for analyte detection. In these approaches, laborious and time-consuming sample pre-treatment procedures, such as alkaline or acidic hydrolysis, solid-phase extraction, and protein removal, are usually required to obtain reliable analytical results. Notably, complex sample pre-treatment procedures represent a challenge also from the standpoint of possible mistakes in experiment execution.

Since PSs are, in fact, a group of closely related molecules lacking a well-defined structure, their properties and chemical composition may differ substantially from batch to batch. Therefore, quantification methods that detect only some PS components—e.g., oleic [10–12] or lauric acid, total fatty acid content [9, 13], or ethylene glycol released through hydrolysis [14]—often provide imprecise data. Conversely, the results of detection methods that rely on the ability of PSs to form micelles are not affected by PS batch-to-batch variability or even by the use of PS samples supplied by different manufacturers. A commonly used analytical approach is colorimetry, which is based on the formation of complexes between PSs and iron, cobalt, or molybdenum thiocyanates [15, 16], followed by extraction of the said complexes into an organic solvent. Exploitation of the formation of a polysorbate–iodine–starch complex has also been suggested for PS quantification [17]. Another possible analytical technique is based on the inclusion of a fluorescent dye into PS micelles, followed by fluorescence detection and quantitation [18, 19].

The aim of this work was to develop an optimized spectrophotometric method for PS quantification that relies on PS reactivity with ferric thiocyanate, so as to improve the previously described technique [1]. We also report the validation of PS80 analysis in the presence of darbepoetin alfa and eculizumab, the drugs that appeared to interfere with the results of the analysis performed with the previously developed approach [1].

MATERIALS AND METHODS

Chemicals and reagents

All reagents (analytical grade) were purchased from *Sigma-Aldrich*, USA. Biopharmaceuticals were drug substance solutions (or active pharmaceutical ingredients) of darbepoetin alfa and eculizumab, both manufactured by *PHARMAPARK*, Russia.

Assay procedure

The eculizumab drug substance, normally containing a PS80 concentration of 0.02%, was diluted five-fold before analysis. Conversely, the darbepoetin alfa drug substance, containing 0.005% PS80, was analyzed without dilution.

In detail, 1000 µL of acetone was added to 400 µL of standard (0.002–0.008% PS80 solutions in ddH_2O) and sample solutions. The contents were briefly mixed and centrifuged at 10000 rpm for 10 min in a 5417C centrifuge (*Eppendorf*, Germany). Subsequently, 1000 µL of each supernatant was placed in a fresh tube and the solvent removed by evaporation on a vacuum rotary evaporator RVC2-18HCL (*Martin-Christ*, Germany) for 2 h at 25°C. The dried samples were dissolved in 100 µL of 2 M sodium chloride. To the obtained solutions were then added 400 µL of freshly prepared derivatization reagent, which consists of equal volumes of 1 M iron(III) chloride and 6.4 M ammonium thiocyanate. Finally, 500 µL of dichloromethane (kept at −20°C) were added, and the capped tubes were vigorously shaken for 5 min using a Bullet Blender BBX24 (*Biostep*, Germany). The tubes were then subjected to centrifugation at 10000 rpm for 10 min at room temperature. The optical density (OD) of the lower phase (the organic solvent layer) was measured at 510 nm on an Ultrospec 7000 instrument (*General Electric*, USA) against a blank consisting of deionized water. The concentrations of PS80 were determined by linear regression using a calibration curve obtained with the standard samples.

Validation

All validation procedures were carried out in accordance with the State Pharmacopeia of the Russian Federation (14th edition) and the ICH Q2(R1) guidelines. Specificity, linearity, analytical range, precision, accuracy, limit of detection (LOD), and limit of quantification (LOQ) were all evaluated.

RESULTS AND DISCUSSION

Specificity

To evaluate the analytical technique's specificity, we used pre-formulated PS-free protein substances of darbepoetin alfa and eculizumab that were characterized by concentrations of 2.1 and 15.1 mg/mL, respectively. The values of the optical density of these solutions, OD_{matrix}, were compared with the OD of the PS80 standard solution at the LOQ (OD_{LOQ}), 0.01 mg/mL. The matrix interference (MI) index can be used to quantitatively appreciate interference from sample matrix on method specificity. MI was calculated by the following equation:

$$MI = \frac{OD_{matrix}}{OD_{LOQ}} \times 100\%$$

For darbepoetin alfa, the MI was 12.9%, and for eculizumab it was 15.1%. Both values did not exceed the MI limit of 20% [15].

Linearity

The relationship between the OD and PS80 concentration was evaluated for five PS80 concentrations in the 0.02–0.08 mg/mL range—each in triplicate. The calibration curve thus obtained is reported in Fig. 1a, and the residuals' plot (the plot of the deviation of the actual data points from the regression line) is reported in Fig. 1b.

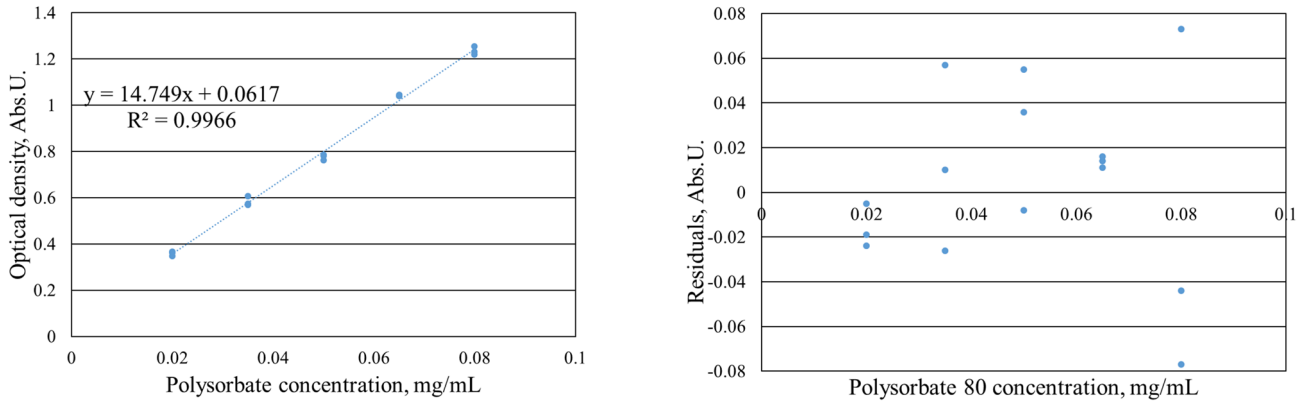

a b

Fig. 1. Regression of the optical density *vs*. the concentration of polysorboate 80 (a). Residual values of the optical density plotted against polysorbate 80 concentration (b).

As can be evinced from Fig. 1a, the value for the correlation coefficient R^2 of the regression of the OD *vs*. PS80 concentration is 0.9966. Based on this high value and the fact that the residual values (reported in Fig. 1b) do not depend on PS80 concentration, we conclude that the method meets the linearity criterion.

Accuracy

For the estimation of the method's accuracy, darbepoetin alfa and eculizumab solutions, initially PS80-free, were spiked with PS80 to reach the final concentration of 0.02, 0.05, and 0.08 mg/mL, in the case of darbepoetin alfa, and 0.08, 0.20, and 0.36 mg/mL, in the case of eculizumab. After PS80 quantification (as described), the recovery rate at every concentration was calculated. In the case of darbepoetin alfa, the recovery rate remained in the 98–102% range for all concentrations; in the case of eculizumab, the corresponding range was 97–100% (Table 1). The recovery results for both drug substances were thus narrowly scattered around the 100% value, and no sample exceeded the recovery range limit of 85–115%; within this range, the values are considered to be free of systematic error and provide true PS80 concentration for the tested samples).

Repeatability and precision

The analytical technique's repeatability was assessed using the data of the linear regression (n = 3). The relative standard deviation (RSD) was calculated for each concentration. Since protein precipitation could affect PS80 extraction and alter analysis results, commercial samples of darbepoetin alfa and eculizumab (already containing 0.05 and 0.2 mg/mL PS80, respectively) were also analyzed (n = 6). For the evaluation of the intermediate precision, the same analyses were conducted in two additional replicates, and the RSD values of overall PS80 concentrations for each sample were compared. The relevant data are listed in Table 2. In the case of no sample, the repeatability limit of 5% or intermediate precision limit of 8% was exceeded.

LOD and limit of quantification

The LOD and LOQ values were determined using the standard deviation of the response, and the slope of the calibration plot. The LOQ was determined to be 0.010 mg/mL and the LOD 0.003 mg/mL.

Robustness

In order to evaluate the analytical method's robustness, we analyzed the effect of varying the following parameters (the usual value is shown in **bold**):

–evaporation temperature (**25**, 30, and 35°C);

–derivatization time (2, **5**, 10, and 20 min).

Standard solutions of PS80, as well as darbepoetin alfa and eculizumab drug substances spiked with PS80, were analyzed. The recovery of eculizumab and darbepoetin alfa was used as robustness criterion. One should expect PS80 concentration differences of no greater than 8% compared with the results obtained using standard procedure.

Table 1. Accuracy estimation

Product	Theoretical polysorbate 80 concentration, mg/mL	Obtained polysorbate 80 concentration, mg/mL	Recovery rate, %
Darbepoetin alfa	0.02	0.0202	101
		0.0198	99
		0.0196	98
	0.05	0.0512	102
		0.0505	101
		0.0511	102
	0.08	0.0810	101
		0.0817	102
		0.0814	102
Ecuizumab	0.08	0.0802	100
		0.0794	99
		0.0788	99
	0.2	0.1936	97
		0.1952	98
		0.1930	97
	0.36	0.3531	98
		0.3597	100
		0.3553	99

Table 2. Repeatability and intermediate precision

Sample		RSD of repeatability, %	RSD of intermediate precision, %
PS80, mg/mL	0.020	2.6 (n = 3)	2.7
	0.035	3.4 (n = 3)	3.1
	0.050	1.6 (n = 3)	1.8
	0.065	1.2 (n = 3)	2.0
	0.080	1.4 (n = 3)	2.1
Darbepoetin alfa, 2.1 mg/mL		2.5 (n = 6)	3.4
Eculizumab, 16.2 mg/mL		4.6 (n = 6)	5.2

Note: PS80: polysorbate 80; RSD: relative standard deviation.

When the evaporation temperature was elevated to 35°C, no effect was observed on the recovery of darbepoetin alfa and eculizumab. However, the recovery RSD value increased two-fold at this temperature with respect to the 25°C case, which could be explained by an increased rate of evaporation, splashing, and/or partial loss of the sample. Changes in the derivatization time did not have much impact on the recovery of the drug formulations either. Notably, implementation of a 2-min derivatization resulted in a decrease of the samples' OD.

Subsequently, the stability of the polysorbate–iron thiocyanate complex was monitored for 1 h. The PS80 standard and darbepoetin alfa drug substance samples spiked with PS80 (at 0.02, 0.05, and 0.08 mg/mL final concentrations) were analyzed at five time points: 10, 20, 30, 40, and 60 min. Between measurements, the solutions were stored in polypropylene tubes at room temperature. In Fig. 2 is reported the graph whereby the OD is plotted against the incubation time. The OD values did not differ from the initial value by more than 8% over the 1-h period, for any sample.

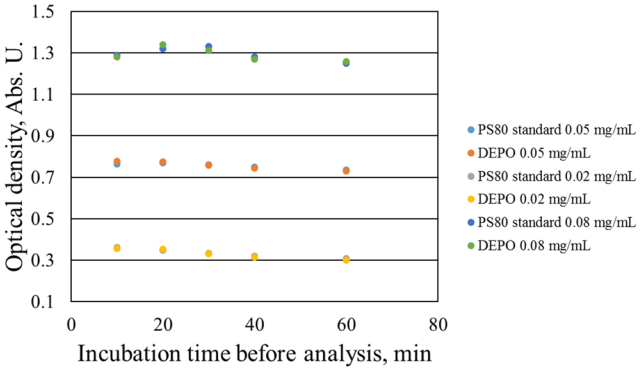

Fig. 2. Effect of incubation time on the optical density of polysorbate 80 (PS80) standards at different concentrations and darbepoetin alfa drug substance samples spiked with PS80 to the specified final concentrations (DEPO).

Analytical range

We have established the linearity, accuracy, and precision of our technique to determine the concentration of PS80 in the 0.02–0.08 mg/mL range. Therefore, evidence indicates that the PS80 analytical range is 0.02–0.08 mg/mL when darbepoetin alfa is present. However, we need to note that eculizumab was diluted five-fold before analysis in all experiments; therefore, in this case the PS80 analytical range is 0.1–0.4 mg/mL.

Selection of the derivatization reagent

PS80 is able to form colored complexes with thiocyanates of transition metals, especially iron(III), molybdenum(V), and cobalt(II). Notably, PS80–metal thiocyanate complexes are soluble in organic solvents [16]. In non-polar organic solvents, furthermore, all these complexes display absorbance peaks in the UV-Vis spectrum. The PS80–cobalt(II) thiocyanate complex displays two UV-Vis peaks, at 320 nm (higher intensity) and 620 nm; PS80–molybdenum(V) thiocyanate displays two peaks, at 323 and 475 nm; and PS80–iron(III) thiocyanate displays one peak at 510 nm. The extinction coefficients of the peaks just listed decrease in the following order: Fe (510 nm) > Co (320 nm) > Mo (323 nm) ≈ Mo (475 nm) > Co (620 nm). As we previously discussed [1], the most useful complex from the standpoint of our analysis is iron(III) thiocyanate because its detection relies on a relatively long wavelength; it interferes minimally with the background, sample matrix, and the presence of UV-absorbing impurities in reagents, and it is characterized by the highest sensitivity among the tested metal thiocyanates.

A considerable issue associated with PS80 derivatization is the high volatility of dichloromethane, which could result in quantification errors and increased RSD values. Attempts to replace dichloromethane with polar organic solvents (e.g., ethyl acetate, butyl acetate, or their mixtures with acetonitrile) have failed due to the intense color and almost opaque appearance of the organic layer, even in the case of blank samples, which is caused by the high solubility of the complexes in these solvents. However, the use of non-polar organic solvents, such as chloroform, carbon tetrachloride, toluene, and benzene, yielded similar results to those obtained using dichloromethane, although analyte sensitivity was 2–4 times lower in all these solvents than in dichloromethane. Moreover, collecting the toluene

and benzene layers proved difficult, since these solvents' densities were lower than that of the aqueous layer. In order to minimize dichloromethane volatility, we cooled the metal thiocyanate complex solutions to −20°C before adding them to the PS80-containing solutions.

Cuvette fouling

The measurements of the OD were carried out in quartz cuvettes. The cuvettes' surfaces were noticeably stained after 3–4 measurements. In order to lessen cuvette fouling and maintain the stability of the colored complexes, we added 10% sulfuric acid to the derivatization reagent [16]. In our previous report [1], we recommended rinsing the cuvettes with 96% ethanol and dichloromethane after each measurement, although complete stain removal was not achieved by this approach. In the present study, we revised the composition of the derivatization reagent.

According to some sources [20, 21], sodium and potassium ions stabilize polyoxyethylene complexes with iron(III) thiocyanate. To investigate the effect of such ions on PS-based complexes, we added either sodium or potassium chloride into the derivatization reagent to the final concentrations of 0.1, 0.4, 1.0, and 2.0 M. To estimate the stability of the complexes in quartz cuvettes, the absorbance of derivatized 0.4 mg/mL PS80 samples was determined in six replicates for all sodium and potassium chloride ion concentrations. When a derivatization reagent containing at least a 0.4 M concentration of either sodium or potassium was utilized, the cuvette was observed to be much cleaner than in the case whereby the derivatization reagent contained no sodium/potassium ions or a 0.1 M concentration of them. We conclude that the addition of 0.4 M sodium chloride (or potassium chloride) is useful for preventing cuvette fouling.

Removal of proteins from PS solutions

Our previous attempt to quantify PS80 in darbepoetin alfa and eculizumab formulations using solid-phase extraction [1] produced ambiguous results, due to PS80 adsorption onto the proteins. Performing a preliminary protein denaturation with chaotropic agents, such as guanidine hydrochloride or urea, partially addressed the problem. In this study, we observed no interaction between the precipitated protein and PS80 in organic solvent–water mixtures. To investigate this issue further, we used different organic solvents to precipitate the protein, while causing no PS80 loss. Darbepoetin alfa, being a highly sialylated protein, was difficult to precipitate, and only the use of a mixed water–organic solvent with at least 50% acetone content afforded the complete removal of the protein from solution. Eculizumab precipitation was carried out in the same manner, and the recovery rate was quite similar, close to 100% (see ***Accuracy*** subsection in RESULTS AND DISCUSSION section).

CONCLUSIONS

The reported spectrophotometric method based on ferric thiocyanate complexation was suitable for PS quantification in biopharmaceutical formulations in the PS concentration range of 0.02–0.08 mg/mL. PS extraction was achieved by protein precipitation using an organic solvent, followed by supernatant evaporation in vacuum. PS was derivatized using an optimized, stable ferric thiocyanate reagent, and the derivative was extracted into dichloromethane to conduct OD measurements.

The optimal conditions for each step of the analysis were identified. The accuracy of the technique in the mentioned analytical range was 97–102%; the RSD of the repeatability did not exceed 5%; the LOQ value was 0.01 mg/mL. The approach was validated for PS80 quantification in darbepoetin alpha and eculizumab drug substances. The proposed method was more sensitive and precise than the previously reported technique [1], and we did not detect any MI.

The authors declare no conflicts of interest.

REFERENCES

1. Askretkov A.D., Isaykina P.M., Cherepushkin S.A., Orlova N.V. Determination of polysorbates by spectrophotometry in drugs based on recombinant proteins. *Drug development & registration.* 2017;(3):124-129 (in Russ.).

2. Hillgren A., Lindgren J., Aldén M. Protection mechanism of Tween 80 during freeze-thawing of a model protein, LDH. *Int. J. Pharm*. 2002;237(1-2):57-69. https://doi.org/10.1016/s0378-5173(02)00021-2

3. Arakawa T., Kita Y. Protection of bovine serum albumin from aggregation by Tween 80. *J. Pharm. Sci.* 2000;89(5):646-651. https://doi.org/10.1002/(SICI)1520-6017(200005)89:5%3C646::AID-JPS10%3E3.0.CO;2-J

4. Kiese S., Pappenberger A., Friess W., Mahler H.C. Shaken, not stirred: mechanical stress testing of an IgG1 antibody. *J. Pharm. Sci.* 2008;97(10):4347-4366. https://doi.org/10.1002/jps.21328

5. Kerwin B.A. Polysorbates 20 and 80 used in the formulation of protein biotherapeutics: structure and degradation pathways. *J. Pharm. Sci.* 2008;97(8):2924-2935. https://doi.org/10.1002/jps.21190

6. Kreilgaard L., Jones L.S., Randolph T.W., Frokjaer S., Flink J.M., Manning M.C., Carpenter J.F. Effect of Tween 20 on freeze-thawing- and agitation-induced aggregation of recombinant human factor XIII. *J. Pharm. Sci.* 1998;87(12):1597-1603. https://doi.org/10.1021/js980126i

7. Wang W., Wang Y.J., Wang D.Q. Dual effects of Tween 80 on protein stability. *Int. J. Pharm.* 2008;347(1-2):31-38. https://doi.org/10.1016/j.ijpharm.2007.06.042

8. Tani T.H., Moore J.M., Patapoff T.W. Single step method for the accurate concentration determination of polysorbate 80. *J. Chromatogr. A.* 1997;786(1):99-106. https://doi.org/10.1016/S0021-9673(97)00540-2

9. Ilko D., Braun A., Germershaus O., Meinel L., Holzgrabe U. Fatty acid composition analysis in polysorbate 80 with high performance liquid chromatography coupled to charged aerosol detection. *Eur. J. Pharm. Biopharm.* 2015;94:569-574. https://doi.org/10.1016/j.ejpb.2014.11.018

10. Őszi Z., Pethő G. Quantitative determination of polysorbate 20 in nasal pharmaceutical preparations by high-performance liquid chromatography. *J. Pharm. Biomed. Anal.* 1998;18(4-5):715-720. https://doi.org/10.1016/S0731-7085(98)00265-9

11. Adamo M., Dick L.W. Jr., Qiu D., Lee A.H., Devincentis J., Cheng K.C. A simple reversed phase high-performance liquid chromatography method for polysorbate 80 quantitation in monoclonal antibody drug products. *J. Chromatogr. B.* 2010;878(21):1865-1870. https://doi.org/10.1016/j.jchromb.2010.04.039

12. Puschmann J., Evers D.H., Müller-Goymann C.C., Herbig M.E. Development of a design of experiments optimized method for quantification of polysorbate 80 based on oleic acid using UHPLC-MS. *J. Chromatogr. A.* 2019;1599:136-143. https://doi.org/10.1016/j.chroma.2019.04.015

13. Tomlinson A., Demeule B., Lin B., Yadav S. Polysorbate 20 Degradation in Biopharmaceutical Formulations: Quantification of Free Fatty Acids, Characterization of Particulates, and Insights into the Degradation Mechanism. *Mol. Pharm.* 2015;12(11):3805-3815. https://doi.org/10.1021/acs.molpharmaceut.5b00311

14. Wei Z., Bilbulian S., Li J., Pandey R., O'Connor E., Casas-Finet J., Cash P.W. Universal method for the determination of nonionic surfactant content in the presence of protein. *J. Sep. Sci.* 2015;38(8):1318-1325. https://doi.org/10.1002/jssc.201400766

15. Kim J., Qiu J. Quantitation of low concentrations of polysorbates in high protein concentration formulations by solid phase extraction and cobalt-thiocyanate derivatization. *Anal. Chim. Acta.* 2014;806:144-151. https://doi.org/10.1016/j.aca.2013.11.005

16. Savjani N., Babcock E., Khor H.K., Raghani A. Use of ferric thiocyanate derivatization for quantification of polysorbate 80 in high concentration protein formulations. *Talanta.* 2014;130:542-546. https://doi.org/10.1016/j.talanta.2014.07.052

17. Cucakovich N.B. Determination of Tween 80 in tissue culture media, vaccines, and related products. *Anal. Biochem.* 1971;40(1):183-186. https://doi.org/10.1016/0003-2697(71)90090-X

18. Khossravi M., Kao Y.H., Mrsny R.J., Sweeney T.D. Analysis methods of polysorbate 20: A new method to assess the stability of polysorbate 20 and established methods that may overlook degraded polysorbate 20. *Pharm. Res.* 2002;19(5):634-639. https://doi.org/10.1023/a:1015306112979

19. Brito R.M., Vaz W.L. Determination of the critical micelle concentration of surfactants using the fluorescent probe N-phenyl-1-naphthylamine. *Anal. Biochem.* 1986;152(2):250-255. https://doi.org/10.1016/0003-2697(86)90406-9

20. Yokoyama Y., Atsumi H., Yoshida S., Sone N., Ueda K. Conformational Study for Ionic Aggregates of Poly(oxyethylene) Dodecyl Ethers with Ferric-Thiocyanate Anion through the Intermediary of Potassium Ion. *Anal. Sci.* 2010;26:1047-1052. https://doi.org/10.2116/analsci.26.1047

21. Yokoyama Y., Hirajima R., Morigaki K., Yamaguchi Y., Ueda K. Alkali-cation affinities of polyoxyethylene dodecylethers and helical conformations of their cationized molecules studied by electrospray mass spectrometry. *J. Am. Soc. Mass Spectrom.* 2007;18(11):1914-1920. https://doi.org/10.1016/j.jasms.2007.08.004

About the authors:

Aleksandr S. Seregin, Postgraduate Student, Scientific Center "Kurchatov Institute," Research Institute for Genetics and Selection of Industrial Microorganisms (1, 1st Dorozhnyi pr., Moscow, 117545, Russia). E-mail: penpney@mail.ru. https://orcid.org/0000-0002-5842-7344

Natalya V. Orlova, Cand. of Sci. (Biology), Head of Research Laboratory, Scientific Center "Kurchatov Institute," Research Institute for Genetics and Selection of Industrial Microorganisms (1, 1st Dorozhnyi pr., Moscow, 117545, Russia). E-mail: orlova.chemist@gmail.com. https://orcid.org/0000-0003-4161-5880

Aleksandr D. Askretkov, Chief Chemist-Analyst, PHARMAPARK LLC (8, b. 1, Nauchnyi pr., Moscow, 117246, Russia). E-mail: askretkov.a.d@gmail.com. https://orcid.org/0000-0003-0110-8323

Dmitry I. Zybin, Chief Chemist-Analyst, PHARMAPARK LLC (8, b. 1, Nauchnyi pr., Moscow, 117246, Russia). E-mail: zybin@pharmapark.ru. ResearcherID P-8049-2016, https://orcid.org/0000-0002-5542-982X

Yuri A. Seregin, Cand. of Sci. (Biology), Deputy Director, Scientific Center "Kurchatov Institute," Research Institute for Genetics and Selection of Industrial Microorganisms (1, 1st Dorozhnyi pr., Moscow, 117545, Russia). E-mail: yuriy.seregin@pharmapark.ru. ResearcherID I-1874-2017

Об авторах:

Серегин Александр Сергеевич, аспирант Национального исследовательского центра «Курчатовский институт» – ГосНИИгенетика (117545, Россия, Москва, 1-й Дорожный проезд, д. 1). E-mail: penpney@mail.ru. https://orcid.org/0000-0002-5842-7344

Орлова Наталья Владимировна, кандидат биологических наук, заведующая испытательной лабораторией Национального исследовательского центра «Курчатовский институт» – ГосНИИгенетика (117545, Россия, Москва, 1-й Дорожный проезд, д. 1). E-mail: orlova.chemist@gmail.com. https://orcid.org/0000-0003-4161-5880

Аскретков Александр Дмитриевич, старший химик-аналитик ООО «Фармапарк» (117246, Россия, Москва, Научный проезд, д. 8, стр. 1). E-mail: askretkov.a.d@gmail.com. https://orcid.org/0000-0003-0110-8323

Зыбин Дмитрий Игоревич, старший химик-аналитик ООО «Фармапарк» (117246, Россия, Москва, Научный проезд, д. 8, стр. 1). E-mail: zybin@pharmapark.ru. ResearcherID P-8049-2016, https://orcid.org/0000-0002-5542-982X

Серегин Юрий Александрович, кандидат биологических наук, заместитель директора Национального исследовательского центра «Курчатовский институт» – ГосНИИгенетика (117545, Россия, Москва, 1-й Дорожный проезд, д. 1). E-mail: yuriy.seregin@pharmapark.ru. ResearcherID I-1874-2017

Submitted: November 4, 2019; Reviewed: March 25, 2020; Accepted: May 18, 2020.

The text was submitted by the author in English.
Edited for English language and spelling by Enago, an editing brand of Crimson Interactive Inc.

MIREA – Russian Technological University.
78, Vernadskogo pr., Moscow, 119454, Russian Federation.
Publication date June 30, 2020.
Not for sale

МИРЭА – Российский технологический университет.
119454, РФ, Москва, пр-кт Вернадского, д. 78.
Дата опубликования 30.06.2020 г.
Не для продажи